Tropical Cyclone

Hyeong-Seog Kim

Korea Maritime and Ocean University

Tropical cyclone (TC)

- A tropical cyclone is an atmospheric cyclonic system that originates the tropical oceans, and is driven principally by heat transfer from the ocean.

- Tropical cyclones are usually categorized according to their maximum wind speed (V_{max} at 10m): tropical depressions if Vmax < 17 m/s, tropical storm if $17 <$ Vmax < 33 m/s, and hurricanes or typhoon if Vmax > 33 m/s.

Tropical Cyclone Structure

- A rapidly rotating storm system characterized by a low-pressure center, strong winds, and a spiral arrangement of thunderstorms that produce heavy rain.

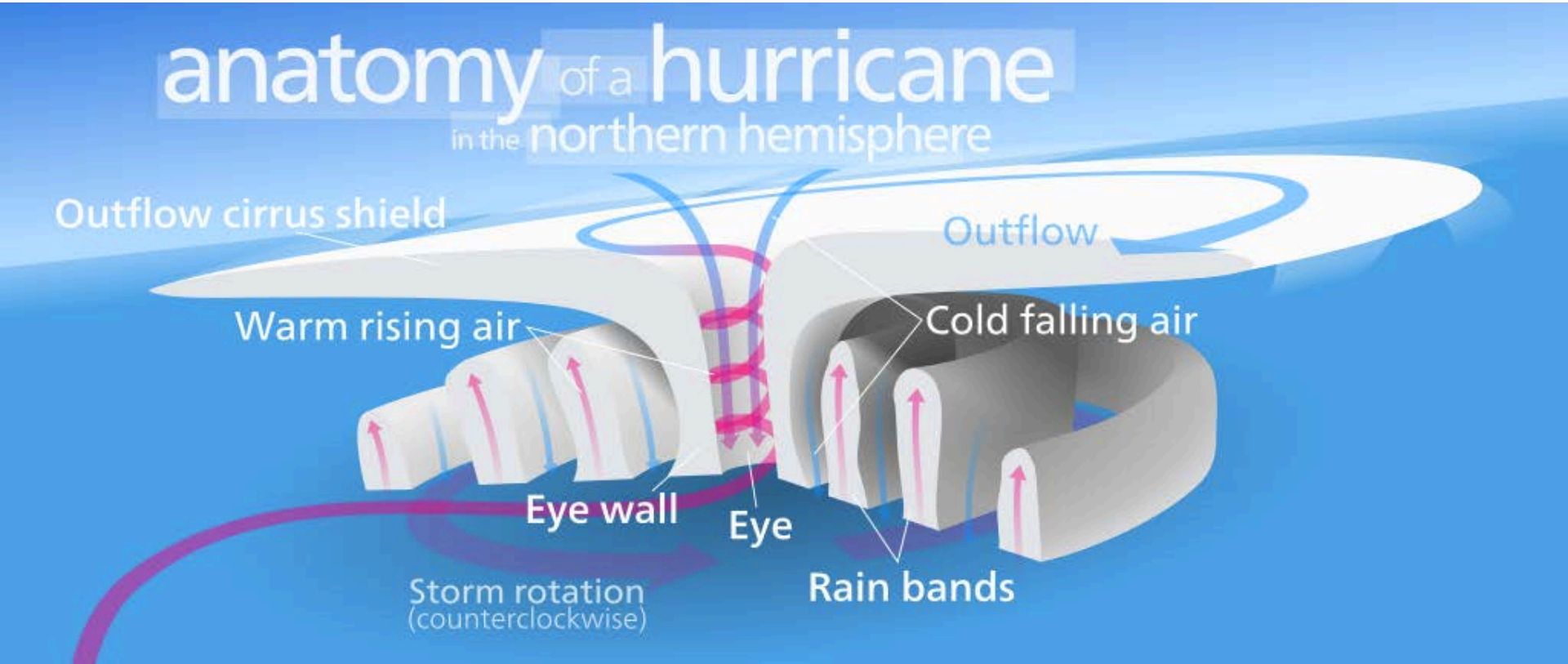

Global Distribution

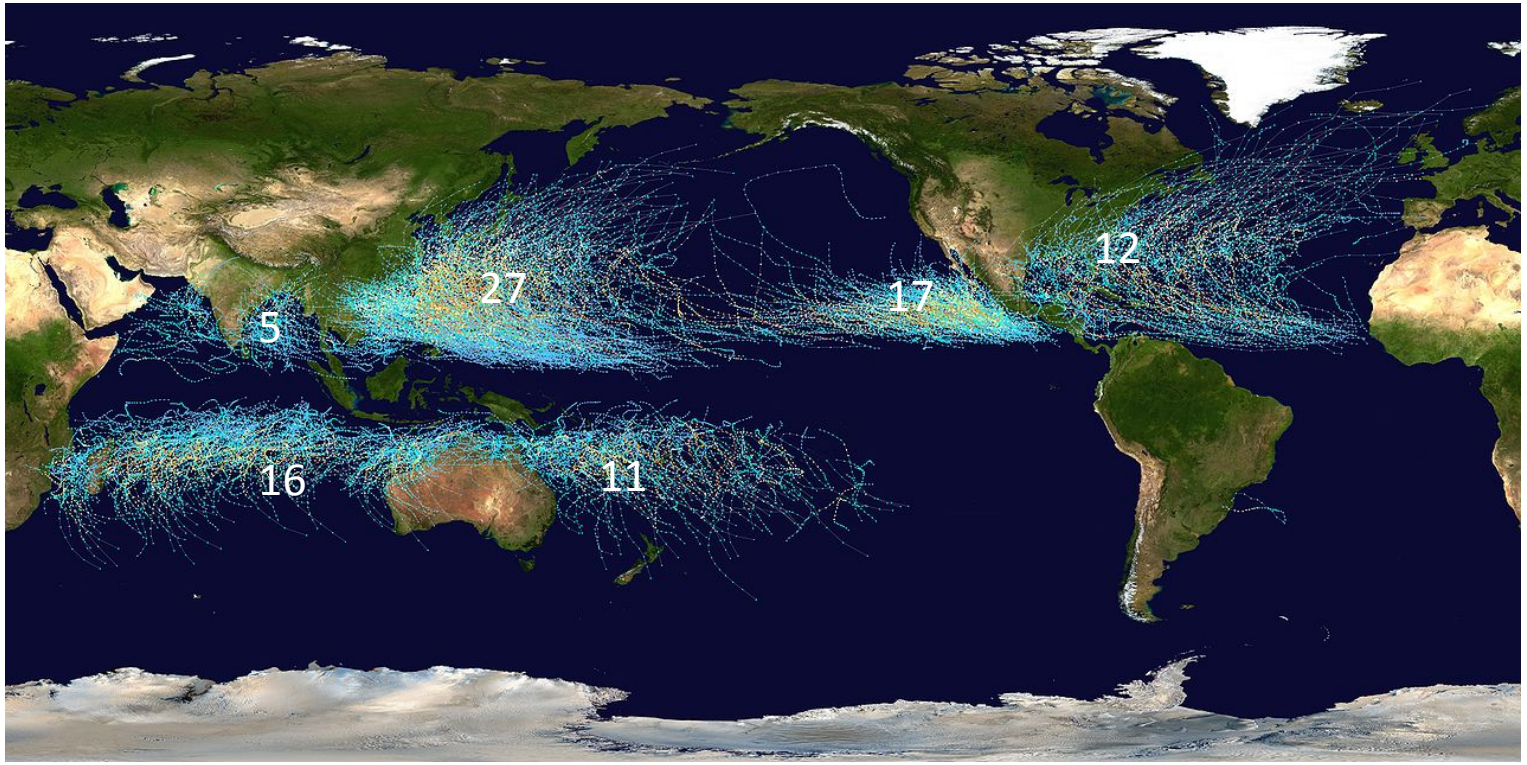

Environmental parameters for TC

- High Sea Surface Temperature (SST) (>26 °C)
  - Energy source for TC development

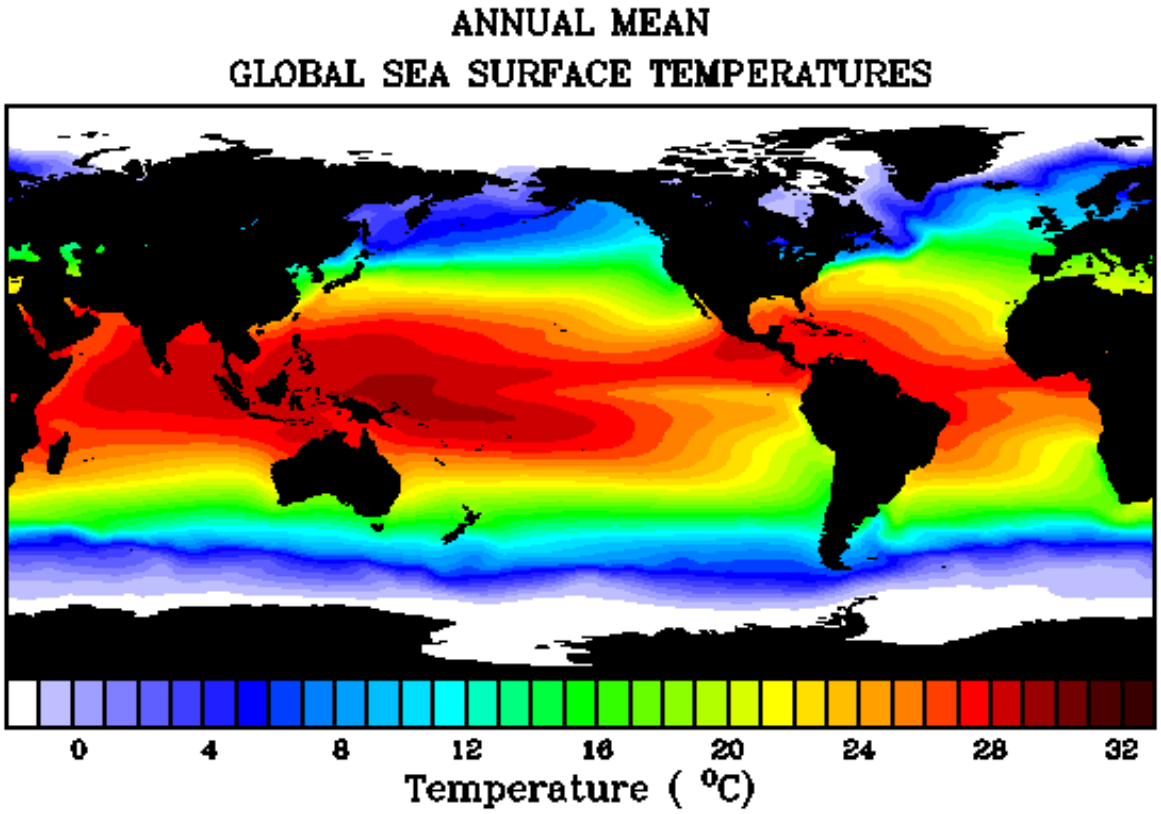

Interaction between TC and Ocean

Cold Wake

Cold wake from Ioke (2006)

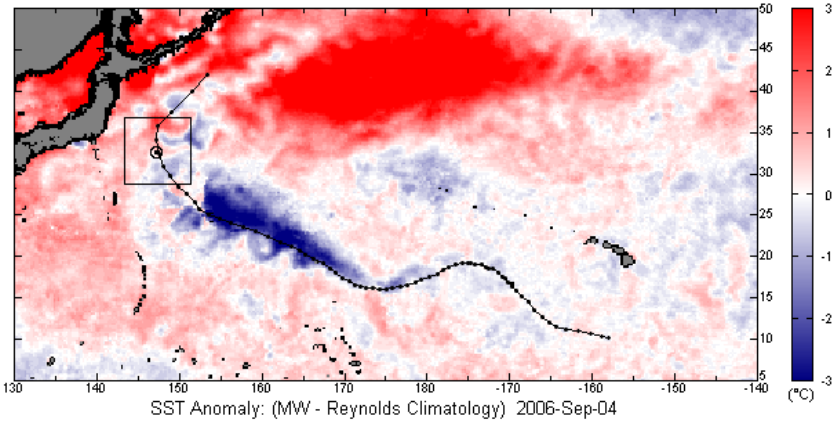

Cold wake at Katrina

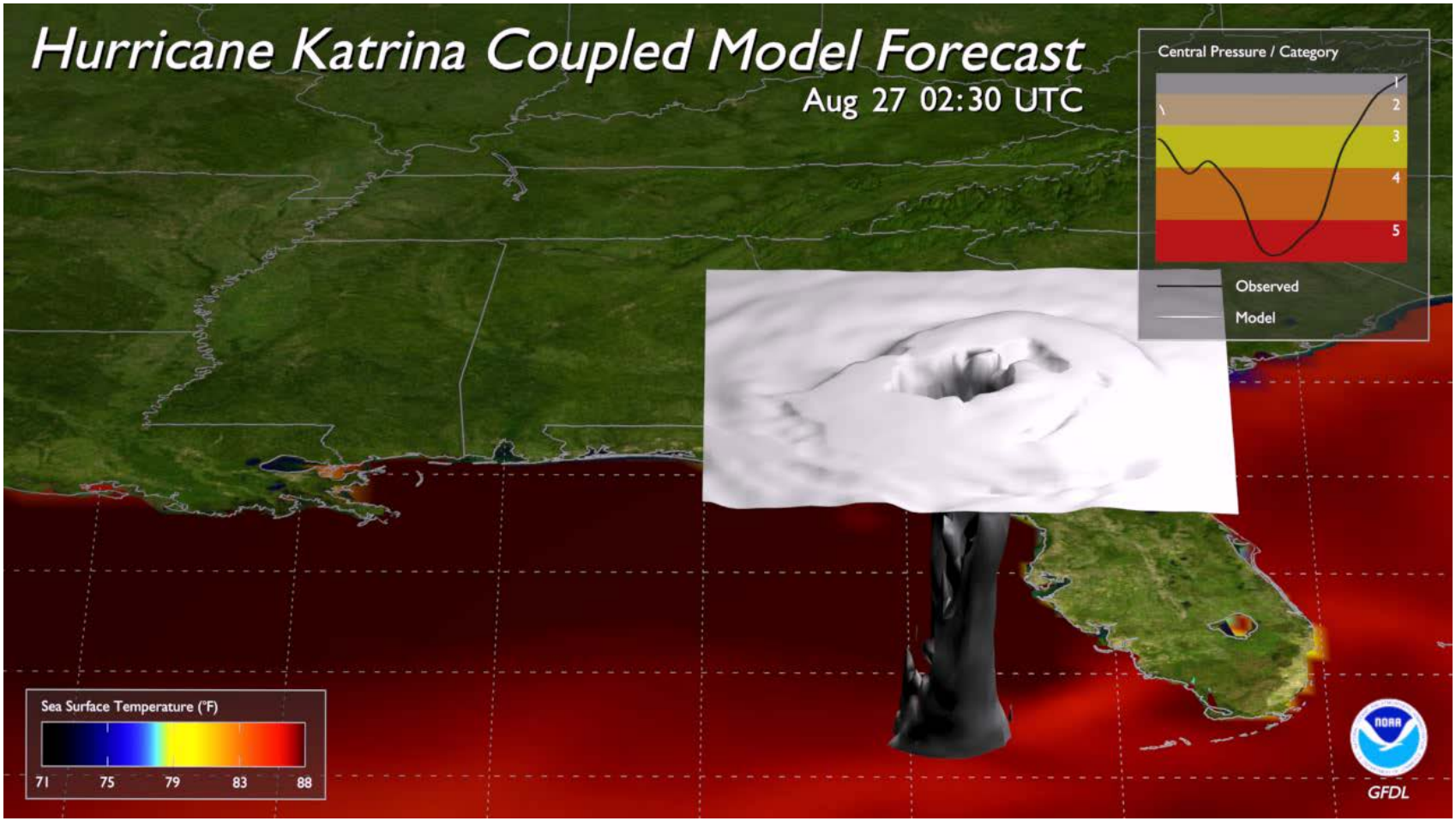

Environmental parameters for TC

- High Relative Humidity
  - Moisture transports the energy from ocean to atmosphere by releasing latent heat and induce rising motion

- Low-level vorticity
  - A cyclonic circulation causes more air to flow in the circulation's center… pulling more air into the developing storm.. Meaning that more air can rise and release its latent heat.

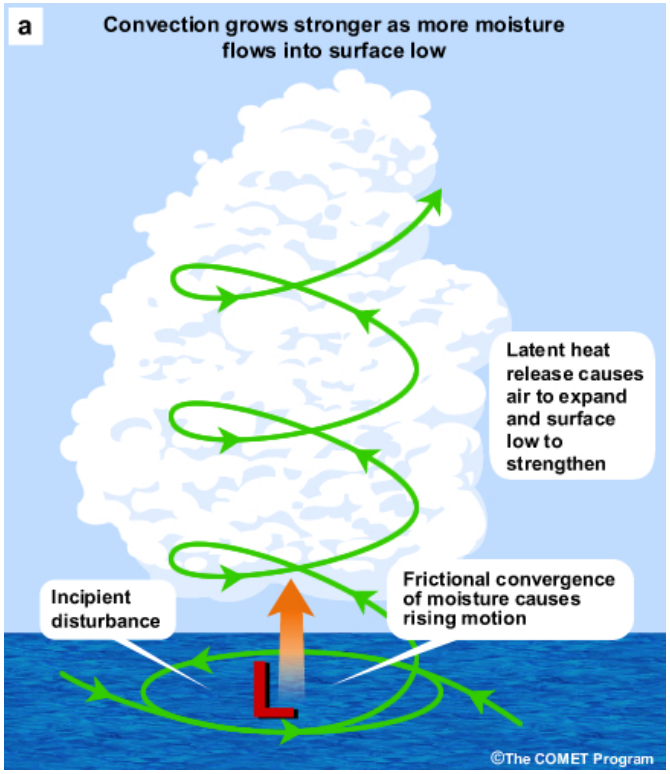

Environmental parameters for TC

- Low vertical wind shear
  - Vertical wind shear is the magnitude of vector difference between winds at high level (~200hPa) and low level (~850hPa)
  - The center of the latent heat being released aloft needs to stay above the surface low pressure center so that the pressure drop being driven by the heating aloft cant work in conjunction with the surface low pressure

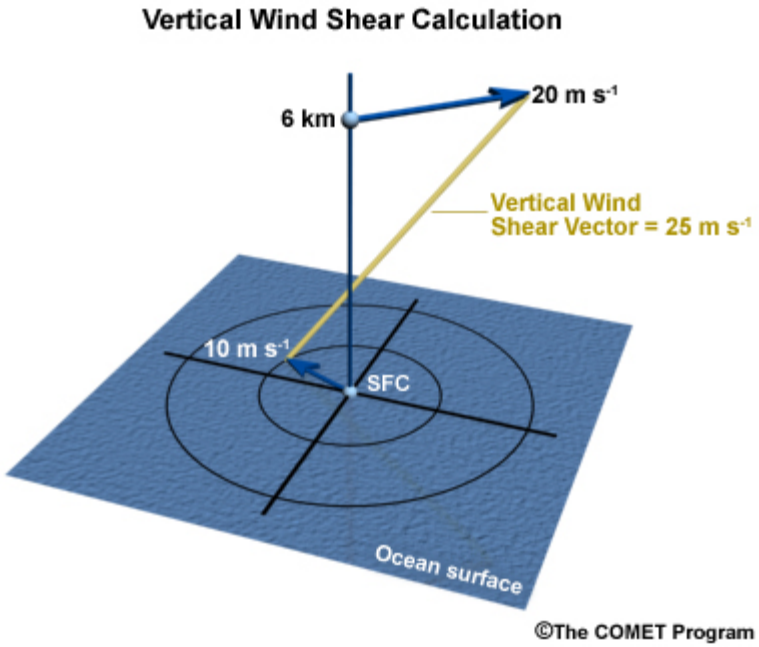

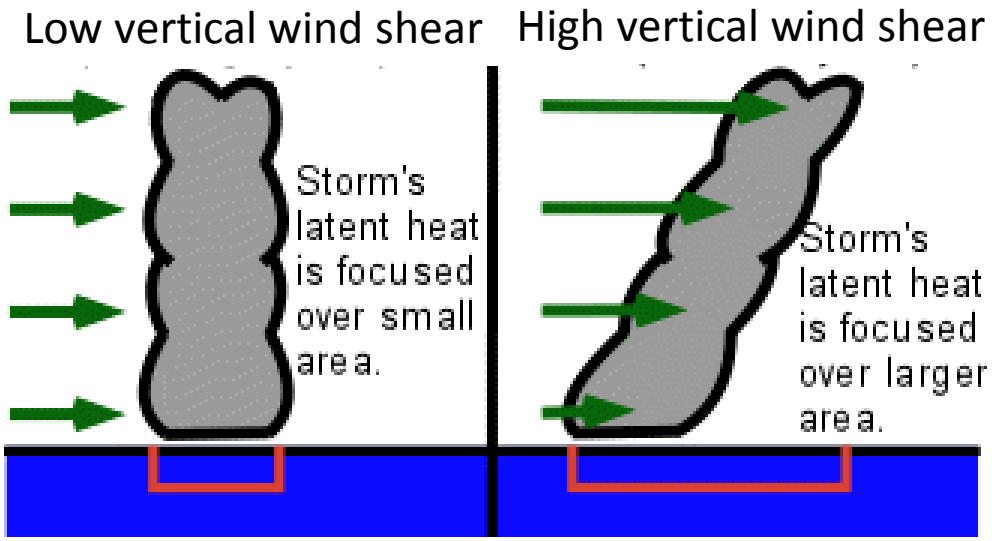

Vertical Wind Shear

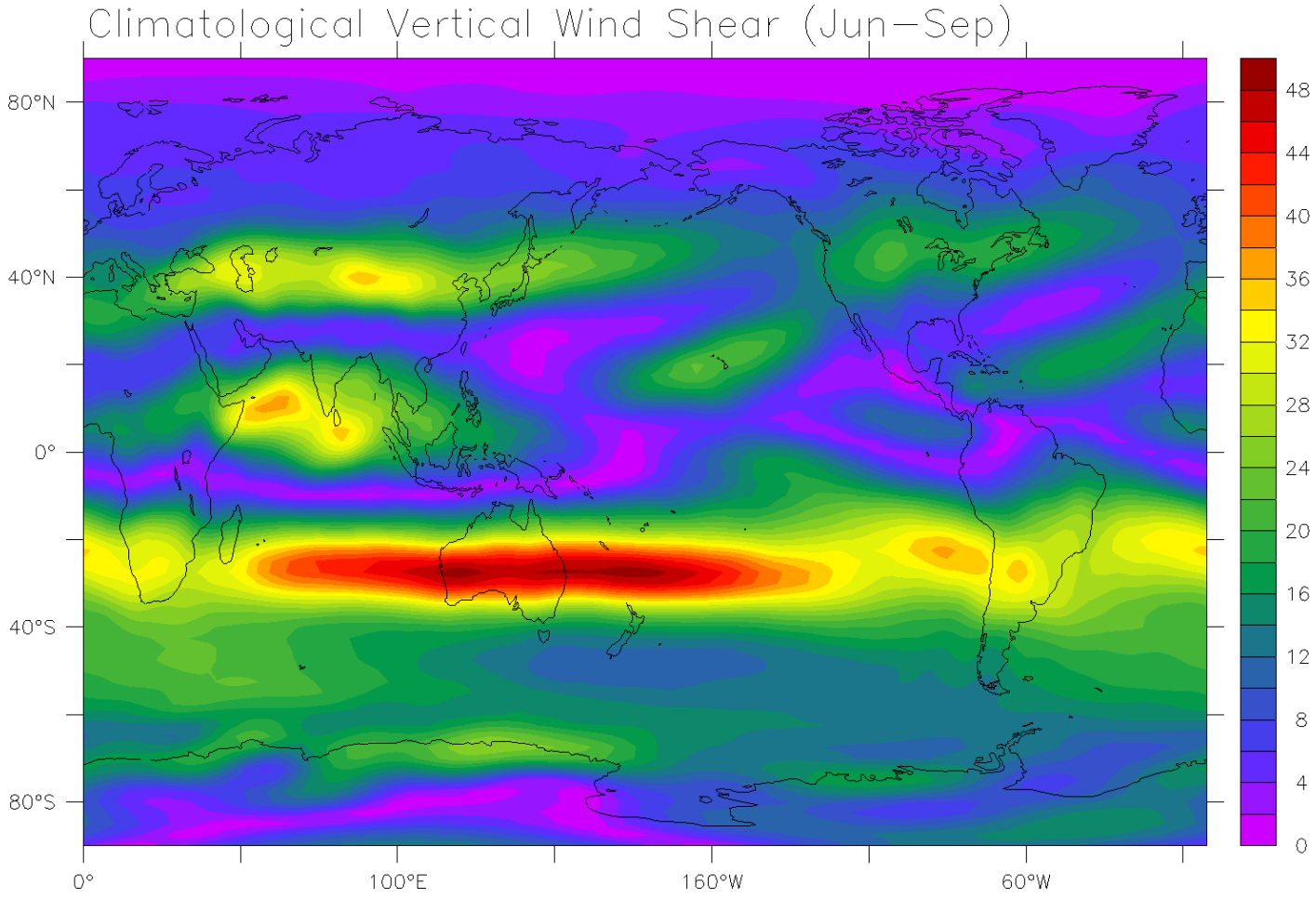

“Necessary but not sufficient”

- The aforementioned parameters for TC formation are “necessary” but “not sufficient” for tropical cyclone formation.

- It means that all of these conditions must be present simultaneously before tropical cyclone formation, but even if all of these conditions are met, tropical cyclone formation may not occur.

Tropical Cyclone Formation Forecast: Statistical Method

INPUT PARAMETERS:

Abbreviation	Screening parameter	Data source	Elimination criteria		
			Atlantic	Eastern Pacific	Western Pacific
LAT	Lat (°N)	Domain definition	<5.0	<5.0	<5.0
PLAND	Land coverage (%)	Land mask	≥100.0	≥100.0	≥100.0
DSTRM	Distance to nearest TC (° lat–lon)	Best tracks	<2.5	<2.5	<2.5
CSST	Max climatological SST (°C)	Levitus SST	<21.0	<21.0	<21.0
VSHEAR	200–850-hPa vertical shear ($m\ s^{-1}$)	NCEP	>25.2	>15.9	>19.5
CIRC	850-hPa circulation ($m\ s^{-1}$)	NCEP	<−1.5	<−1.2	<−0.9
THDEV	Vertical instability (°C)	NCEP	<−2.6	<−3.0	<1.6
HDIV	850-hPa horizontal divergence ($\times 10^{-5}\ s^{-1}$)	NCEP	>1.0	>0.7	>0.5
PCCOLD	Cold pixel count (%)	SAT WV	<2.8	<5.0	<3.0
BTWARM	Avg cloud-cleared brightness temperature (°C)	SAT WV	>−25.4	>−23.1	>−27.8

The formation probability is calculated by a three-step algorithm.

1. Input parameter values exceed predetermined thresholds are screened out
2. Compute the linear discriminant function value from the input parameters at each grid point.
3. Determine the probability of TC formation based on the statistically-derived relationship between the linear discriminant function value and the corresponding past TC formation frequecy.

Schumacher, A. B., M. DeMaria, J. A. Knaff, 2009: Objective Estimation of 24-h Probability of Tropical Cyclone Formation. *Wea. Forecasting*, **24**, 456-471

Tropical Cyclone Formation Forecast: Statistical Method

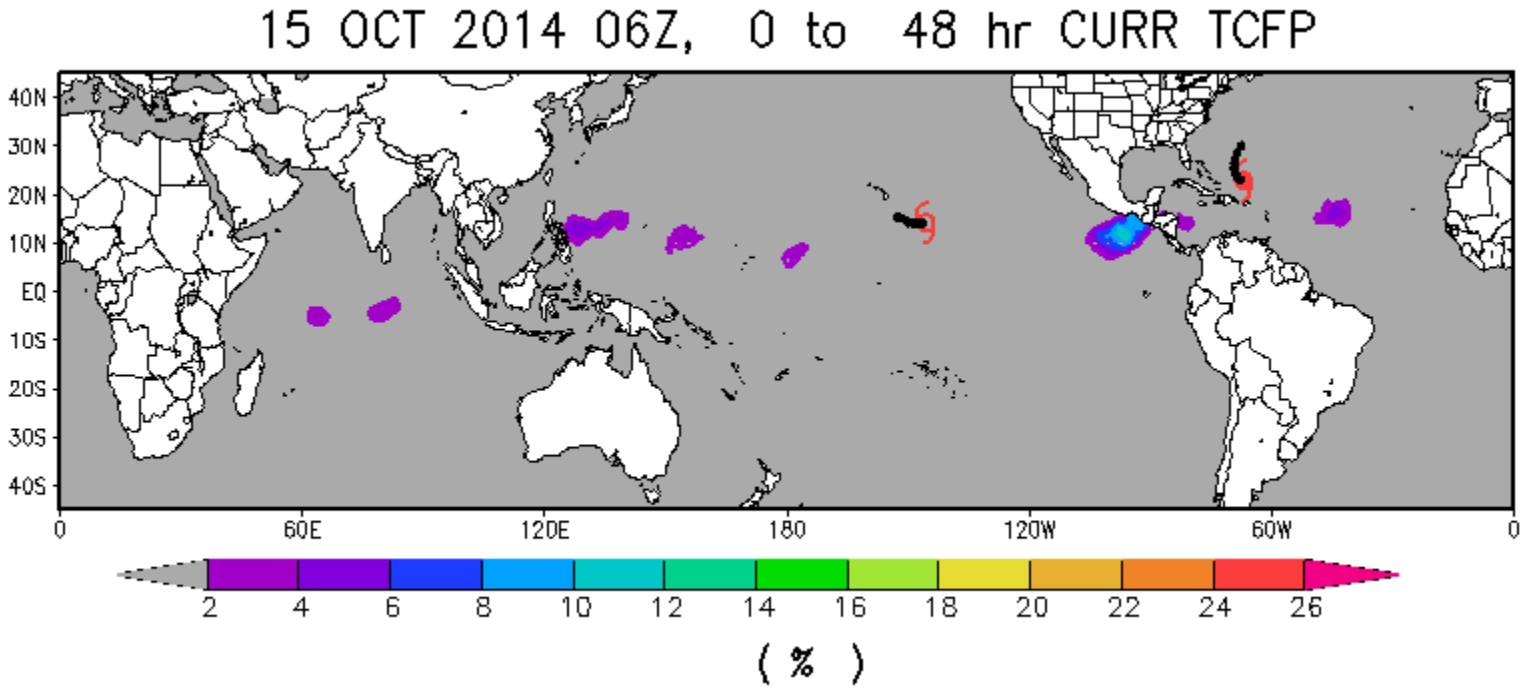

www.ssd.noaa.gov/PS/TROP/TCFP/index.html

Influence of large-scale variability

- TC activities depend on environmental parameters (e.g., SST, relative humidity, low-level vorticity, vertical wind shear).

- If there are temporal or spatial changes induced by the large-scale variability such as El Nino/Southern Oscillation (ENSO), Madden-Julian Oscillation (MJO), the thermodynamic and dynamic parameters in the TC regions can be modified. These modifications, in turn, alter TC activity.

El Niño-Southern Oscillation (ENSO)

El Niño (Warm Phase)

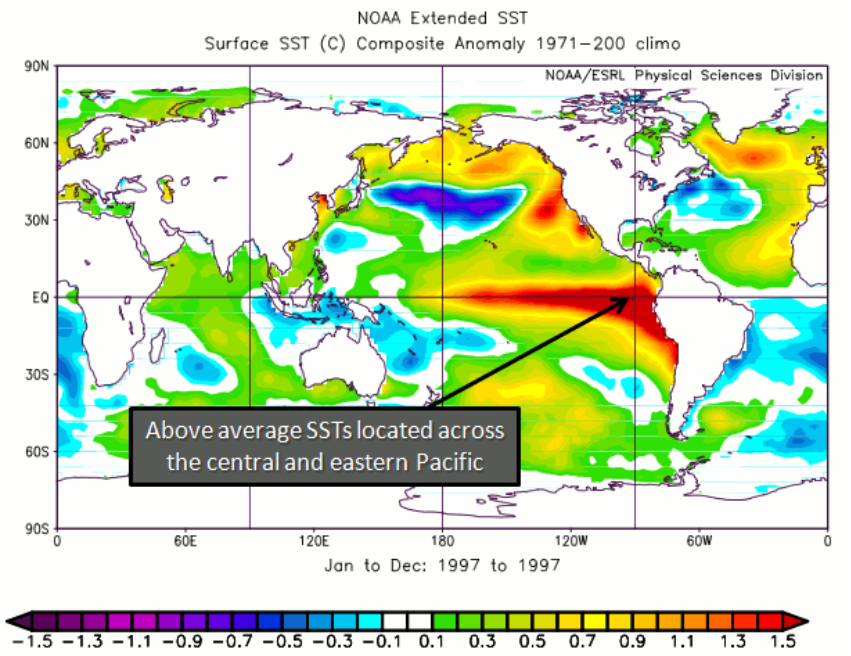

La Niña (Cold Phase)

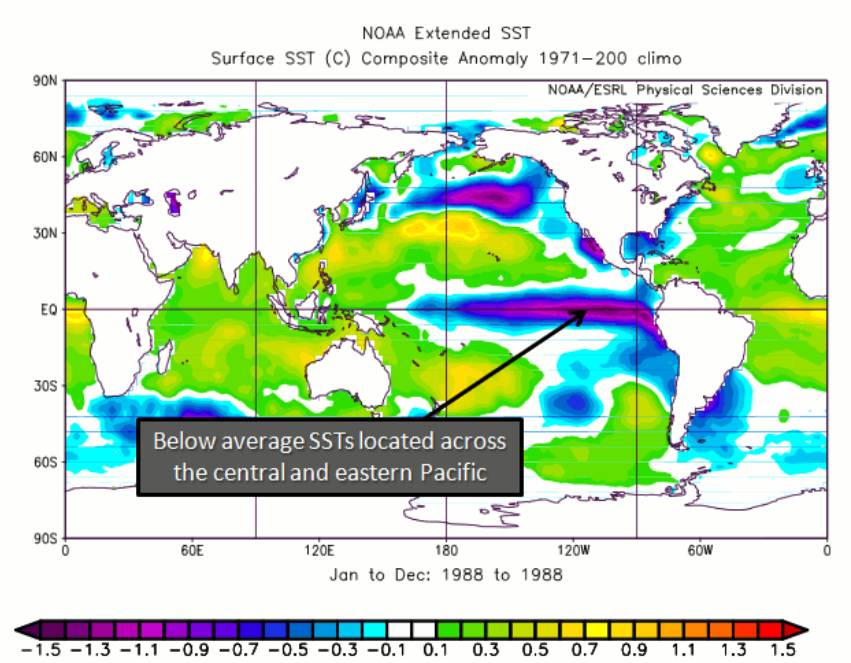

ENSO effect : North Atlantic

La Niña contributes to fewer eastern Pacific hurricanes and more Atlantic hurricanes.

La Niña produces lower vertical wind shear over the Main Development Region (MDR).

There tend to be more Atlantic hurricanes during La Niña because of this expanded area of low vertical wind shear.

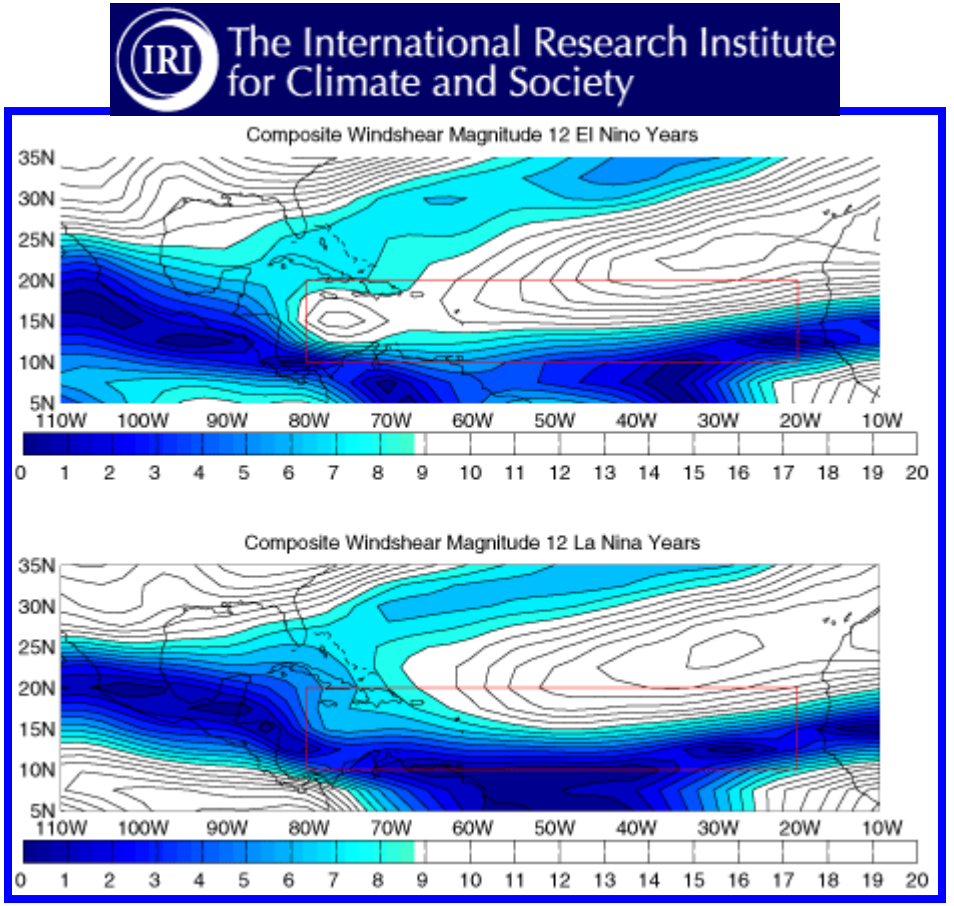

Wind shear magnitudes larger than 7.5-10m/s in the MDR region are unfavorable for hurricane development

ENSO effect : North Atlantic

A more southerly track for hurricanes is favored during ENSO neutral and El Nino phases

A significant increase in landfall frequency occurs during La Nina phase as compared to neutral ENSO.

Probability of two or more North Atlantic hurricanes making landfall along the U.S. coastline to be 28% during El Niño, 48% during the neutral phase, and 66% during La Niña.

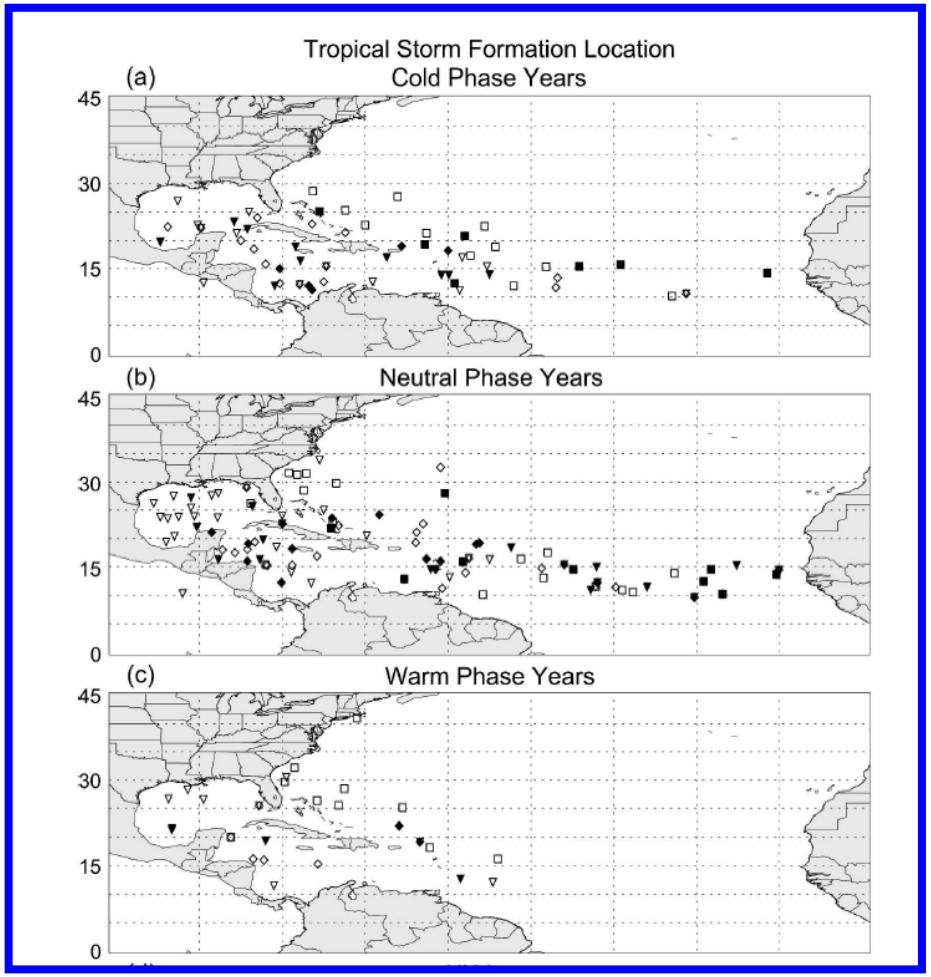

Shawn R. Smith, Justin Brolley, James J. O'Brien, and Carissa A. Tartaglione, 2007: ENSO's Impact on Regional U.S. Hurricane Activity. *J. Climate*,**20**, 1404–1414.

ENSO effect : Western North Pacific

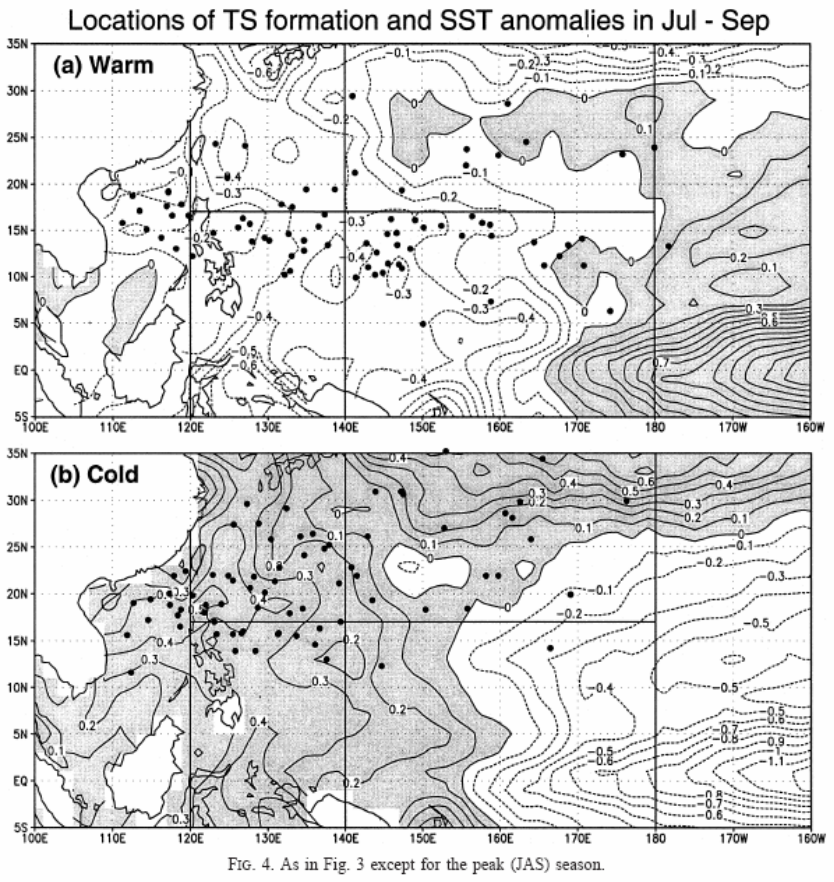

FIG. 4. As in Fig. 3 except for the peak (JAS) season.

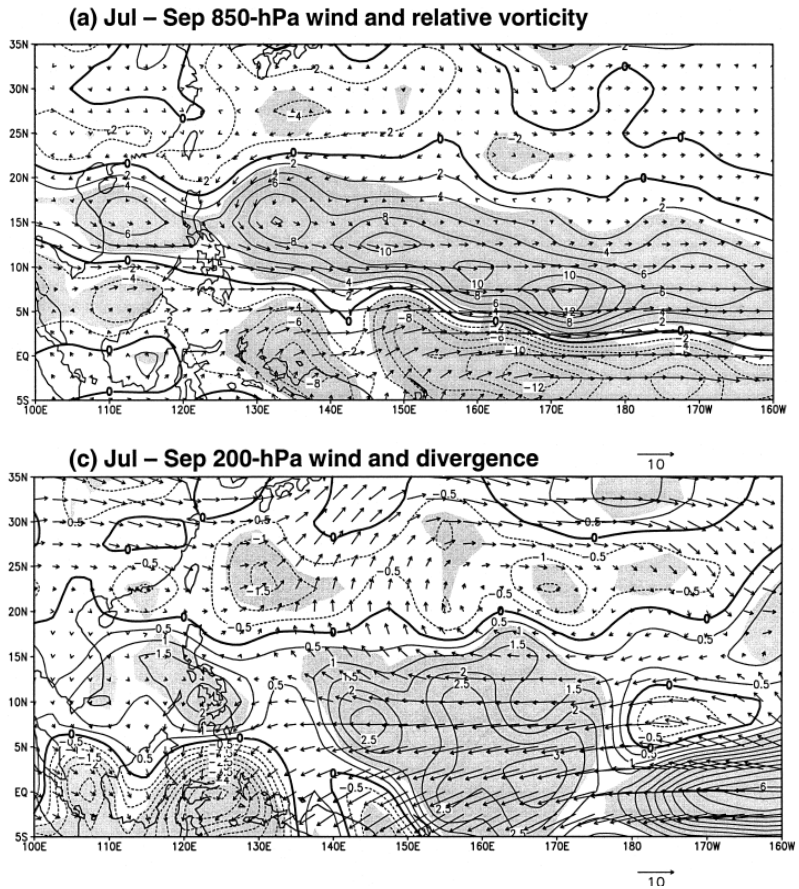

Wang and Chan (2002)

ENSO effect : Western North Pacific

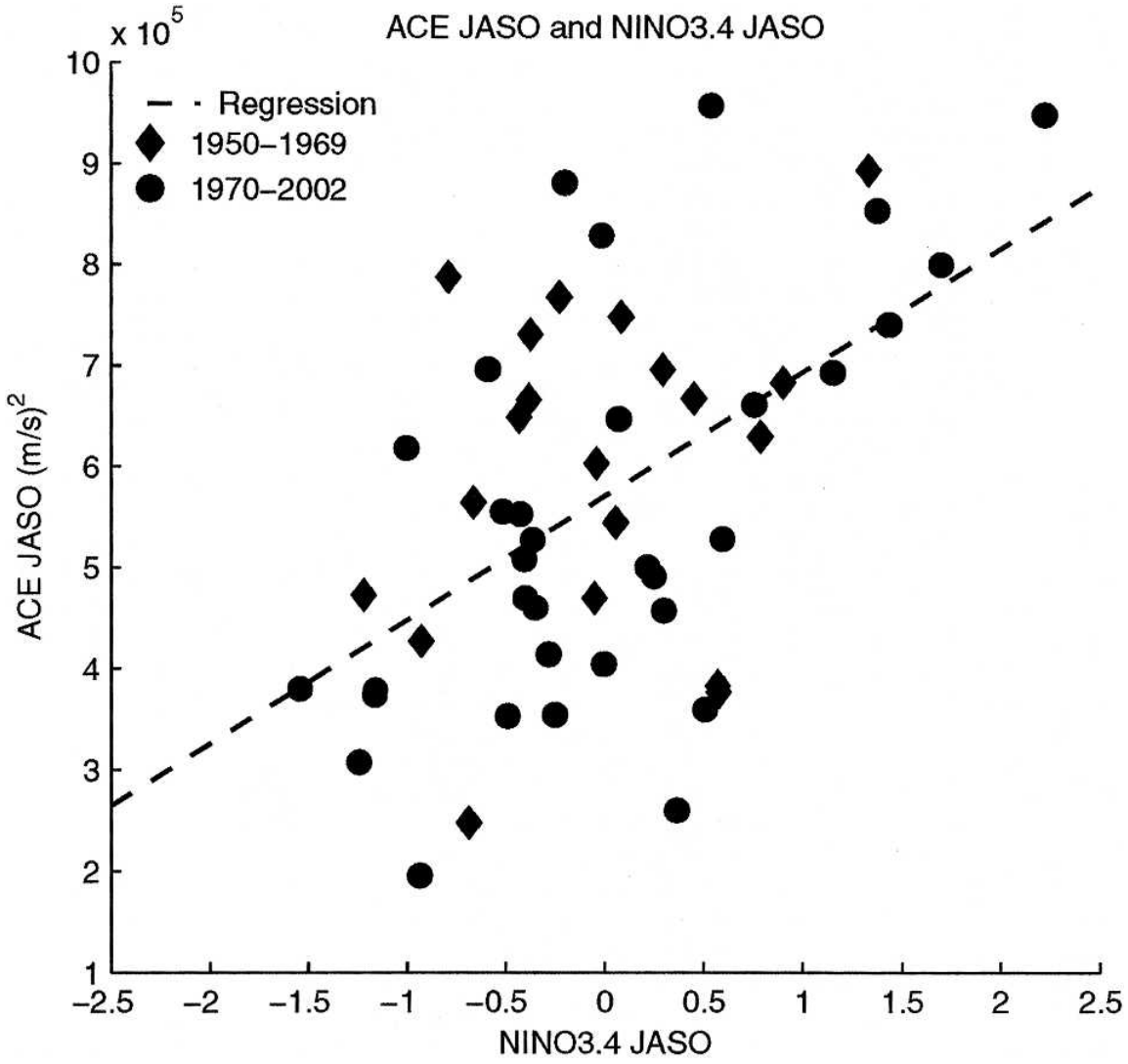

During El Nino, TC intensity in WNP become stronger

Scatterplot of ACE (m s2) and Niño-3.4 (°C) for JASO in the period 1950–2002; the dashed line is the linear regression (Camargo and Sobel 2005)

ENSO effect : Southern Hemisphere

El Nino

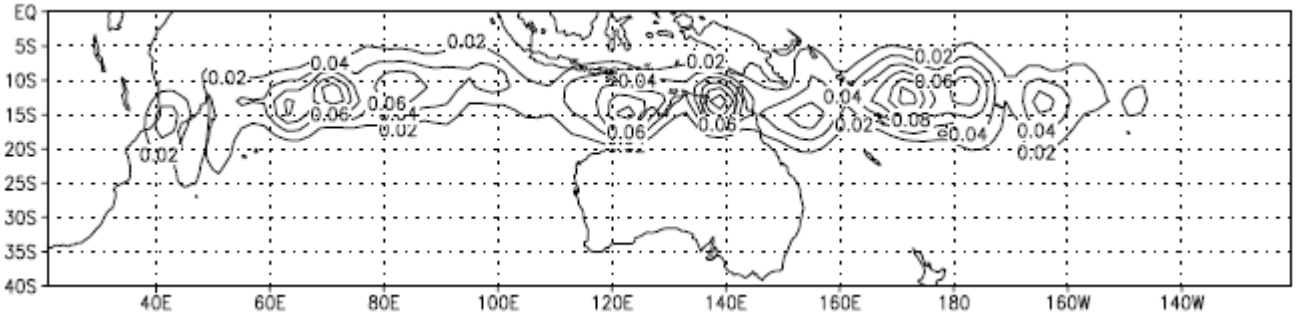

La Niña

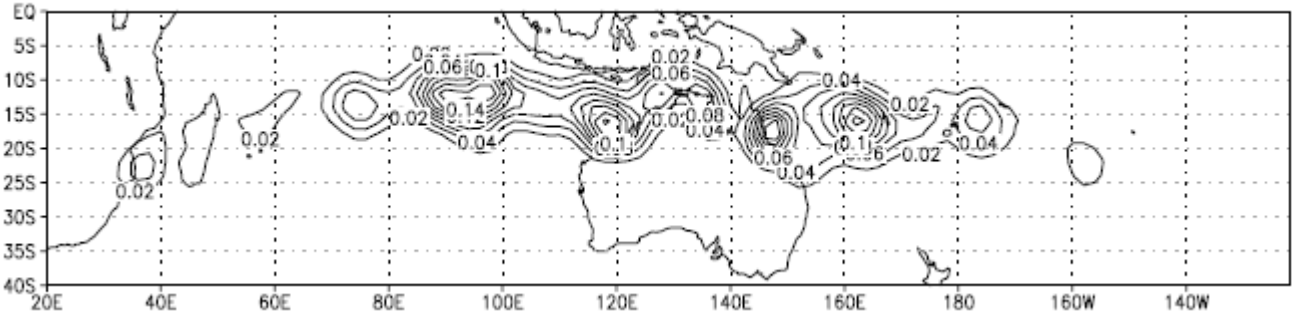

- The TC climatology for El Nino and La Nina years shows a geographical shift in the positions of maxima of TC occurrences in the SH.
- In the SIO, TC occurrences in El Nino (La Nina) years in the area between the east African coast and 75E (between around 75E and 135E) are higher than in La Nina (El Nino) years.
- In the SPO, TC occurrences in El Nino (La Nina) years in the area east of around 170E (between around 140E and 170E) are higher than in La Nina (El Nino) years

Seasonal Prediction of Tropical Cyclone Activity

- Statistical Method
  - Based on the empirical relationship between TC activity and large-scale environments
  - Using time-lagged relationship
  - Cheap
  - Relatively high predictability
- Dynamical Method
  - Using high resolution dynamical model that can resolve tropical cyclones.
  - Expensive
  - Recently, the predictability become comparable to statistical prediction.
- Hybrid Method
  - Combine statistical and dynamical methods.
  - Dynamical model predicts large-scale environments and statistical model predicts TC activity based on the simultaneous relationship between observed TC activity and large-scale environments predicted by dynamical model.
  - Low resolution model can be utilized

Statistical seasonal TC prediction: Example

Seasonal forecasting of typhoons affecting the East Asia

- Typhoons passing through the East China Sea
  - **The TCs striking East Asian countries (Korea, China, and Japan) normally pass over the East China Sea during typhoon season**

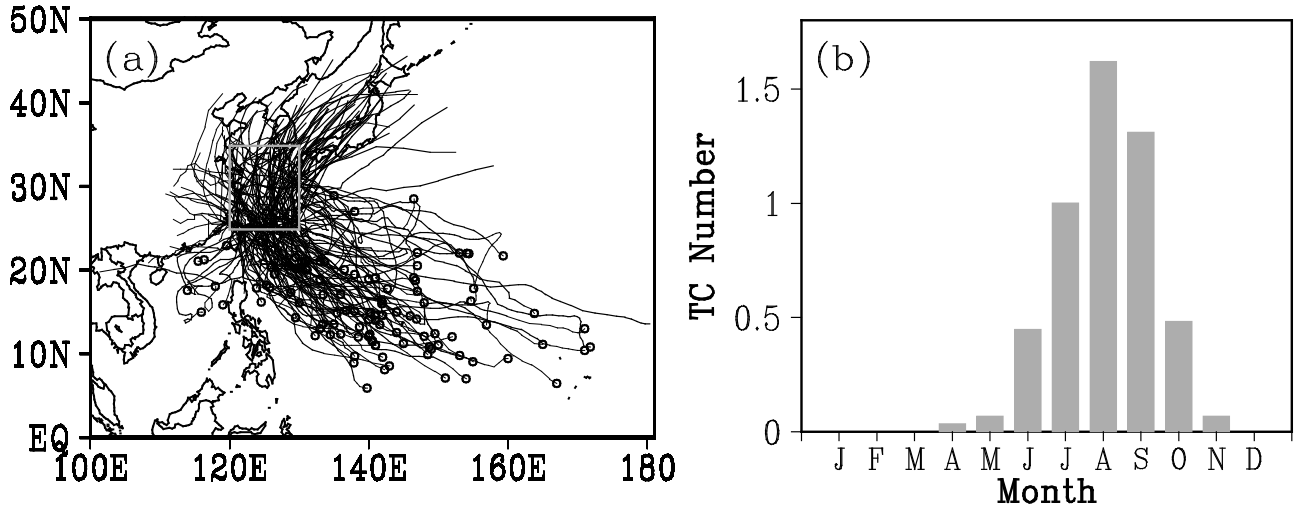

Predictand and Predictors

- **Predictand: the number of TCs passing over the East China Sea during July, August, and September.**

- **Predictors: time-lagged correlated large-scale environments**
  - Lag-correlation analysis for the large-scale environmental parameters, such as the sea surface temperature (SST), sea level pressure (SLP), outgoing longwave radiation (OLR), 850-hPa relative vorticity, and 850-hPa zonal wind during the preceding months.
  - Predictor analysis is performed for the first 25 years (1979–2003)
  - The last 4 years (2004–2007) are reserved as a period independent from the predictor analysis

- **Data**
  - TC : Regional Specialized Meteorological Centre - Tyoko
  - SLP, Wind, vorticity : NCEP/DOE reanalysis-2
  - SST, OLR : National Oceanic and Atmospheric Administration-Climate Diagnostic Center.

Predictors : pre-seasonal environments

Time-lagged correlations between preseason environmental parameters and the predictor

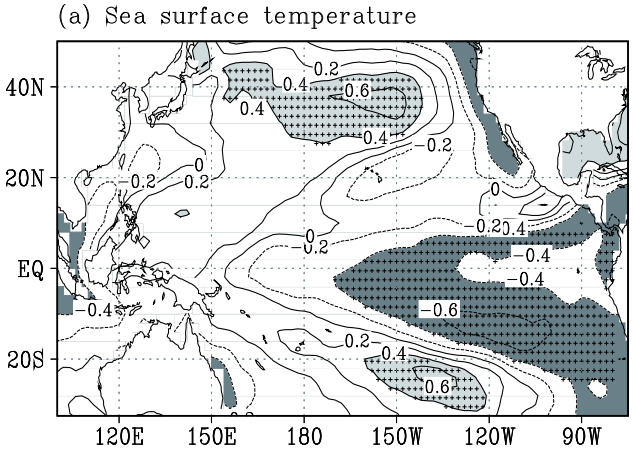

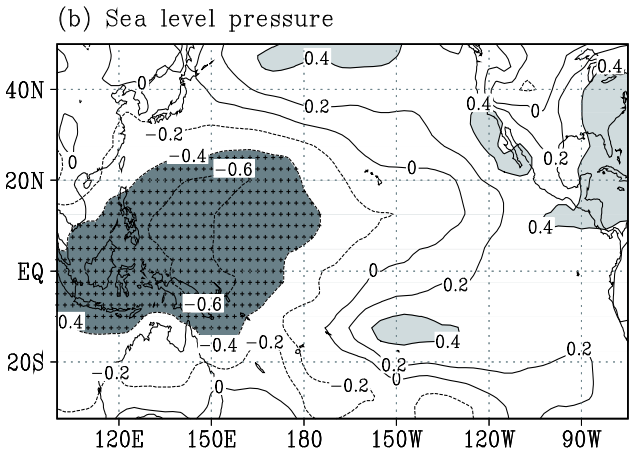

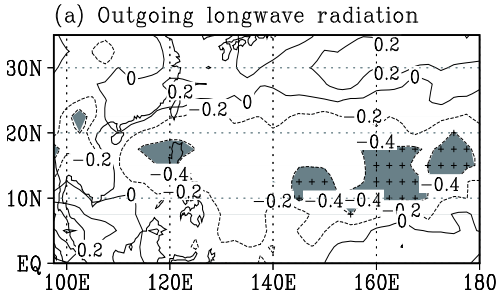

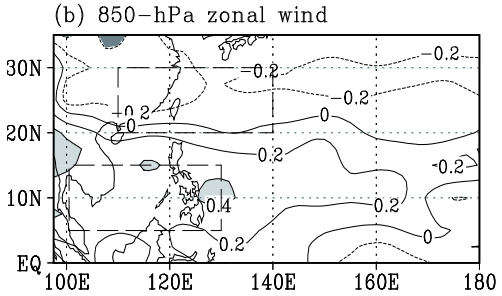

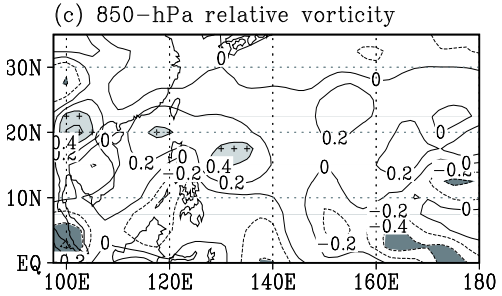

Predictor analysis period is the first 25 years (1979–2003).
The last 4 years (2004–2007) are reserved as an independent period.

Screening predictors

- The inclusion of many potential predictors in the multivariate regression model does not ensure better predictability, even if all of them are dynamically relevant predictors.
- Blindly combining all of the predictors in a regression setting may lead to poor prediction (Wilks, 2006).
- Therefore, a best set of predictors is selected from the pool of potential predictors by stepwise regression.
- SST, 850-hPa relative vorticity, and OLR are selected as the set of predictors for the statistical models to forecast the summertime TC frequency over the East China Sea.

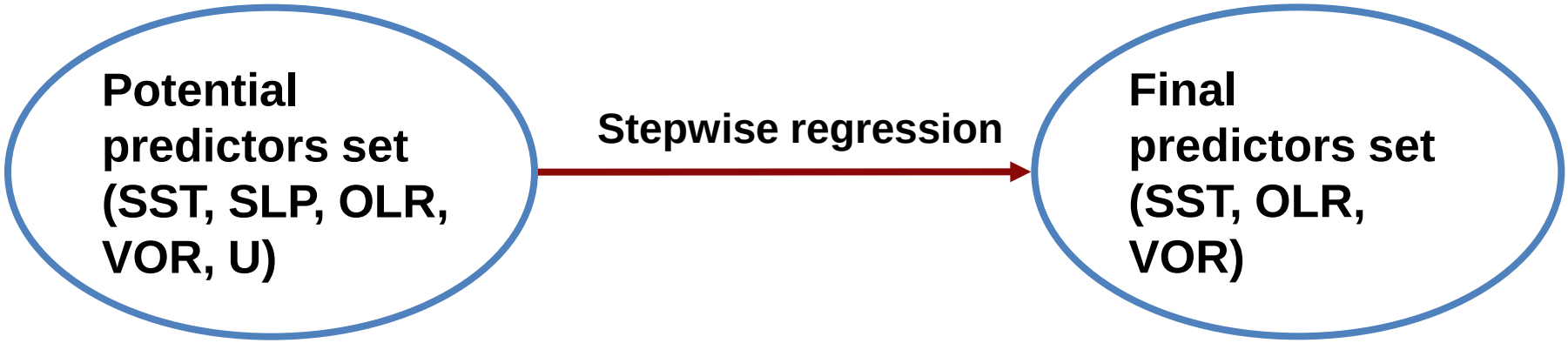

Predictor Screening

Table I. Sum of absolute errors (SAE), R-square (R^2) and regression coefficients (a) in each stage of stepwise LAD regression..

		SST	Sea level pressure (SLP)	OLR	850-hPa zonal wind (U850)	850-hPa relative vorticity (VOR)
1st step	SAE	22.17	27.11	27.45	30.92	23.34
one predictor	R^2	0.53	0.36	0.37	0.17	0.52
	a	$a_{SST} = 1.23$	$a_{SLP} = -1.01$	$a_{OLR} = -0.95$	$a_{U850} = 0.89$	$a_{VOR} = 1.37$
2nd step	SAE		21.11	21.31	21.72	19.27
Two predictors	R^2		0.54	0.55	0.54	0.63
Including SST	a		$a_{SST} = 0.73$ $a_{SLP} = 0.56^*$	$a_{SST} = 0.99$ $a_{OLR} = -0.32$	$a_{SST} = 1.04$ $a_{U850} = 0.30$	$a_{SST} = 0.82$ $a_{VOR} = 0.56$
3rd step	SAE		18.03	17.94	18.18	
Three predictors	R^2		0.65	0.66	0.64	
Including SST and VOR	a		$a_{SST} = 1.14$ $a_{VOR} = 1.00$ $a_{SLP} = 0.62^*$	$a_{SST} = 0.75$ $a_{VOR} = 0.57$ $a_{OLR} = -0.12$	$a_{SST} = 0.57$ $a_{VOR} = 1.22$ $a_{U850} = -0.54^*$	
4th step	SAE		17.78		17.45	
Four predictors	R^2		0.67		0.67	
Including SST, VOR and OLR	a		$a_{SST} = 0.92$ $a_{VOR} = 0.79$ $a_{OLR} = -0.26$ $a_{SLP} = 0.48^*$		$a_{SST} = 0.54$ $a_{VOR} = 1.23$ $a_{OLR} = -0.02$ $a_{U850} = -0.53^*$	

The asterisk (*) denotes that the regression coefficient has an inconsistency in the sign of a correlation coefficient between the predictor and the predictand.

Statistical prediction methods

- **Least absolute deviation (LAD) regression model**
  - –The LAD regression is less sensitive to extreme values and more statistically stable than the least square error regression.
  - –The LAD model is widely used for the statistical prediction of the seasonal TC activity (e.g., Gray et al., 1992, 1993, 1994; Chu et al., 2007).

- **Poisson regression model**
  - –Poisson mode is more suitable for the prediction of TC occurrences because Poisson distribution restricts the possible outcomes to nonnegative integer. (Elsner and Schertmann, 1993; McConnell and Holbrook, 2004).

- **Bayesian regression model**
  - –Bayesian analysis is an efficient way to provide a coherent and rational framework for reducing uncertainties.
  - –Probability prediction is possible by Bayesian model.
  - –This work adopt the Bayesian algorithm developed by Chu and Zhao (2007)
  - –Elsner and Jagger (2004, 2006), Chu and Zhao (2007)

Statistical prediction method

$$Y_{obs}(t) = F[X_m(t)]$$ ***for training period***

Develop the statistical model using observed data

$$\Downarrow$$

$$Y_{fcst}(T) = F[X_m(T)]$$ ***for prediction year***

Y : **predictand** (*seasonal typhoon frequency in each cluster*)

X_m : **predictors from pre-seasonal environment**

F : **statistical model** (*Poisson, LAD, Baysian etc*)

t : **training years** (*1981–2003*)

T : **prediction year (2004-2007)**

Results

- **Leave-one-out cross validation for 1979-2003 (predictor analysis period)**
- **Prediction for 2004-2007 (independent period)**

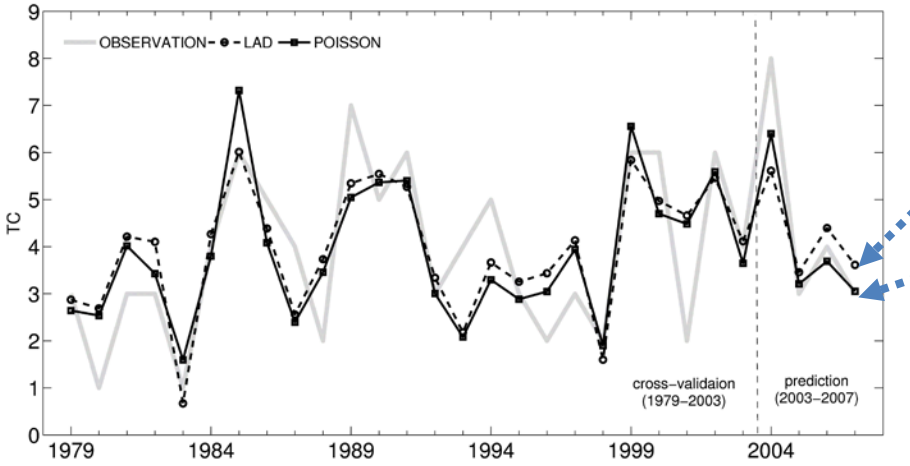

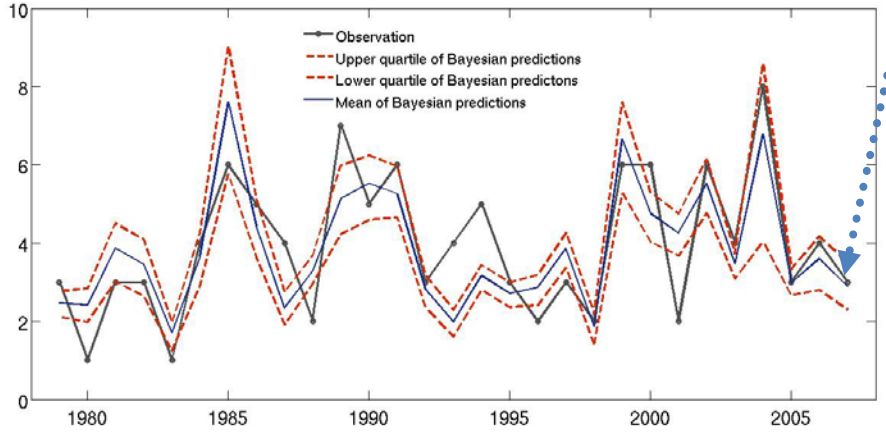

	RMSE	Correlation	MSSS
LAD	1.15	0.75	0.60
Poisson	1.11	0.78	0.63
Bayesian	1.10	0.78	0.65

※Mean Square Skill Score (MSSS) is defined as a ratio of the reduction in the mean square error of the predictions of the models compare to the reference forecasts based on the climatology value (WMO 2002)

Dynamical seasonal TC prediction: Example

Geophysical Fluid Dynamics Laboratory High-Resolution Atmospheric Model (HiRAM) at 25-km resolution

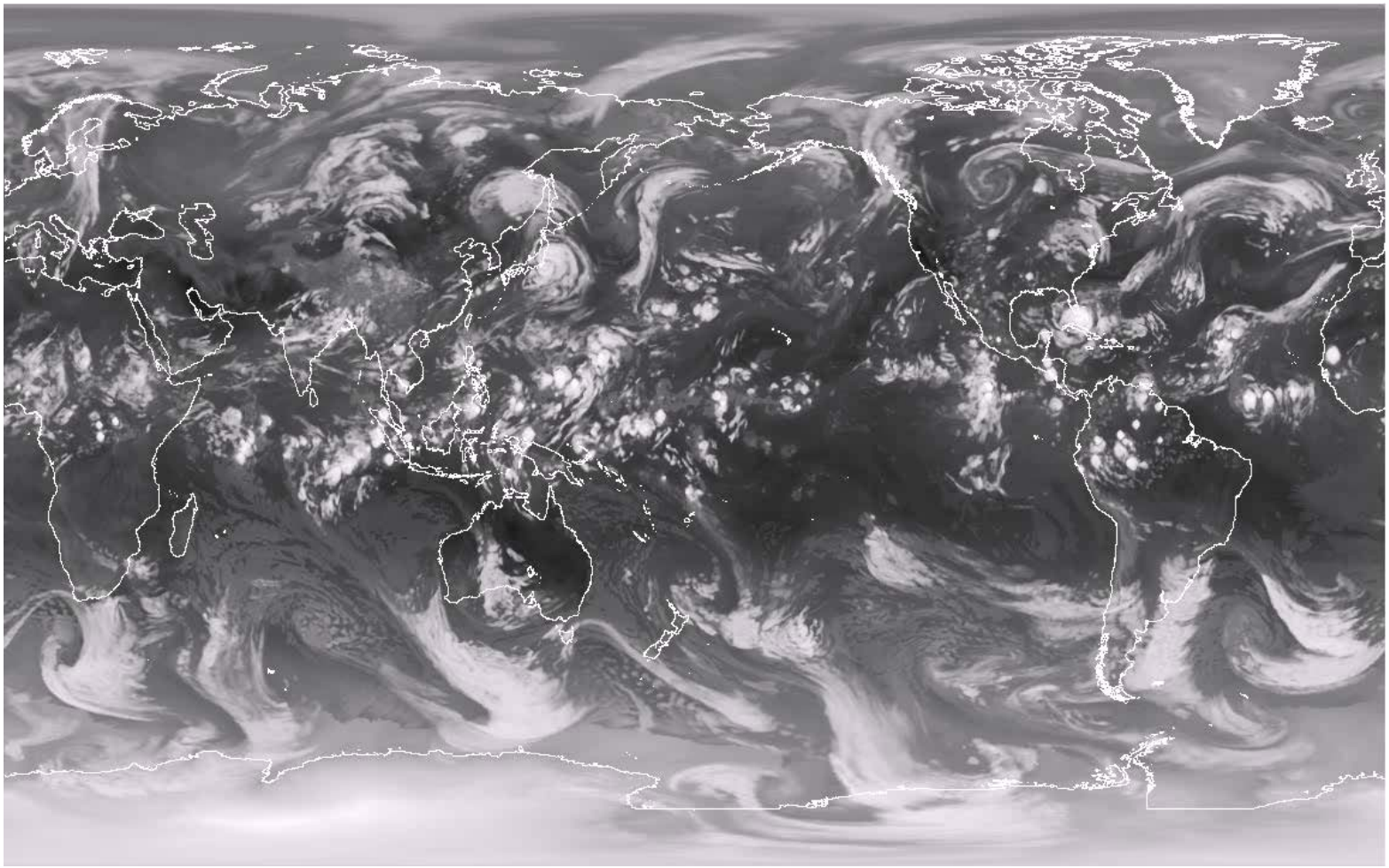

Dynamical seasonal TC prediction: Example

Geophysical Fluid Dynamics Laboratory High-Resolution Atmospheric Model (HiRAM) at 25-km resolution

Prediction from July 1

High predictability in North Atlantic

Low predictability in Western Pacific

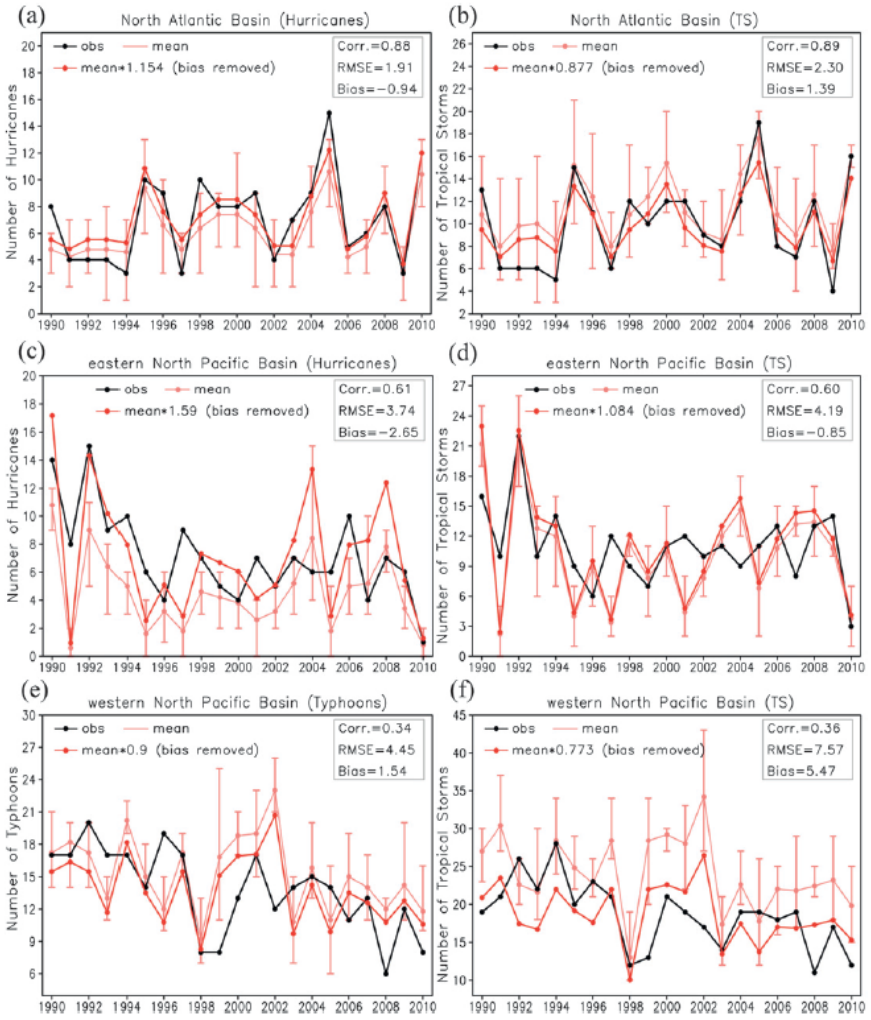

Hybrid prediction method

$$Y_{obs}(t) = F[X_m(t)]$$ ***for training period***

Develop the statistical model using dynamical model forecast

$$\Downarrow$$

$$Y_{fcst}(T) = F[X_m(T)]$$ ***for prediction year***

Y : **predictand** (*seasonal typhoon frequency in each cluster*)

X_m : **predictors from dynamical forecasting model**

F : **statistical model** (*Poisson, LAD, Baysian etc*)

t : **training years**

T : **prediction year**

Hybrid Seasonal TC Prediction: Example

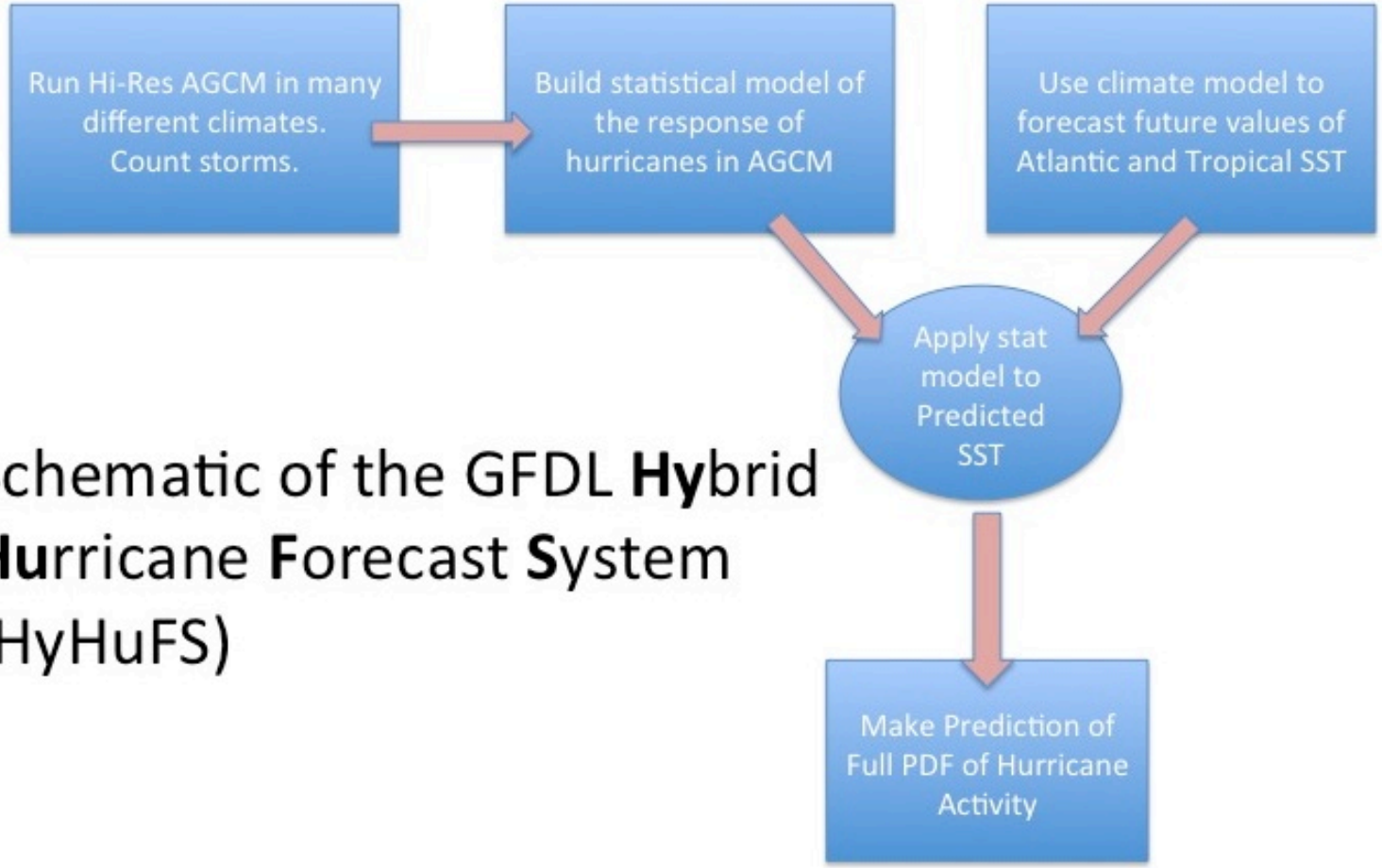

Schematic of the GFDL **Hy**brid **Hu**rricane **F**orecast **S**ystem (HyHuFS)

Hybrid Seasonal TC Prediction: Example

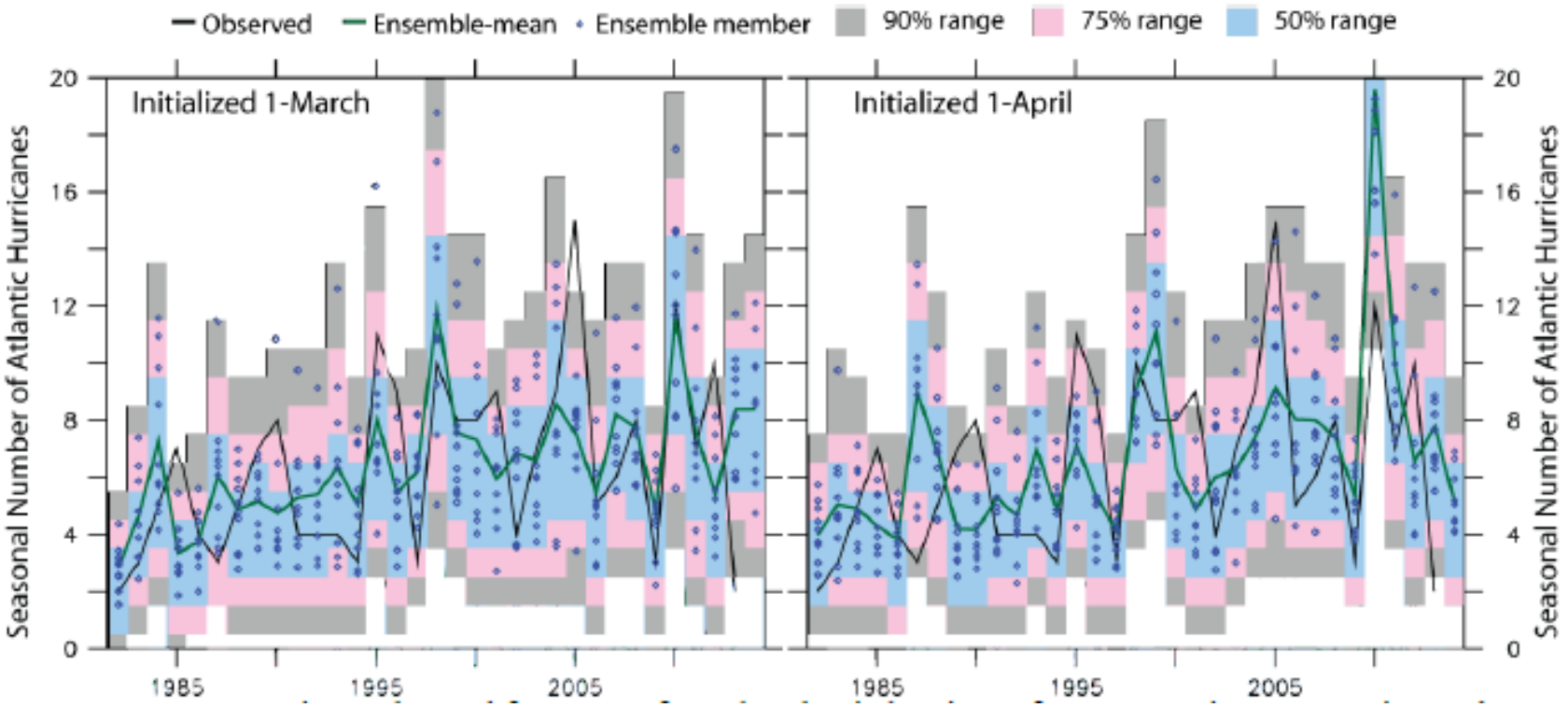

For Sub-seasonal Time Scale TC forecast

- The aforementioned TC forecast methods are developed for seasonal time scale (several months) TC prediction.

- For the sub-seasonal time scale (several weeks), similar methods (statistical, dynamical, hybrid) can be developed.

- One of main large-scale parameters affecting sub-seasonal time scale TC activity is Madden-Julian Oscillation (MJO) that is the dominant mode of intra-seasonal variability in the tropics.

- Thus, to develop and improve the predictability of sub-seasonal TC forecasting, the relationship between MJO and TC should be incorporated into TC forecasting models.

Madden Julian Oscillation (MJO)

The Madden and Julian Oscillation (MJO) is the dominant mode of intraseasonal variability (about 20-100 days) in the tropics with considerable convective precipitation systems propagating eastward from the Indian Ocean towards the West Pacific and decaying near the date line.

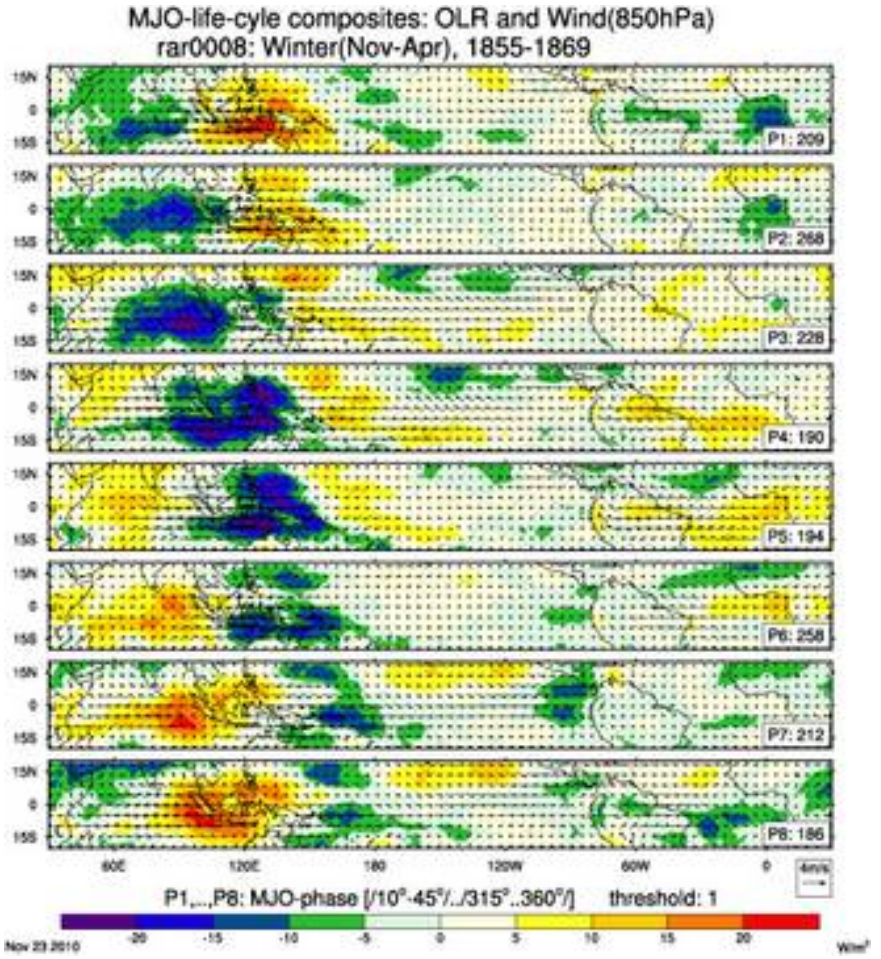

MJO Index

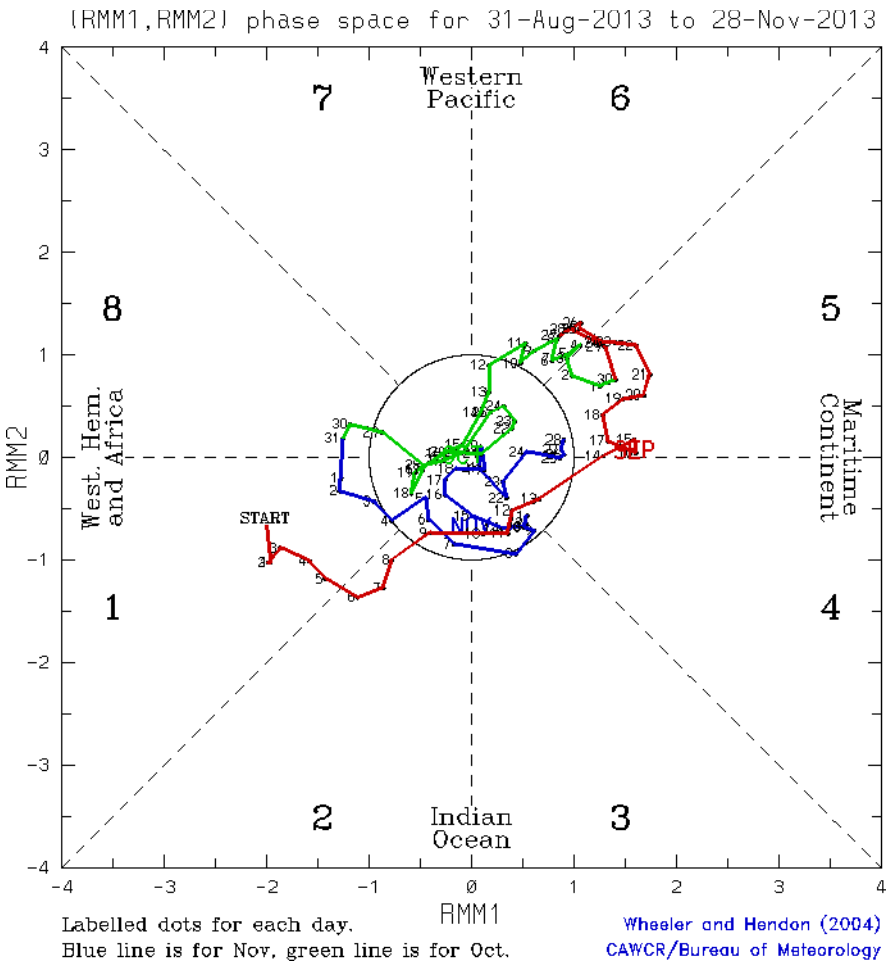

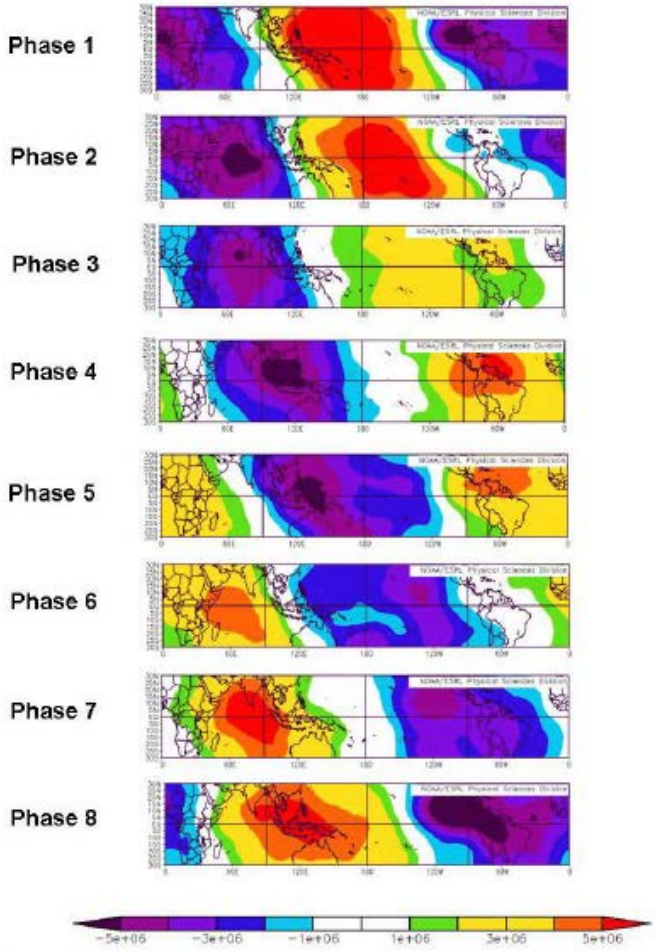

Fig. 1 200-mb velocity potential anomalies ($m^2 s^{-1}$) for the top 200 days for each MJO phase from July-October for each phase of the WH index. Cool colors indicate upper-level divergence while warm colors indicate upper-level convergence.

http://cawcr.gov.au/staff/mwheeler/maproom/RMM/

S2S Prediction and MJO

- Observations studies have shown that tropical storm activity is modulated by the Madden Julian Oscillation.

- Modelling studies have shown that the impact of the MJO on tropical cyclone activity can be simulated by numerical models.

- This suggests that sub-seasonal prediction of tropical storm is possible, and some operational centres are already issuing weekly outlooks of tropical cyclone activity, in addition to the medium-range and seasonal prediction of tropical storms.

Summer MJO life cycle

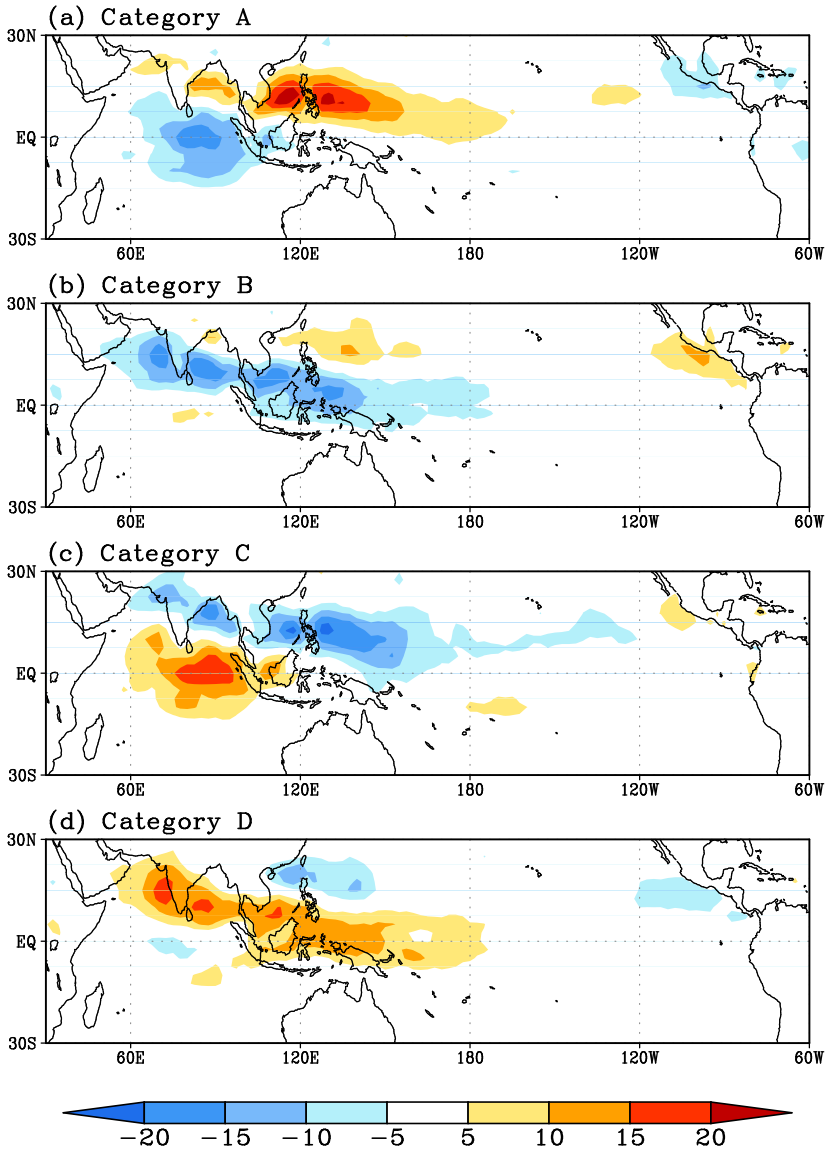

In the category A, the anomalous deep convection dominates in the tropical Indian Ocean.

In the category C, the anomalous deep convection dominates in western north Pacific (WNP)

The convection center propagates both eastward and northward.

MJO vs. TC genesis in WNP

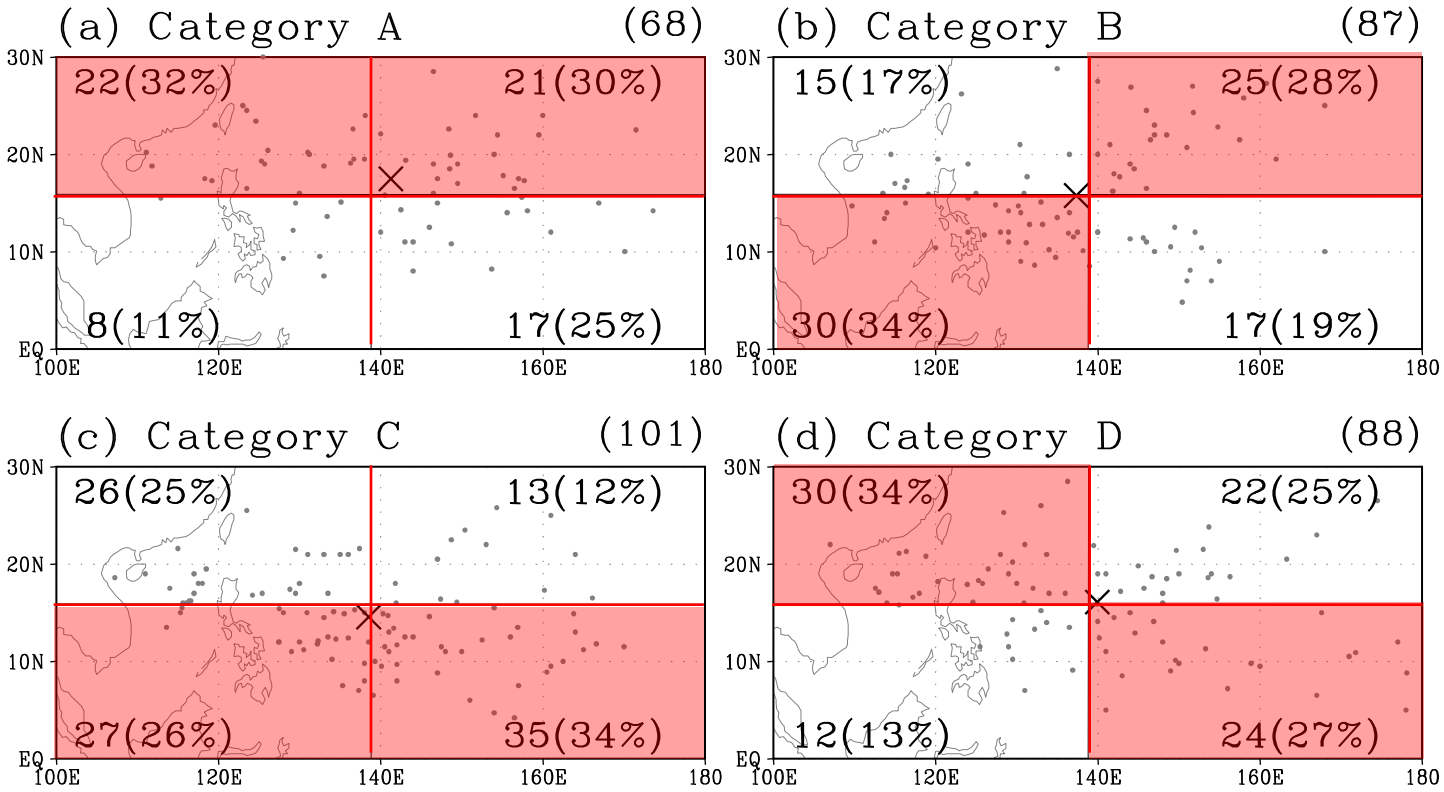

Typhoon genesis number increases from category A to C and decreases from C to A

Red shading region : the proportion of genesis > 25%

MJO vs. Dynamic parameters

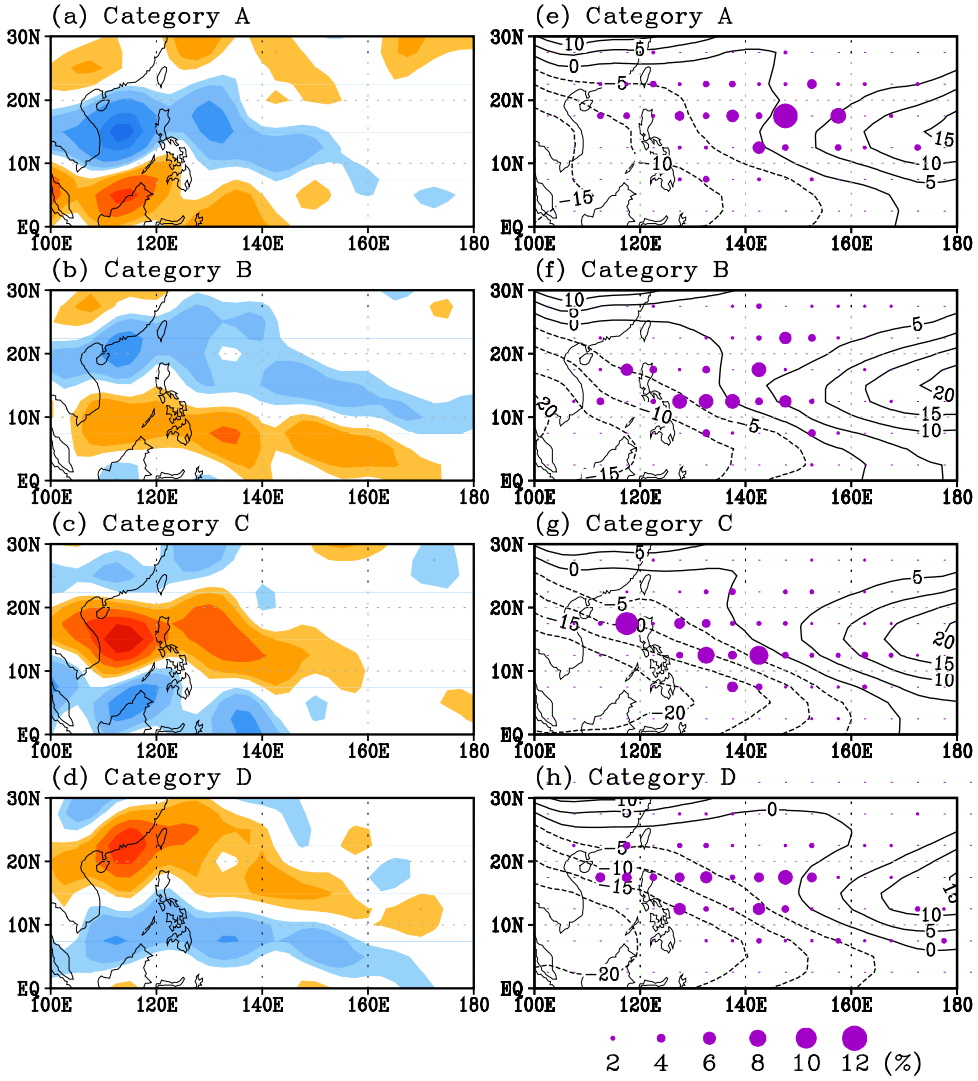

Left : 850-hPa vorticity anomaly
Right : zonal vertical wind shear (line)
typhoon genesis ratio (circle)

- **Positive low level vorticity anomaly in WNP activate typhoon genesis in the category C.**
- **Westward shift of the zero shear line results in slight southwestward shift of major typhoon genesis area.**

MJO vs. TC tracks in WNP

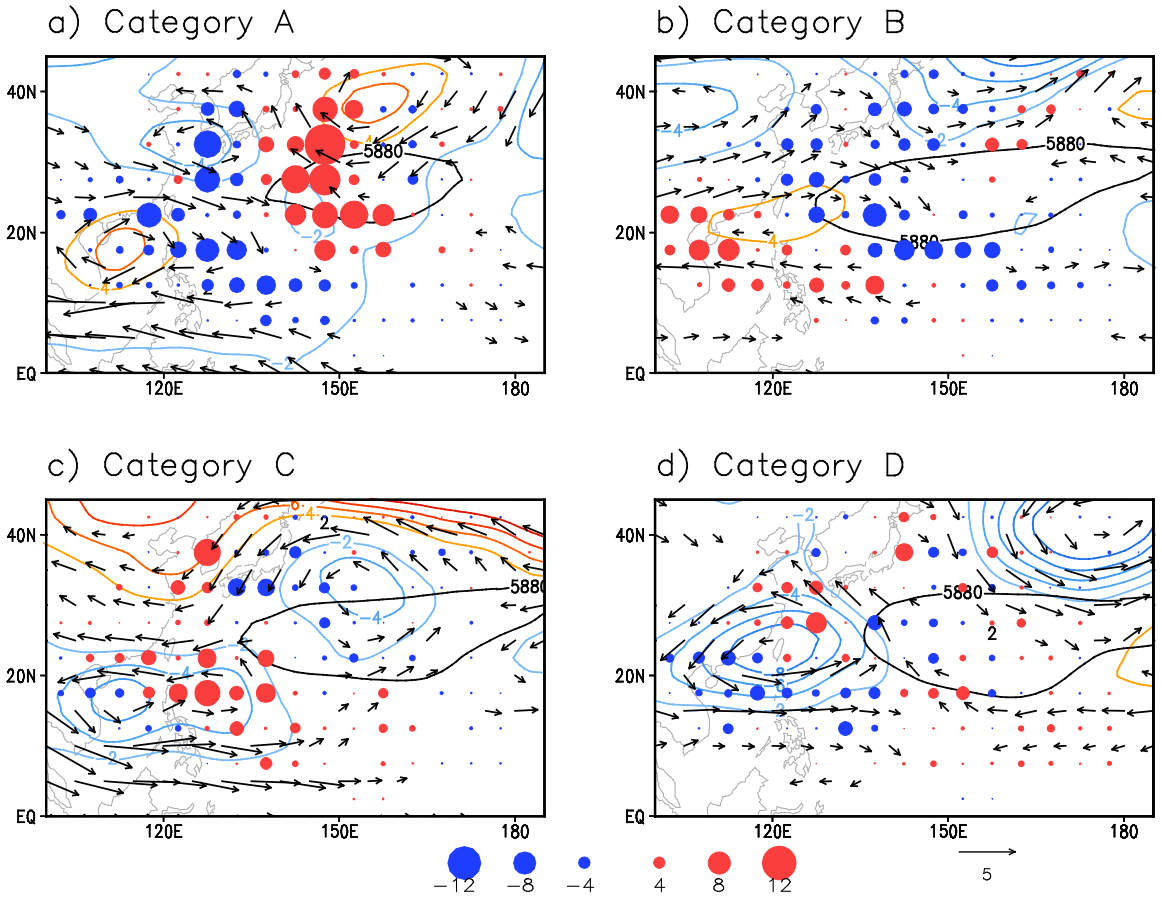

Anomaly map of steering flow (vector, m/s) 500-hpa GPH (contour) typhoon ratio (circle, %)

TC tracks in each MJO category depend on the systematic shift in the main genesis regions at a first-order. Also, they are affected by the prevailing large-scale steering flows in each MJO category

MJO and TC landfalls in WNP

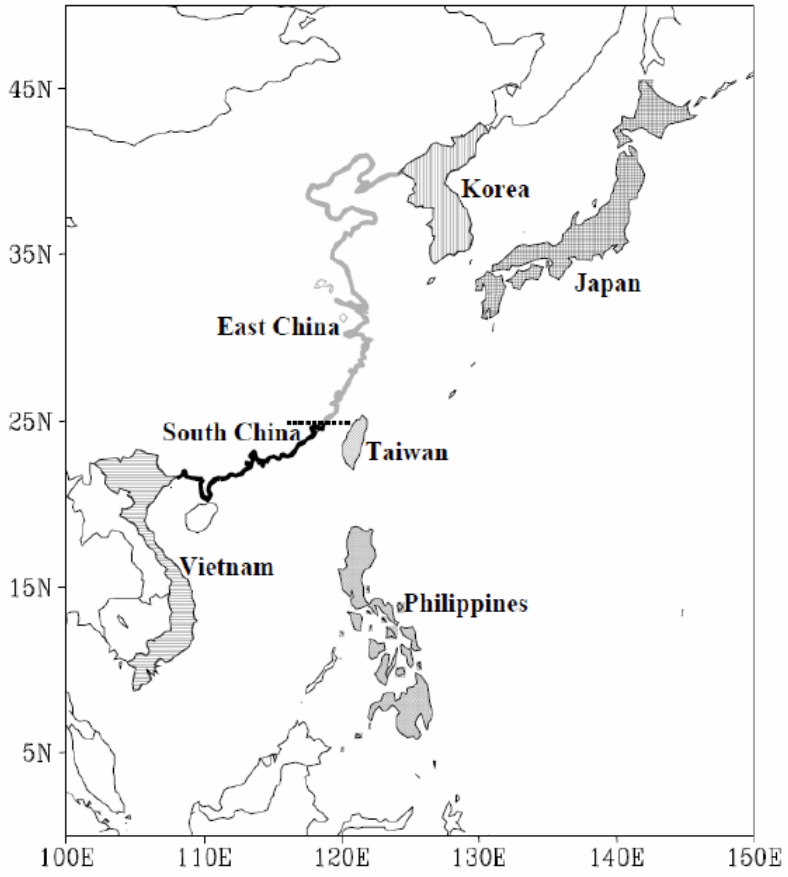

Category	A	B	C	D	NONE	Total
MJO day	722 (22.8)	702 (22.1)	719 (22.7)	658 (21.6)	334 (10.8)	3172 (100.0)
the Philippines	12 (1.7)	20 (2.8)	19 (2.6)	13 (1.9)	7 (2.0)	71 (2.2)
Vietnam	6 (0.8)	17** (2.4)	10 (1.4)	9 (1.3)	6 (1.7)	48 (1.5)
South China	11†† (1.5)	23 (3.3)	29* (4.0)	19 (2.8)	10 (2.9)	92 (2.9)
Taiwan	6 (0.8)	7 (1.0)	16* (1.3)	14 (2.0)	4 (1.2)	47 (1.5)
East China	10 (1.4)	7 (1.0)	9 (1.3)	14 (2.0)	1† (0.3)	41 (1.3)
Korea	2† (0.3)	1†† (0.1)	17** (2.4)	6 (0.9)	2 (0.6)	28 (0.9)
Japan	10 (1.4)	14 (2.0)	13 (1.8)	18 (2.6)	13** (3.8)	68 (2.1)

Schematics for influence of MJO

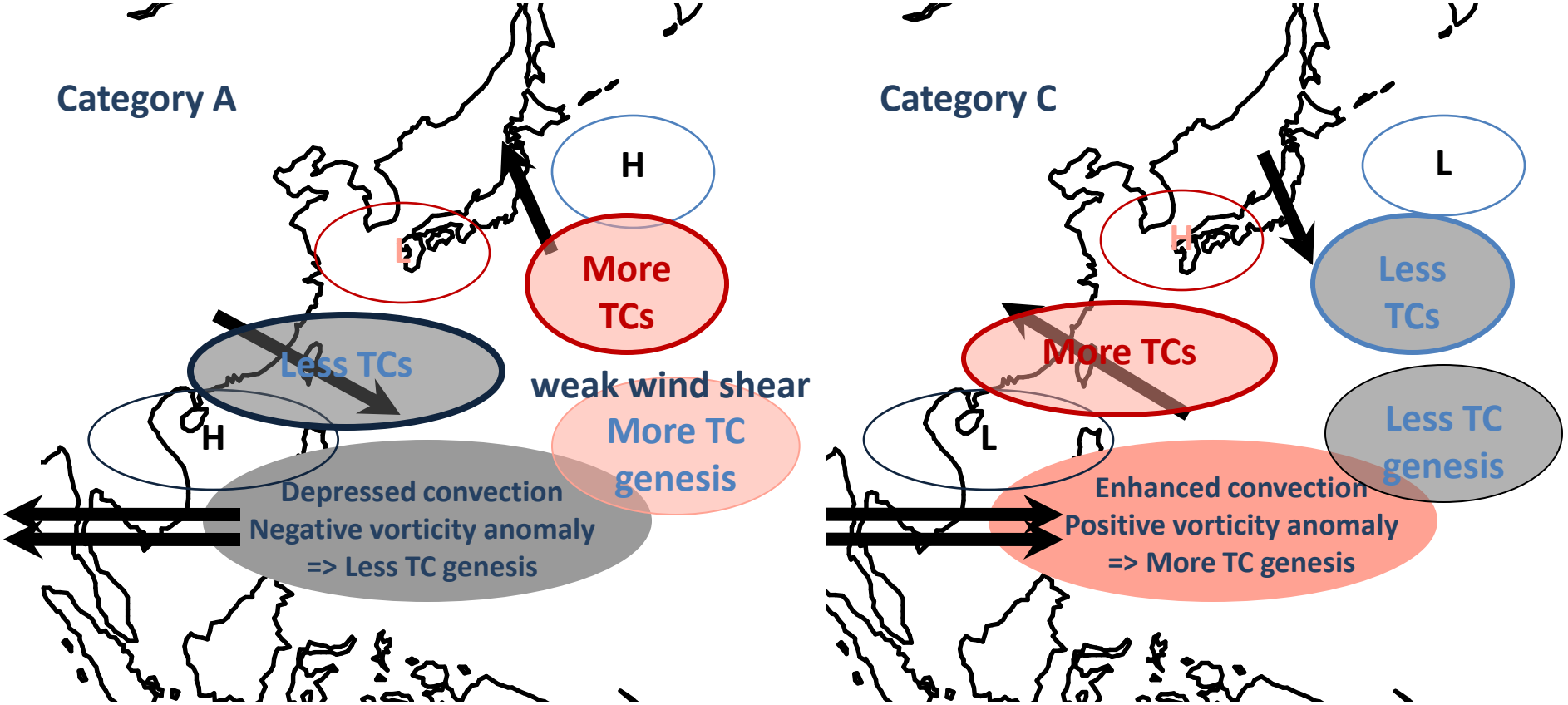

MJO and Atlantic Hurricane

Convection locates Indian Ocean

Convection locates Western Pacific

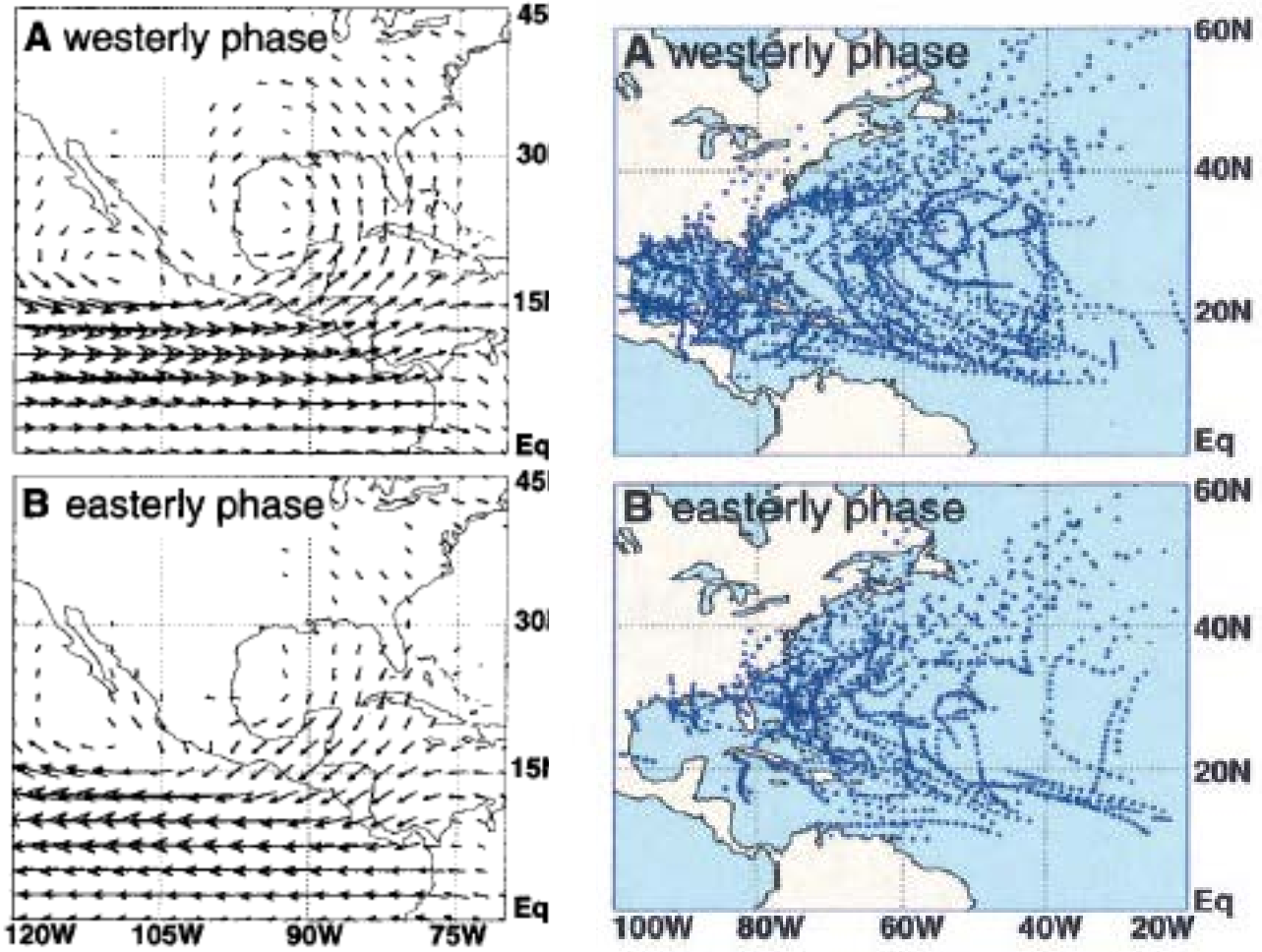

Maloney and Hartmann (2002)

MJO and Tropical Cyclone Activity in the Australian Region

850 hPa vorticity

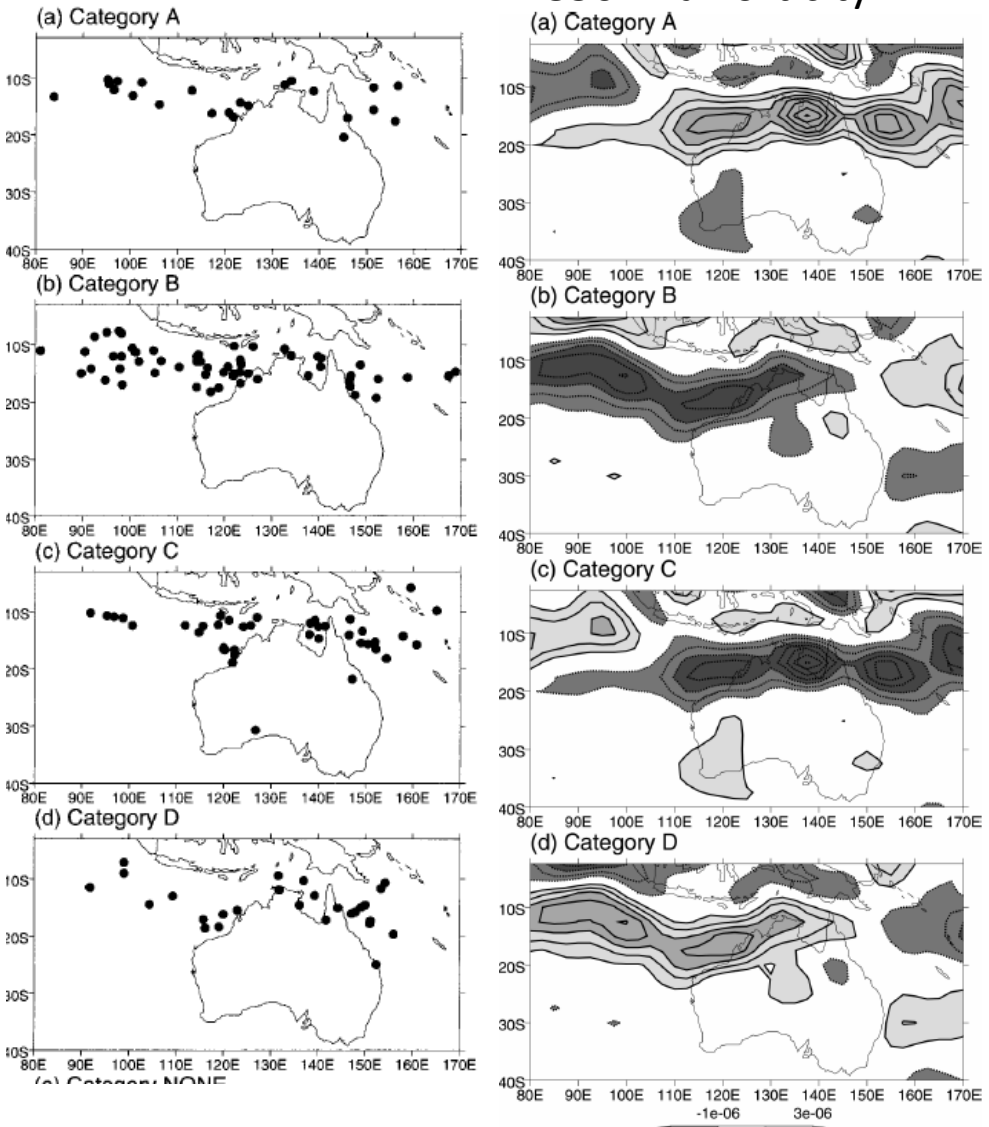

TABLE 1. Summary of tropical cyclone formation within each MJO category. Here, N denotes the number of days for which the MJO was in a particular category (this is shown in brackets as a percentage of the total number of days); N_{WEST} denotes the number of days on which a tropical cyclone formed in the western region (west of 135°E), within that MJO category (this is shown in brackets as a percentage daily genesis rate, i.e., $100 \times N_{WEST}/N$); and N_{EAST} is the corresponding statistic for the eastern region (east of 135°E). Categories where TC numbers were significantly above (below) average at the 90% and 95% significant levels are indicated by * and ** († and ‡), respectively.

MJO category	N	N_{WEST}	N_{EAST}
A	675 (17.5%)	16 (2.4%)†	7 (1.0%)
B	689 (17.8%)	44 (6.4%)**	15 (2.2%)
C	653 (16.9%)	20 (3.1%)	20 (3.1%)**
D	756 (19.6%)	12 (1.6%)‡	14 (1.9%)
NONE	1092 (28.2%)	50 (4.6%)	13 (1.2%)
Total	3865 (100%)	142 (3.7%)	70 (1.8%)

Hall et al (2001)

MJO and Tropical Cyclone Activity in the Fiji Region

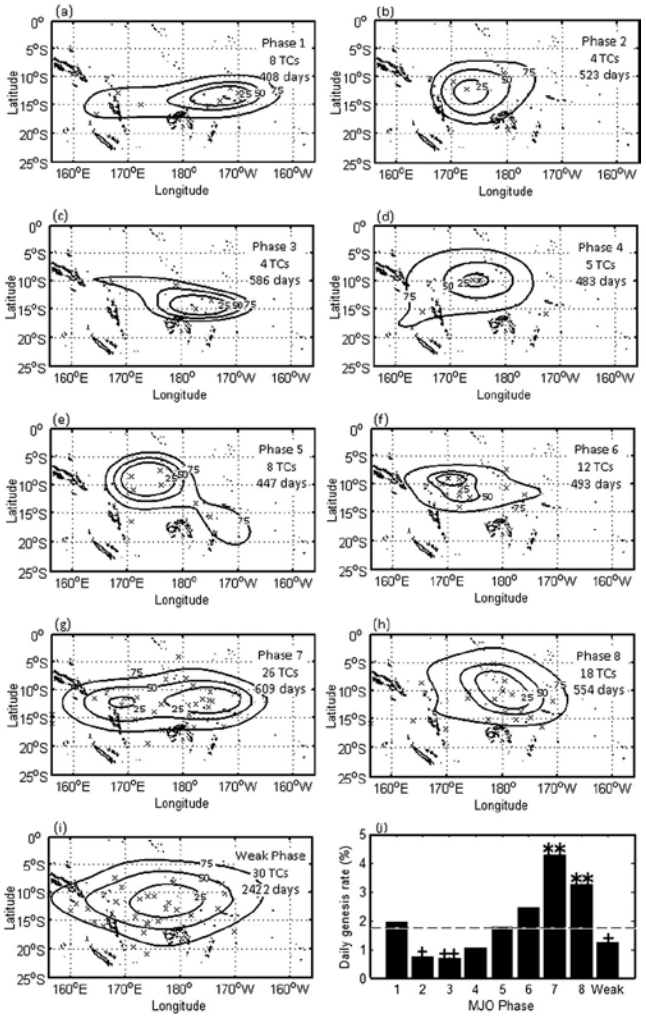

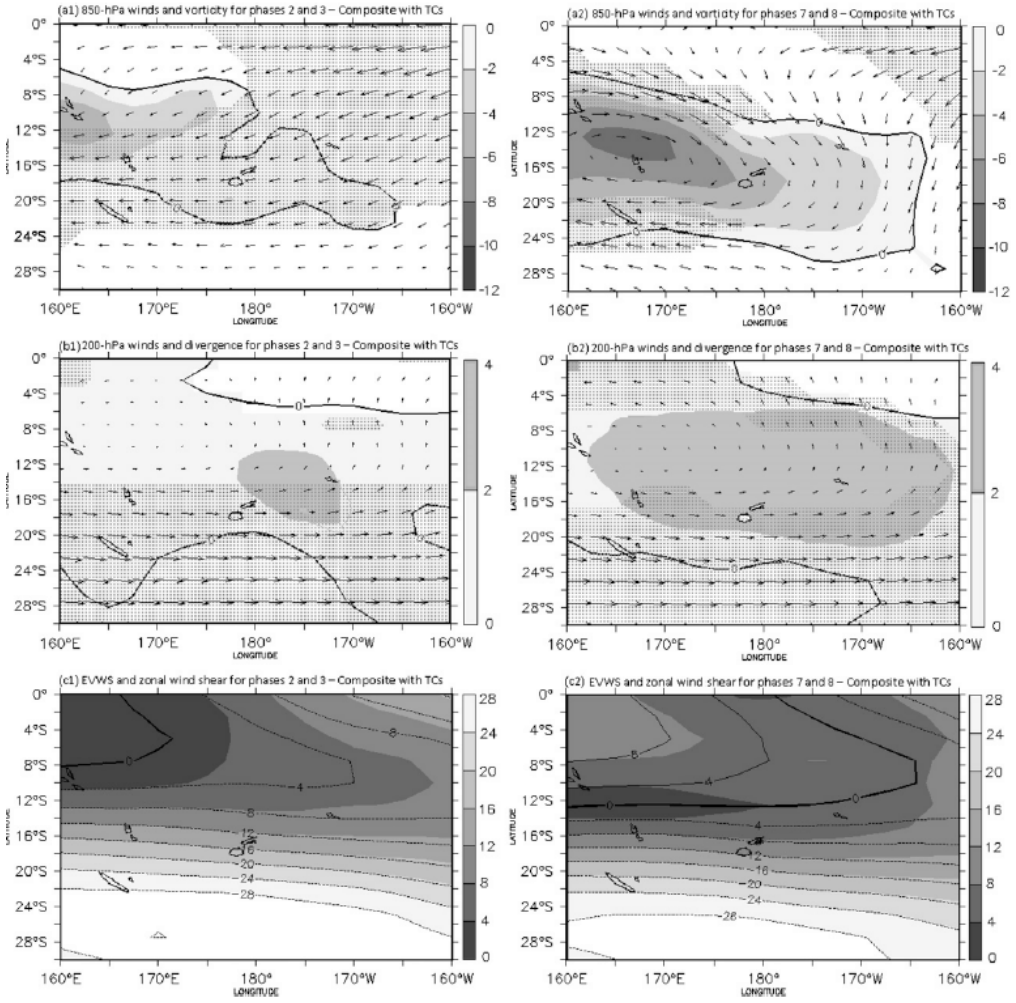

Chand and Walsh (2010)

MJO and Tropical Cyclone Activity in the South Indian Ocean

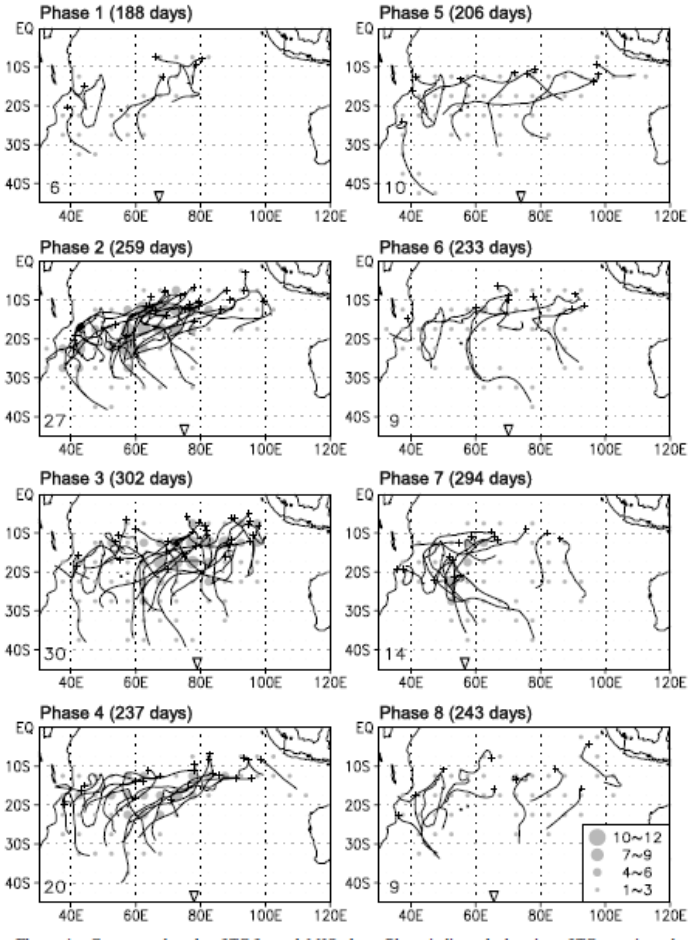

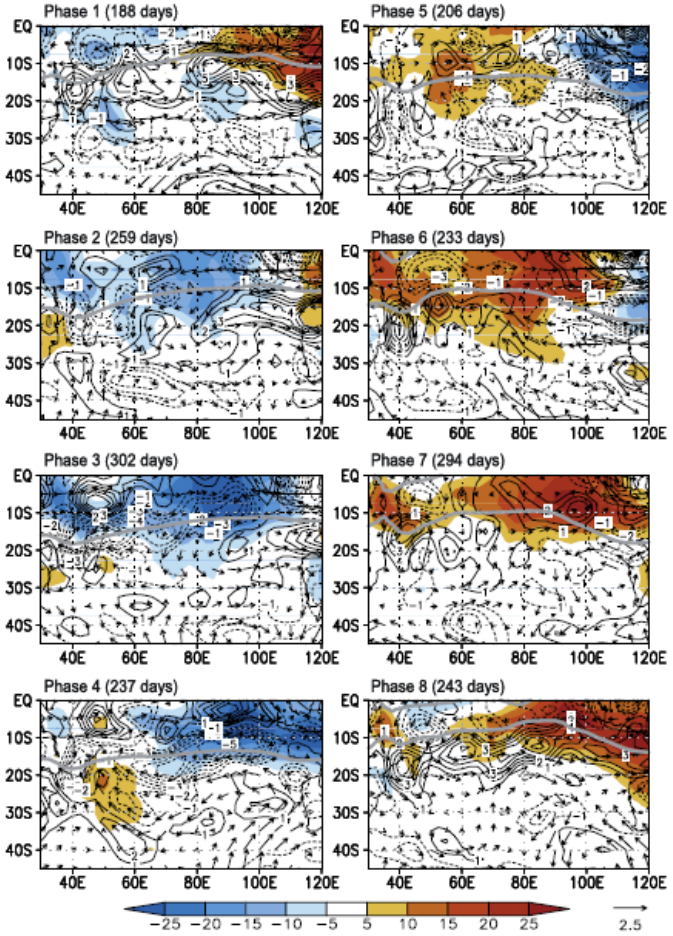

Ho et al. (2009)

MJO and Tropical Cyclone Activity in the Northern Indian Ocean

Boreal Summer Intra Seasonal Oscillation

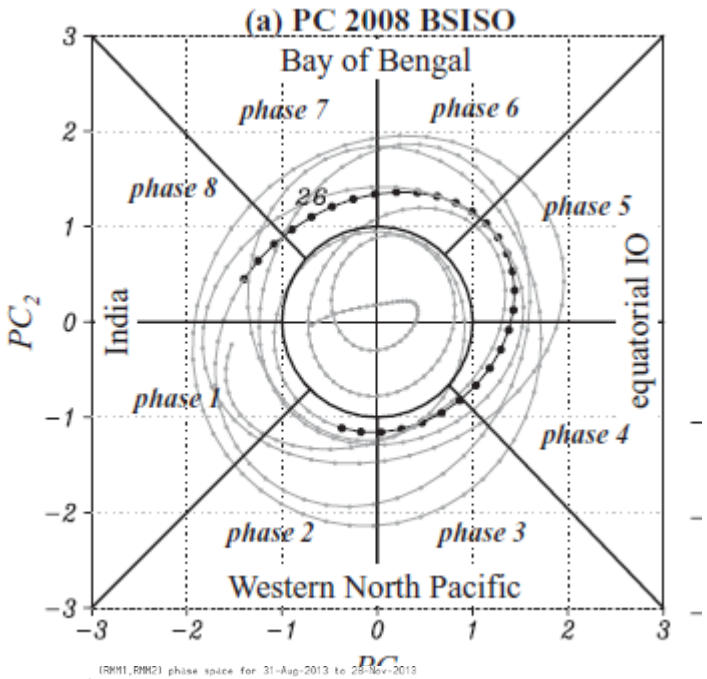

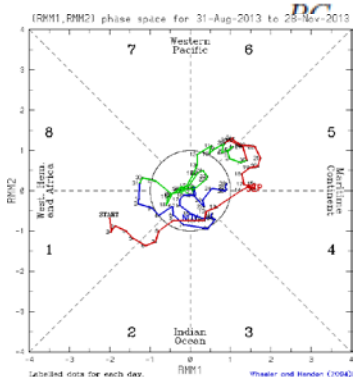

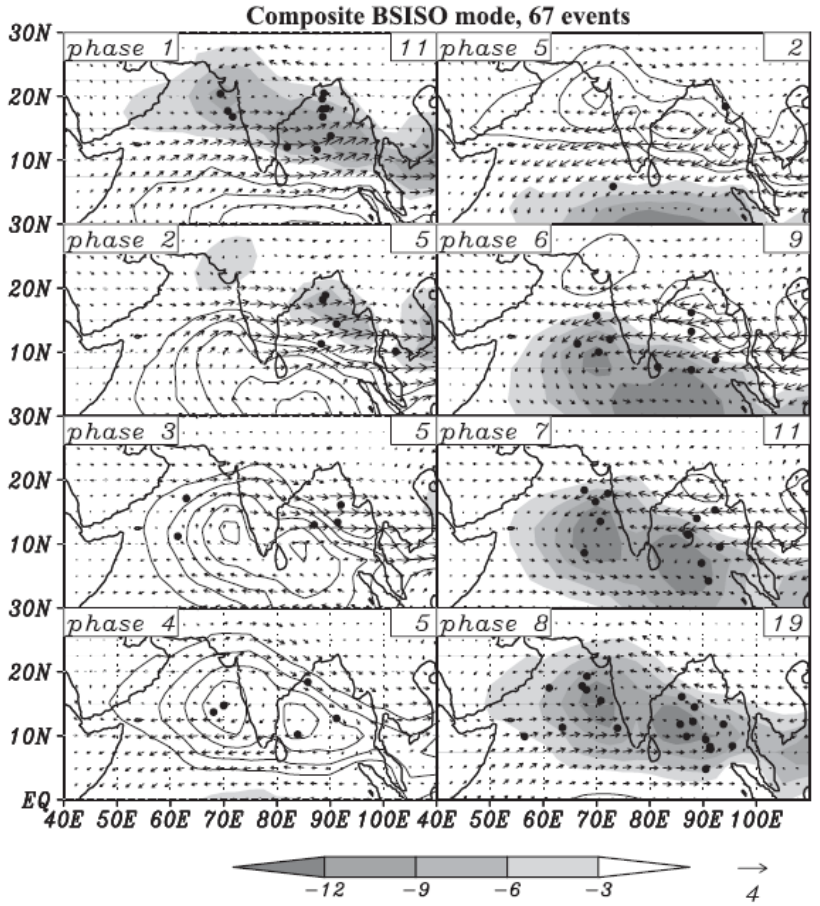

Kikuchi and Wang (2010)

Summary for MJO and TC

- During MJO convection cell locates in Indian Ocean
  - TC activity increases in the North Atlantic, Indian Ocean (including west Australian region) and decreases in the western North Pacific and South Pacific (including Fiji region).

- During MJO convection cell locates in western Pacific
  - TC activity decreases in the North Atlantic, Indian Ocean (including west Australian region) and increases in the western North Pacific and South Pacific (including Fiji region).

Subseasonal TC Forecasting based on the relationship with MJO

- Recently, the predictability of MJO increase (3~4 weeks) by dynamical forecasting models.
- If the MJO can be predicted, the probabilistic sub-seasonal TC prediction is possible using this relationship.

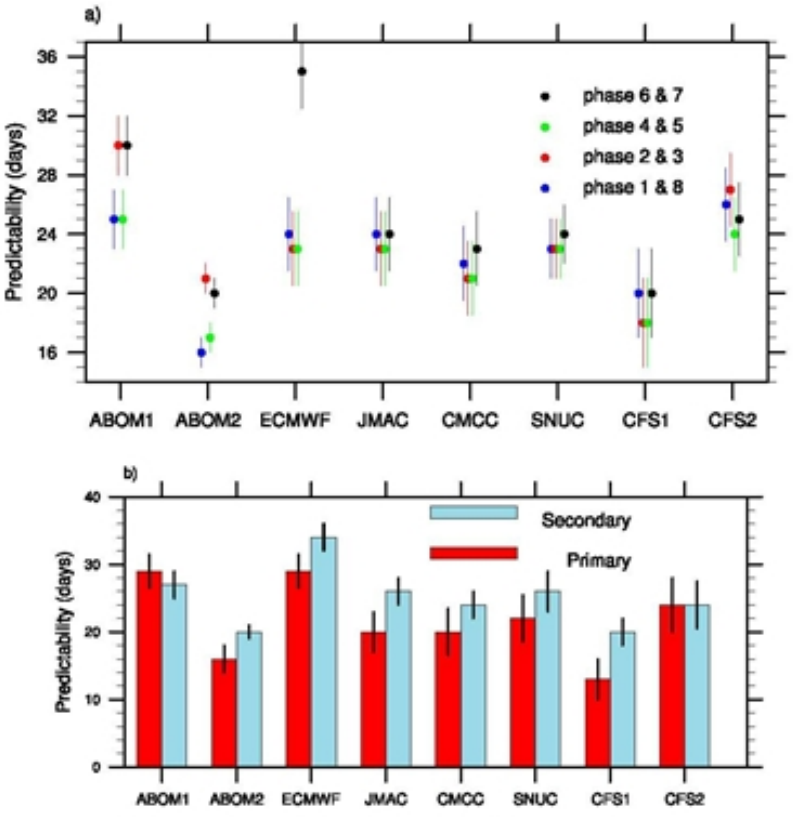

FIG. 3. MJO predictability (days) estimates for the eight models for (a) hindcasts initiated from different MJO phases and (b) primary and secondary MJO events. The error bars represent the 95% confidence interval for the predictability estimates.

Dynamical Subseasonal Prediction of Tropical cyclone

- Dynamical Prediction using high-resolution dynamical model to resolve the tropical cyclone.

- ECMWF 32-day ensemble forecasts
  - 51 members: 50 members plus one control
  - horizontal resolution (CY36R1): ~32 km to Day 10 and then ~65 km
  - coupling with ocean begins at 10 days
  - the real-time forecasts issued every Monday and Thursday (Mondays since 10 Oct. 2011)

- A TC tracker is used by ECMWF to obtain the 12-h tropical cyclone-like vortex track positions predicted by each of the members.

Typhoon Megi

(red: ensemble storm track; white: JTWC best-track)

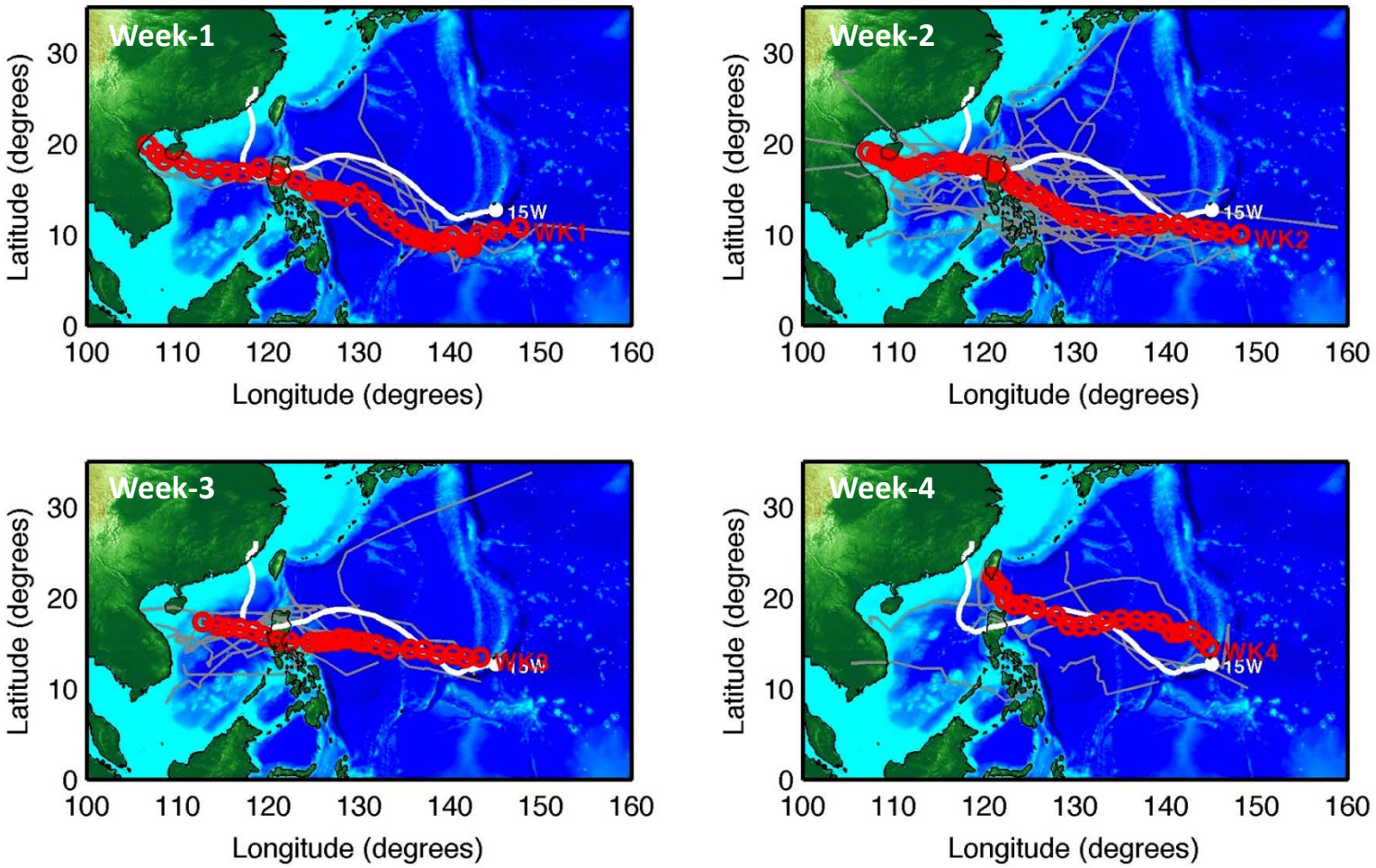

*A Week-1 storm starts in the forecast on the Monday (or Thursday) before the JTWC declares the system to be a Tropical Depression. A storm starting in the Week-2 (3 or 4) forecast is two (three or four) weeks before the corresponding JTWC Tropical Depression existed.

2012 WPAC Hits

As in Typhoon Megi example, multiple ensemble storms starting at slightly different times may be representing the same TC. An objective method being developed for combining these similar ensemble storms will reduce the number of HITS and increase the reliability.

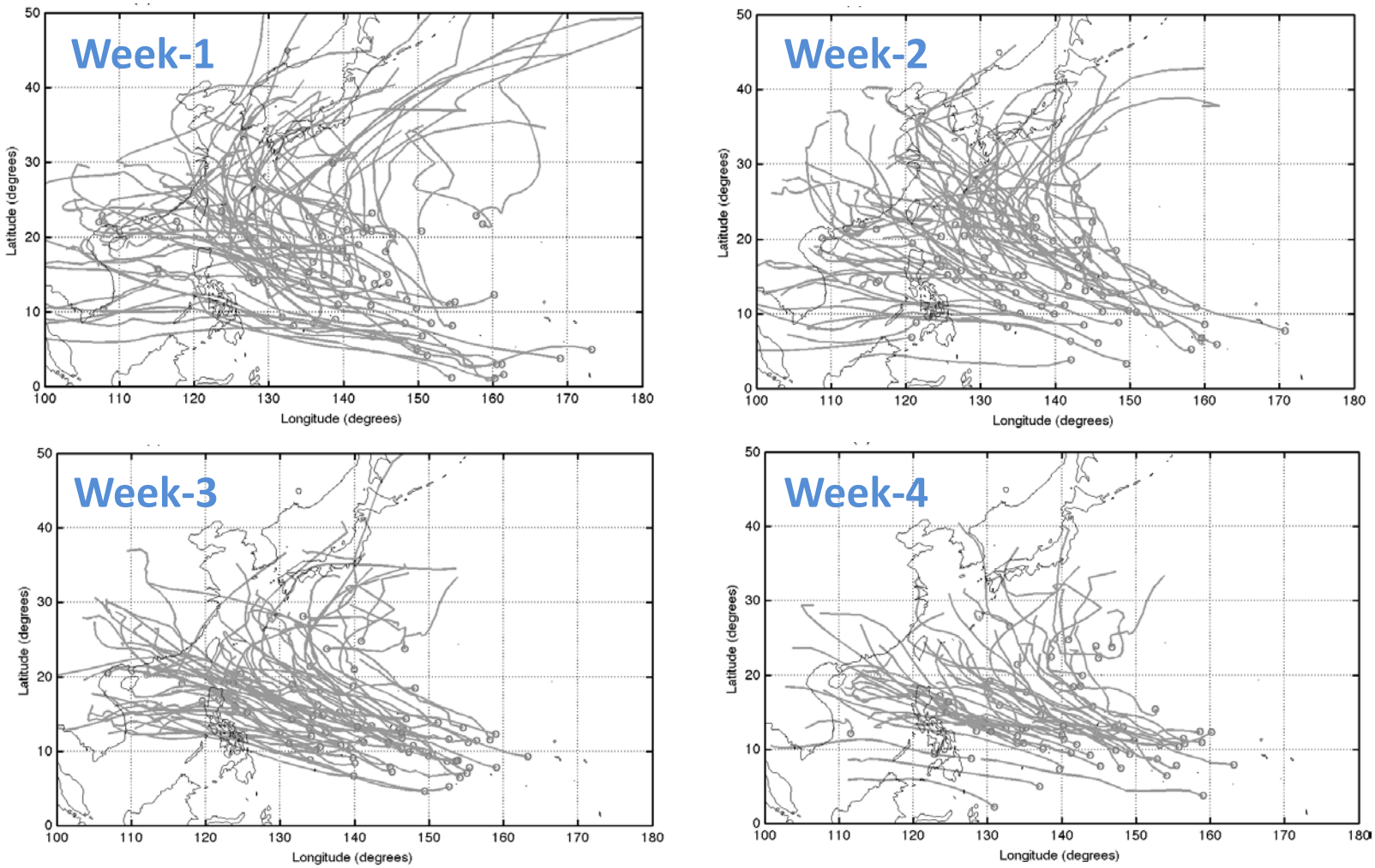

2012 WPAC False Alarms

In Week-1, a large fraction of the 109 FAs began below 10° N and had similar tracks. The objective method for combining similar ensemble storm tracks will considerably reduce the numbers of these easily recognized FAs, and some of the FAs that resemble real storms.

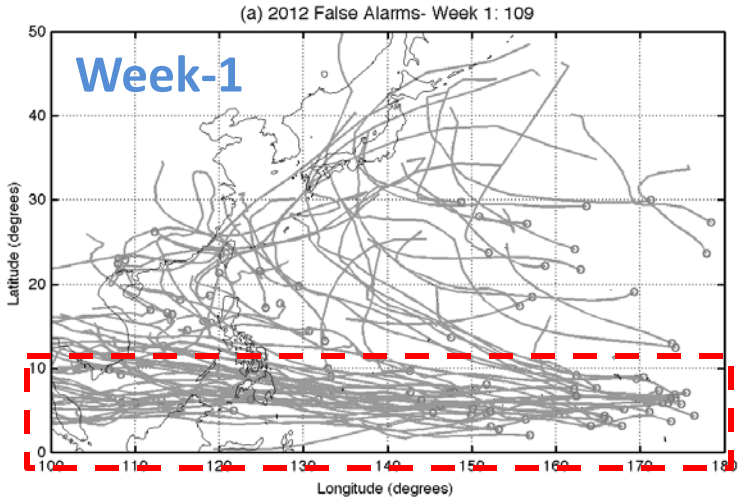

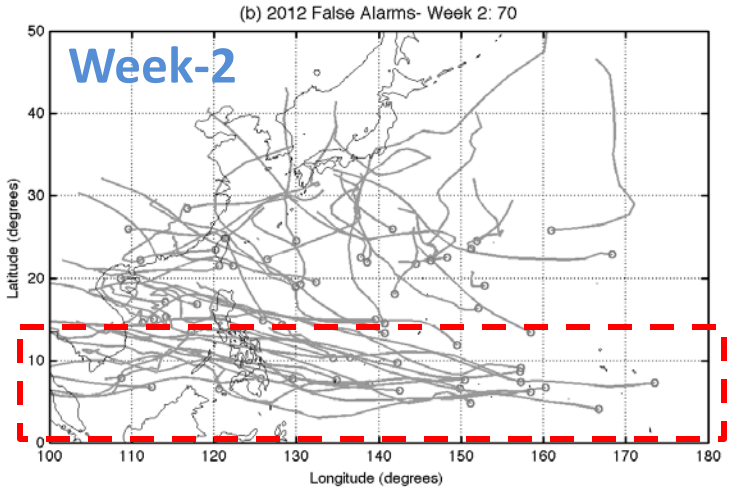

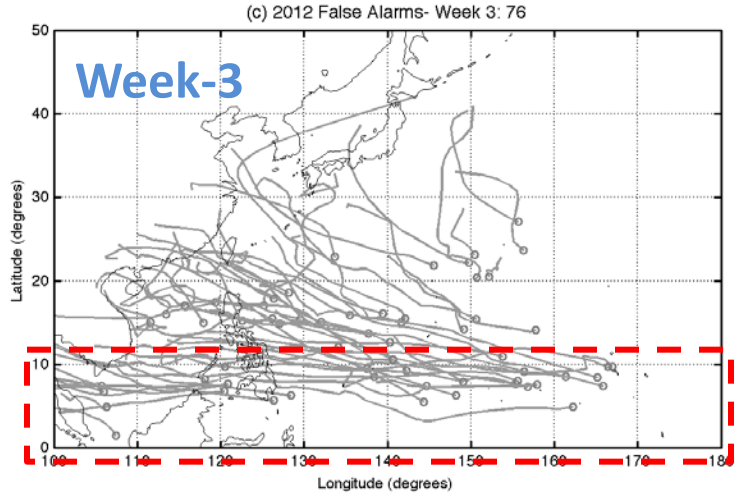

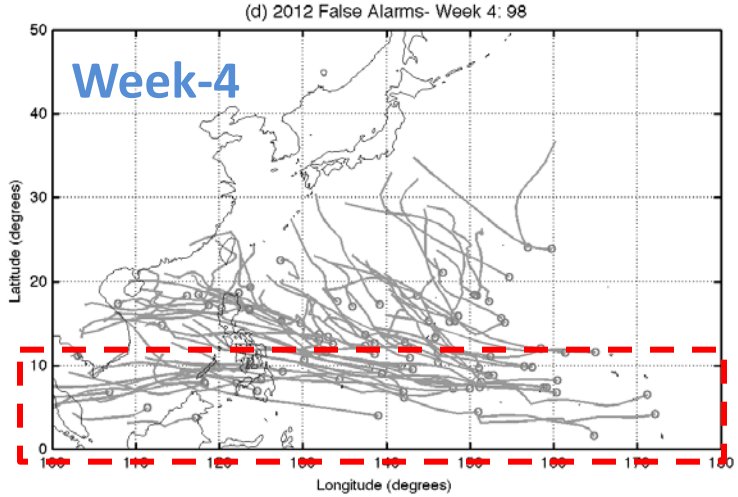

To Improve Subseasonal Predictability for Tropical Cyclone

- Improve understanding the relationship between intraseasonal variability (e.g. MJO) and tropical cyclone activity
- Improve the dynamical model predictability of intraseasonal variability and tropical cyclone by increasing resolution and improving dynamic/physics process in the models

Track-pattern-based model

Introduction

The TC landfalls absolutely depend on *TC tracks* that show the interannual and interdecadal variation as well as the seasonal variation (e.g., Chan 1985; Harr and Elsberry 1991; Ho et al. 2004, 2005; Kim et al. 2005, 2005).

In order to predict the TC landfalls and to mitigate the their damage in advance, it is necessary to understand the characteristics of various TC tracks and to develop the seasonal forecasting model for TC track patterns

Typhoon passages

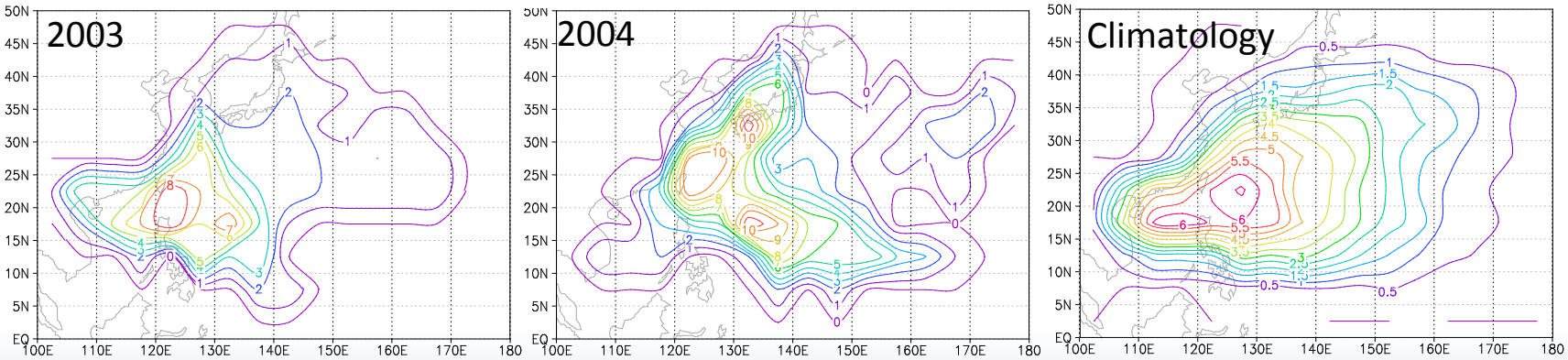

Introduction (continued)

In this study,

We intend to develop the seasonal forecasting model for the summer TC track passage.

At first, we objectively classify the summer TC tracks into several clusters using the fuzzy clustering algorithm.

And then, the dynamical-statistical prediction methodology is developed using the empirical relationship between the TC frequency in each cluster and the large-scale circulation which are produced by dynamical forecasting model.

Data used

- **TC : best track dataset achieved by RSMC Tokyo typhoon center.**
- **Large-scale environments : NCEP/NCAR reanalysis, NOAA SST**
- **Dynamical seasonal forecast : NCEP Climate Forecasting System(CFS)**

Contents

1. Fuzzy clustering of summer typhoon tracks.

2. Application to seasonal prediction.

Fuzzy clustering for TC tracks

The map of typhoon tracks have complex shapes and ambiguity in boundaries for distinctive patterns.

To classify the typhoon tracks, we introduce the fuzzy clustering algorithm.

In the fuzzy clustering algorithm, an object can simultaneously belong to the whole clusters with different membership coefficients. Because of this property, the fuzzy clustering method can produce more natural classification results for typhoon tracks

Tropical cyclone tracks for 1965 – 2006, June – October

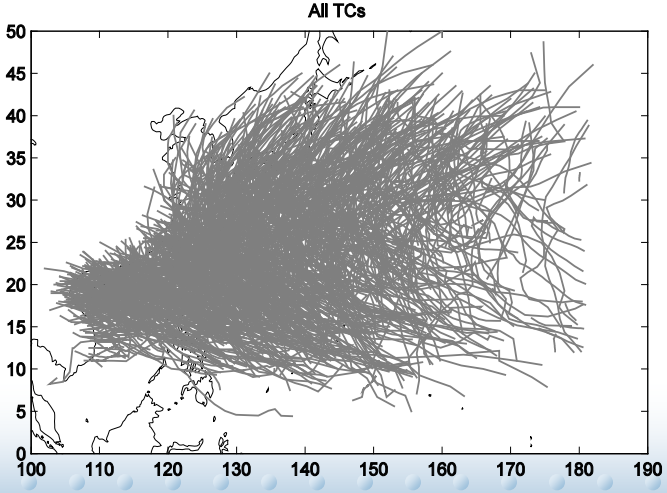

Crisp partitioning (k-means, hieratical clustering)

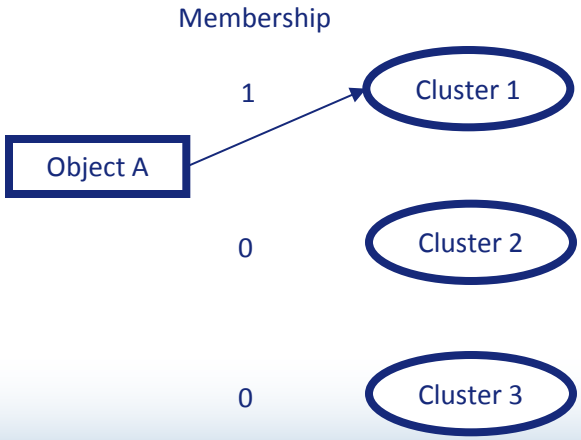

Soft partitioning (fuzzy clustering)

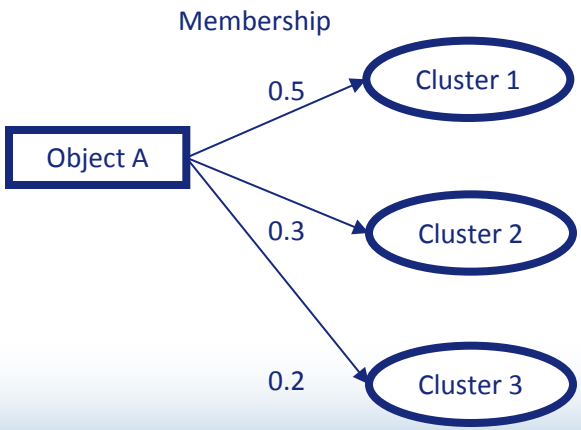

Fuzzy c-means algorithm for typhoon tracks

$$\mathbf{x}_k = [lon_{t=1}, lon_{t=2}, \cdots, lon_{t=21}, lat_{t=1}, lat_{t=2}, \cdots, lat_{t=21}]^T$$

where $k = 1,..., N$,

lon and *lat* are interpolated TC location,

N is the number of TCs.

The Fuzzy c-means clustering algorithm is based on the minimization of an objective function called c-means functional.It is defined as:

$$J = \sum_{i=1}^{c} \sum_{k=1}^{N} (\mu_{ik})^m \left\| \mathbf{x}_k - \mathbf{v}_i \right\|^2$$

Given the data set X, choose the number of clusters $1 < c < N$, the weighting exponent $m > 1$, the termination tolerance $\varepsilon > 0$, and the partition matrix U;

$$\mathbf{U} = \begin{bmatrix} \mu_{1,1} & \mu_{1,2} & \cdots & \mu_{1,c} \\ \mu_{2,1} & \mu_{2,2} & \cdots & \mu_{2,c} \\ \vdots & \vdots & \ddots & \vdots \\ \mu_{N,1} & \mu_{N,2} & \cdots & \mu_{N,c} \end{bmatrix}$$

Initialize the partition matrix $\mathbf{U}^{(0)}$ randomly.

Repeat for l=1,2, …

Step 1. Compute the cluster prototypes (mean):

$$\mathbf{v}_i^{(l)} = \frac{\sum_{k=1}^{N} (\mu_{ik}^{(l-1)})^m \mathbf{x}_k}{\sum_{k=1}^{N} (\mu_{ik}^{(l-1)})^m}, \quad 1 \le i \le c$$

Step 2. Compute the distances (dissimilarities):

$$D_{ik}^2 = (\mathbf{x}_k - \mathbf{v}_i)^T (\mathbf{x}_k - \mathbf{v}_i), \quad 1 \le i \le c, 1 \le k \le N$$

Step 3. Update the partition matrix:

$$\mu_{i,k}^{(l)} = \frac{1}{\sum_{j=1}^{c} (D_{ikA} / D_{jkA})^{2/(m-1)}}$$

,until $\left\| \mathbf{U}^{(l)} - \mathbf{U}^{(l-1)} \right\| < \varepsilon$

Optimum cluster number

We determine the cluster number objectively using five validity measures.

The measures suggest that seven is the optimum cluster number.

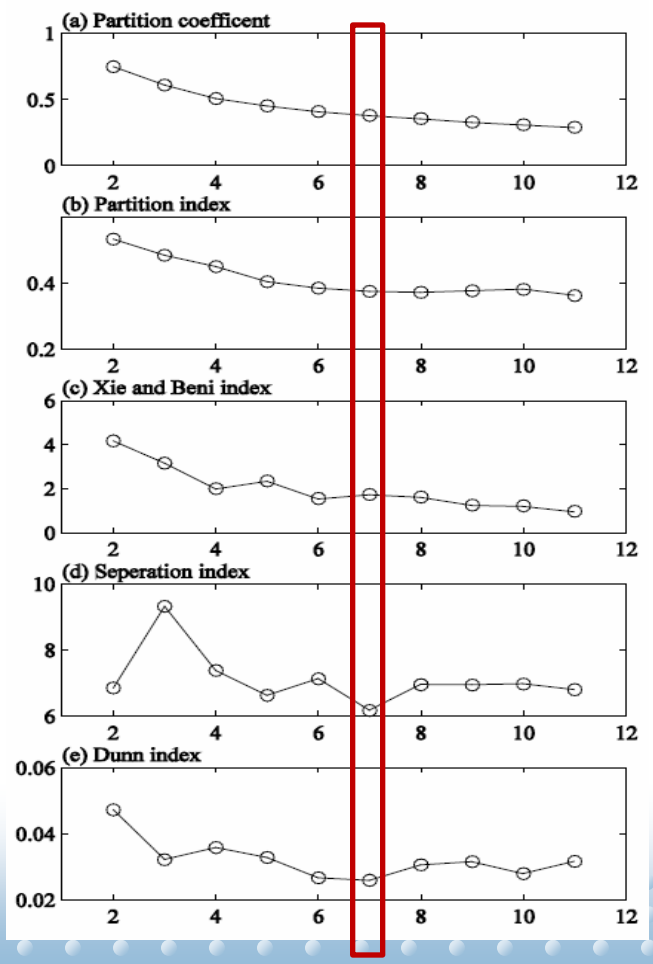

The validity scalars for optimum cluster number

$$\text{Partition coefficient} = \frac{1}{N}\sum_{i=1}^{C}\sum_{j=1}^{N}\mu_{ij}^{2}$$

$$\text{Partition index} = \sum_{i=1}^{C}\frac{\sum_{j=1}^{N}\mu_{ij}^{m}\left\|\mathbf{x}_j-\mathbf{c}_i\right\|^2}{N_i\sum_{k=1}^{C}\left\|\mathbf{c}_k-\mathbf{c}_i\right\|^2}$$

$$\text{Xie and Beni index} = \frac{\sum_{i=1}^{C}\sum_{j=1}^{N}\mu_{ij}^{m}\left\|\mathbf{x}_j-\mathbf{c}_i\right\|^2}{N\min_{i,j}\left\|\mathbf{x}_j-\mathbf{c}_i\right\|^2}$$

$$\text{Separation Index} = \frac{\sum_{i=1}^{C}\sum_{j=1}^{N}\mu_{ij}^{2}\left\|\mathbf{x}_j-\mathbf{c}_i\right\|^2}{N\min_{i,k}\left\|\mathbf{c}_k-\mathbf{c}_i\right\|^2}$$

$$\text{Dunn index} = \min_{i\in C}\left\{\min_{j\in C, i\neq j}\left\{\frac{\min_{x\in Ci, y\in Cj}d(x,y)}{\max_{k\in C}\left\{\max_{x,y\in C}d(x,y)\right\}}\right\}\right\}$$

Fuzzy clustering results

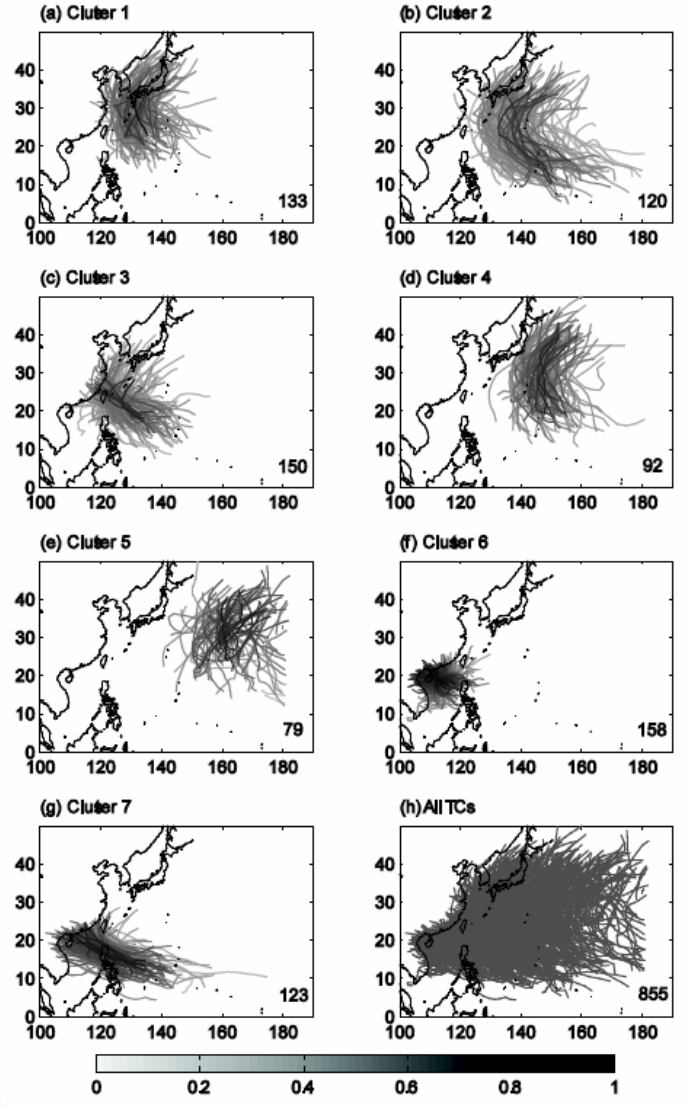

For practical purpose, we assign each TC is assigned to a cluster where its membership coefficient is the largest.

Characteristics in TC landfall and rainfall

TC landfalls on the sub-regions (1965-2006, JJASO)

	C1	C2	C3	C4	C5	C6	C7	All
Philippine	1	0	7	0	0	11	90	109
Vietnam	0	0	0	0	0	62	31	93
South China coast	0	1	15	0	0	55	43	114
East China coast	13	2	35	0	0	0	3	53
Taiwan	3	1	51	0	0	3	5	63
Korea	14	3	6	0	0	0	0	23
Japan	53	27	11	5	0	0	0	96

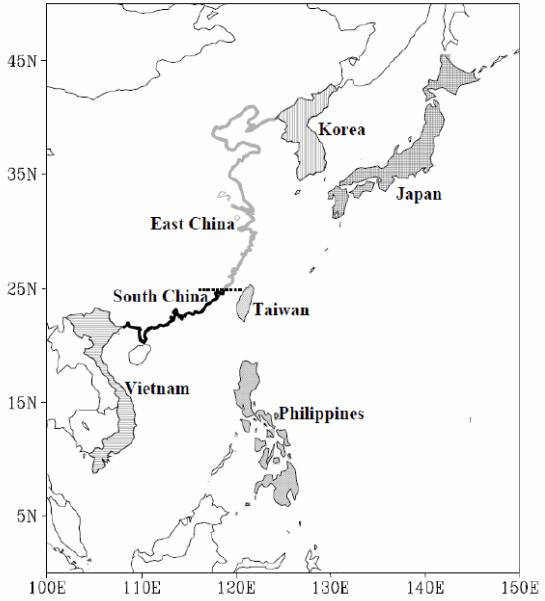

Characteristics in steering circulations

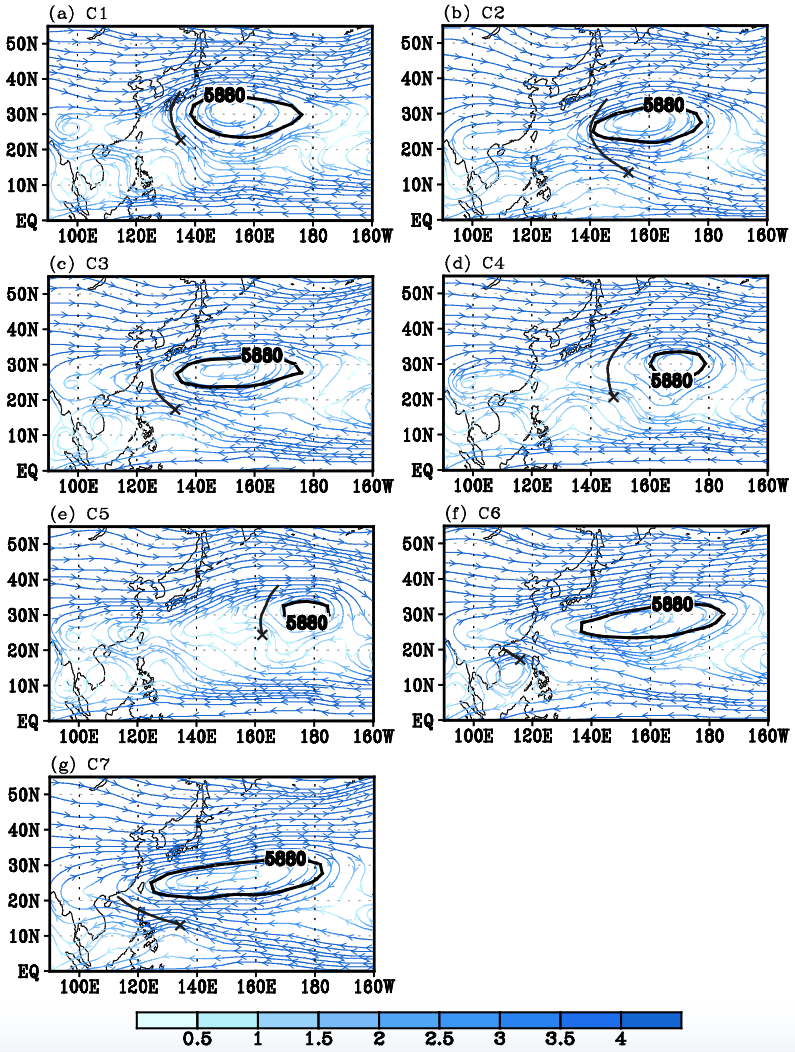

Composites of the tropospheric layer-mean flows (streamline) on the day of TC genesis.

The color depth for streamlines represents the mean flow speed.

The solid contour is the 5880 gpm of the 500-hPa geopotential height composite

Relationship with the ENSO and QBO

ENSO:La Nina

COR(TC_C1, SST) JJASO

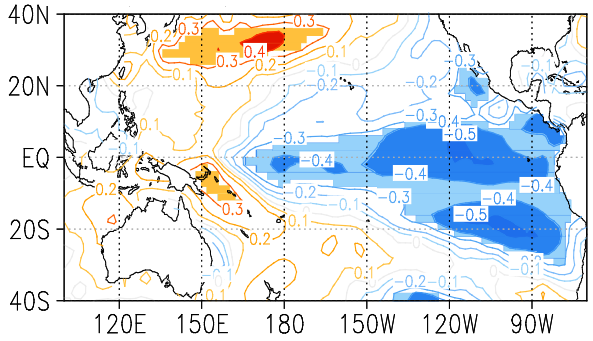

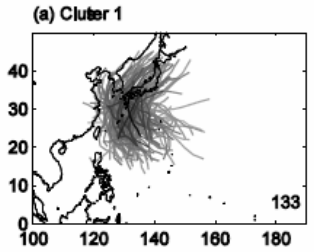

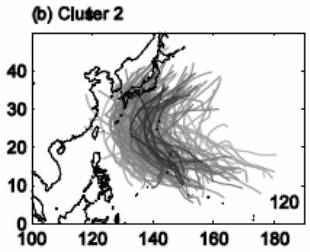

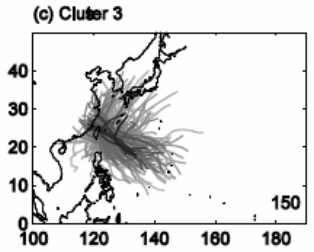

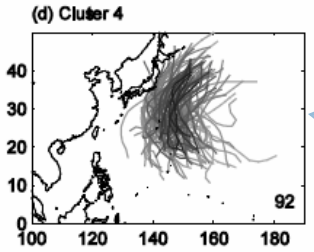

ENSO: El Nino

COR(TC_C2, SST) JJASO

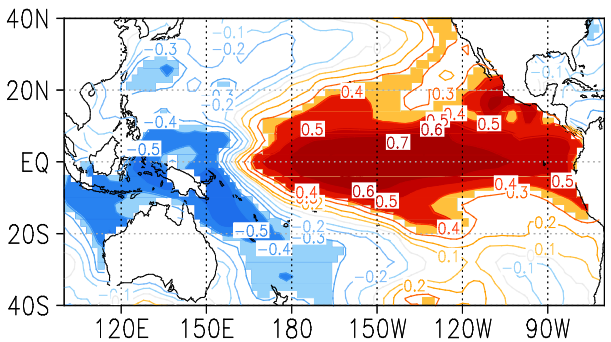

El Nino Modoki

COR(TC_C3, SST) JJASO

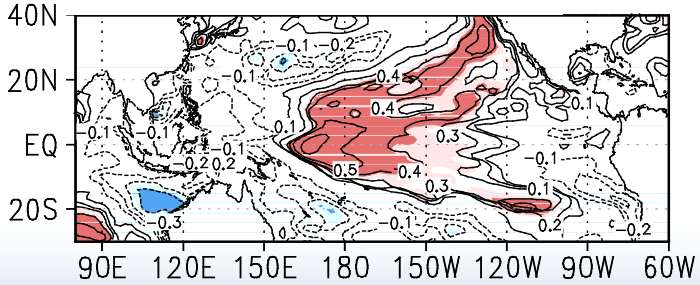

QBO

COR(TC_C4, U50) JJASO

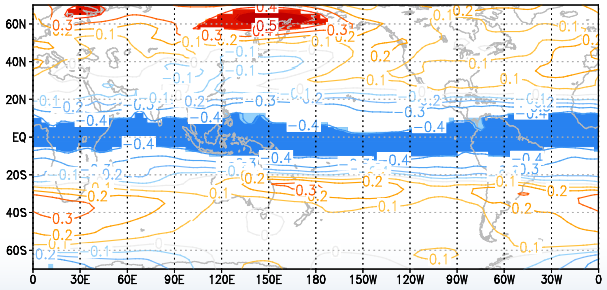

Contents

1. Fuzzy clustering of summer typhoon tracks.

2. Application to the seasonal prediction.

Flow chart for seasonal forecast using the TC clusters

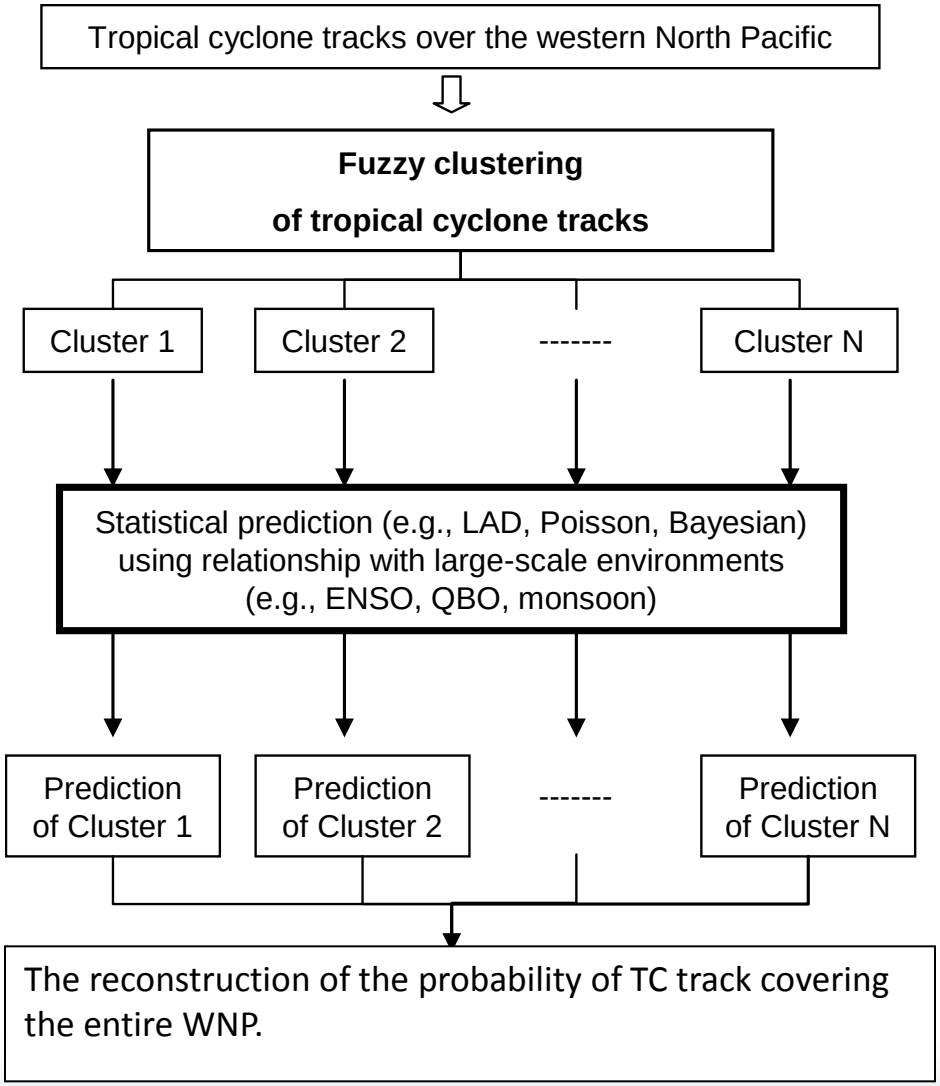

Using dynamical seasonal forecasts

The classified TC track patterns are more related to the simultaneous large-scale circulations rather than the pre-seasonal environments (see below figure).

If the dynamical model provides the environments for the typhoon season, the statistical prediction model for TC track patterns can be developed using the relationship with the large-scale environment.

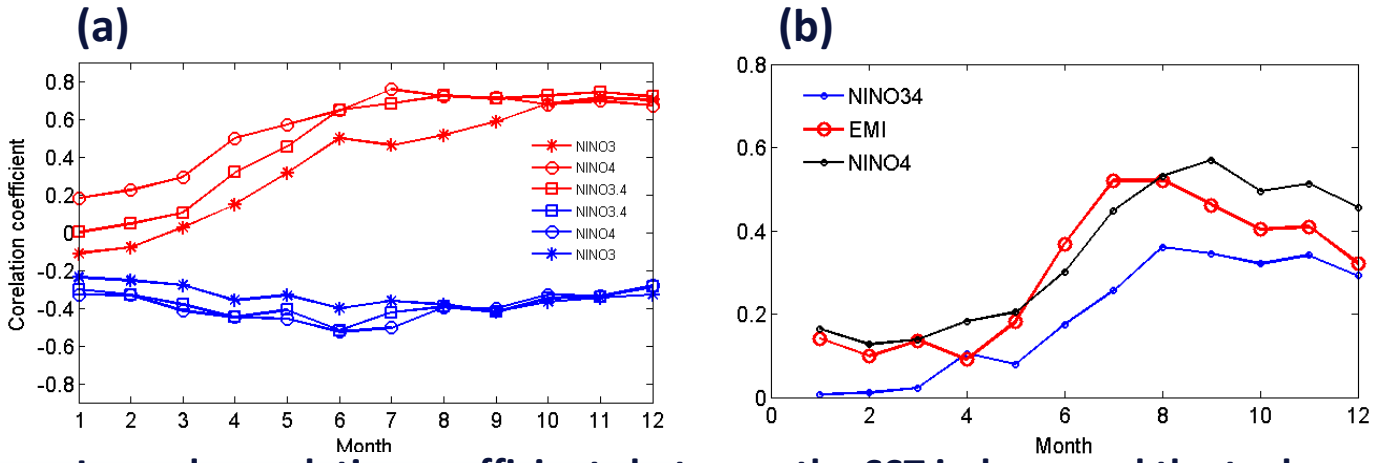

Lagged-correlation coefficients between the SST indexes and the typhoon counts in (a) C1 (blue line) and C2 (red line) and (b) C3.

Dynamical forecasts for large-scale environments

NCEP CFS retrospective forecast data

Dynamical forecast using fully coupled ocean-atmosphere-land model.

It provides 9-month forecasting starting each month with 15 ensemble members.

Available period : 1981−2008

Resolution : dynamic variables : 144x73
physical variables : 192x94
ocean variables : 180x139

CFS forecasts used in this study,

15 ensemble members (initial conditions : mid-April ~ early-May)

Analysis season : June through October

Correlations between SST and TC frequency in each cluster

Observations

CFS forecasts

C1

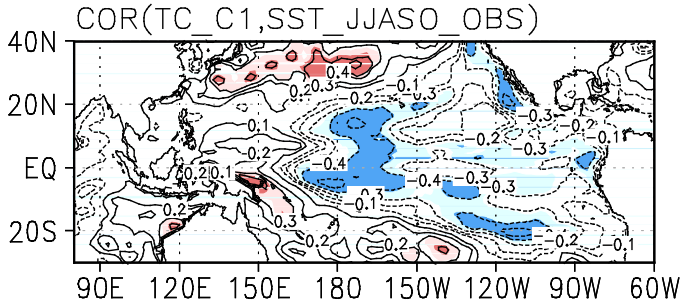

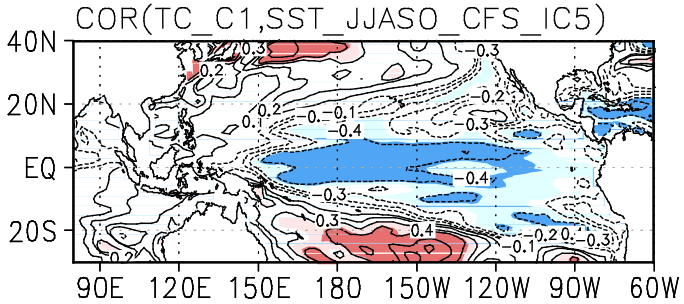

C2

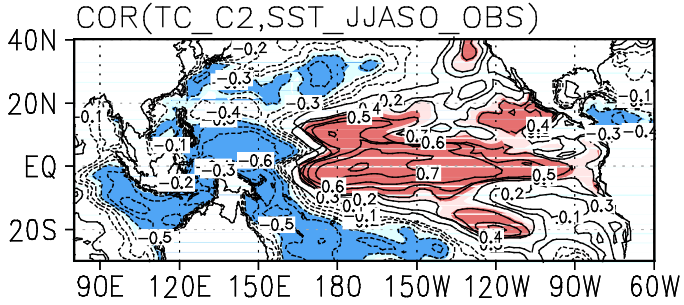

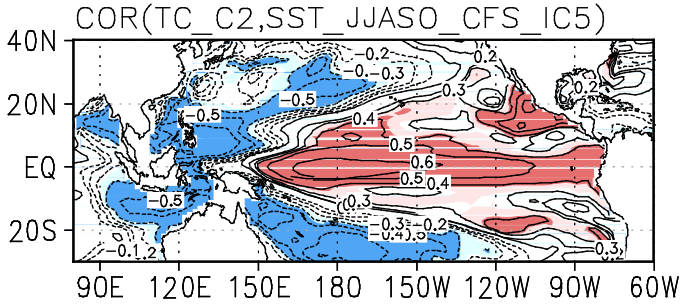

C3

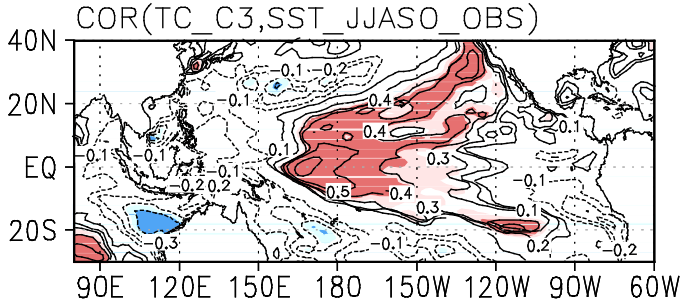

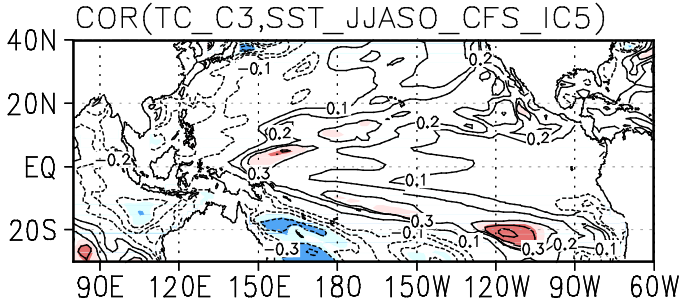

Using ensemble mean

The CFS forecasts show quite similar features to observations.

Correlations between SST and TC frequency in each cluster

Observations

CFS forecasts

C4

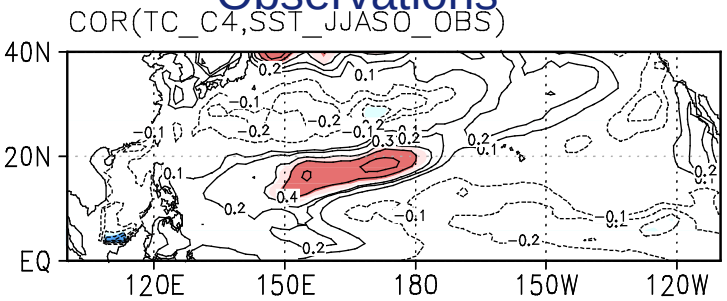

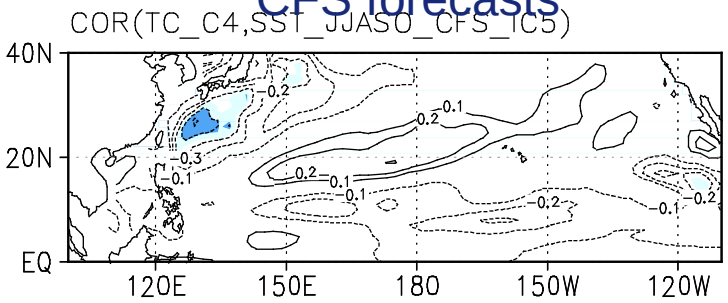

C5

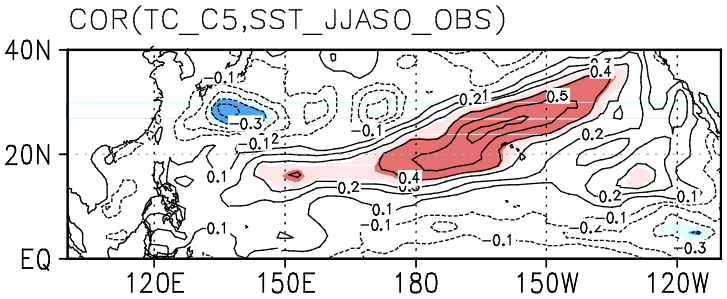

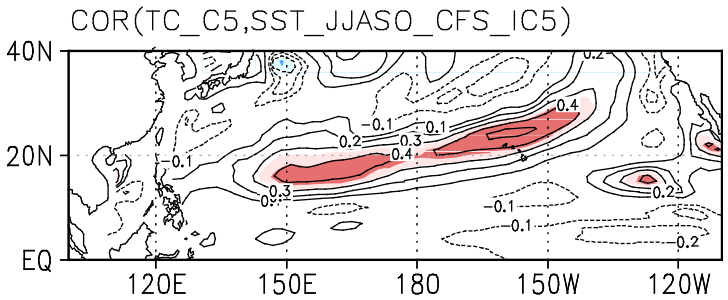

C6

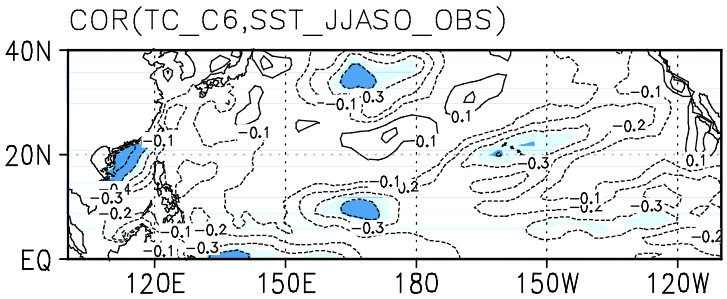

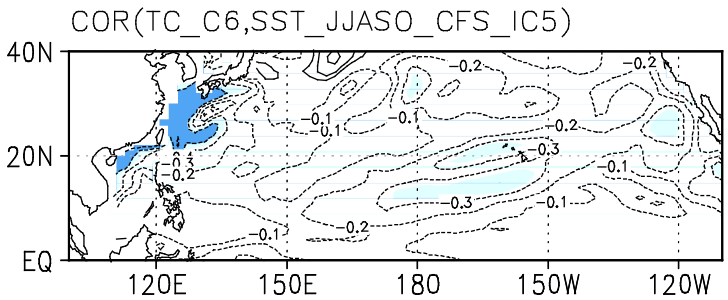

C7

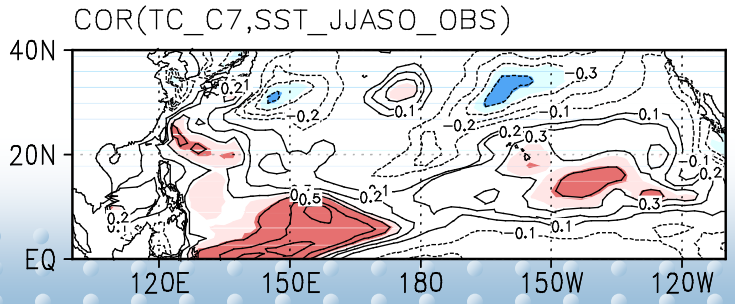

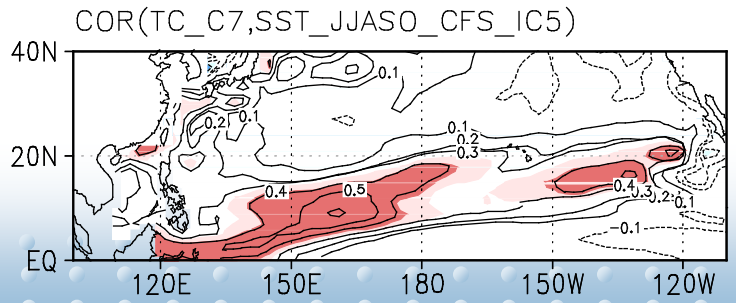

Correlations between C4 TCs and 50hPa zonal wind

Observation

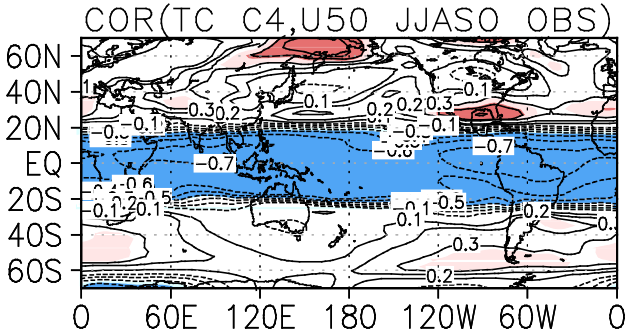

CFS forecast

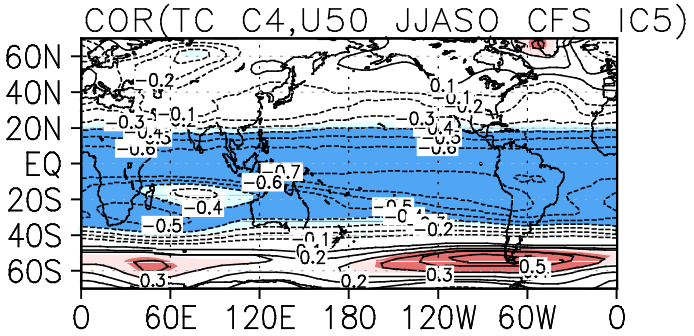

Relationship with the QBO

The relationship with QBO is also well shown in CFS forecast.

Statistical prediction based on dynamical forecast

$$Y_{obs}(t) = F[X_m(t)] \qquad \textit{for training period}$$

$$\Downarrow$$

$$Y_{fcst}(T) = F[X_m(T)] \qquad \textit{for prediction year}$$

Y **: predictand (*seasonal TC frequency in each cluster*)**

X_m **: predictors from dynamical model (*large-scale environment provided by NCEP/CFS seasonal forecast*)**

F **: statistical model (*Poisson regression model*)**

t **: training years (*jackknifed during 1981–2006*)**

T **: prediction year**

Hindcast results (jackknife cross validations)

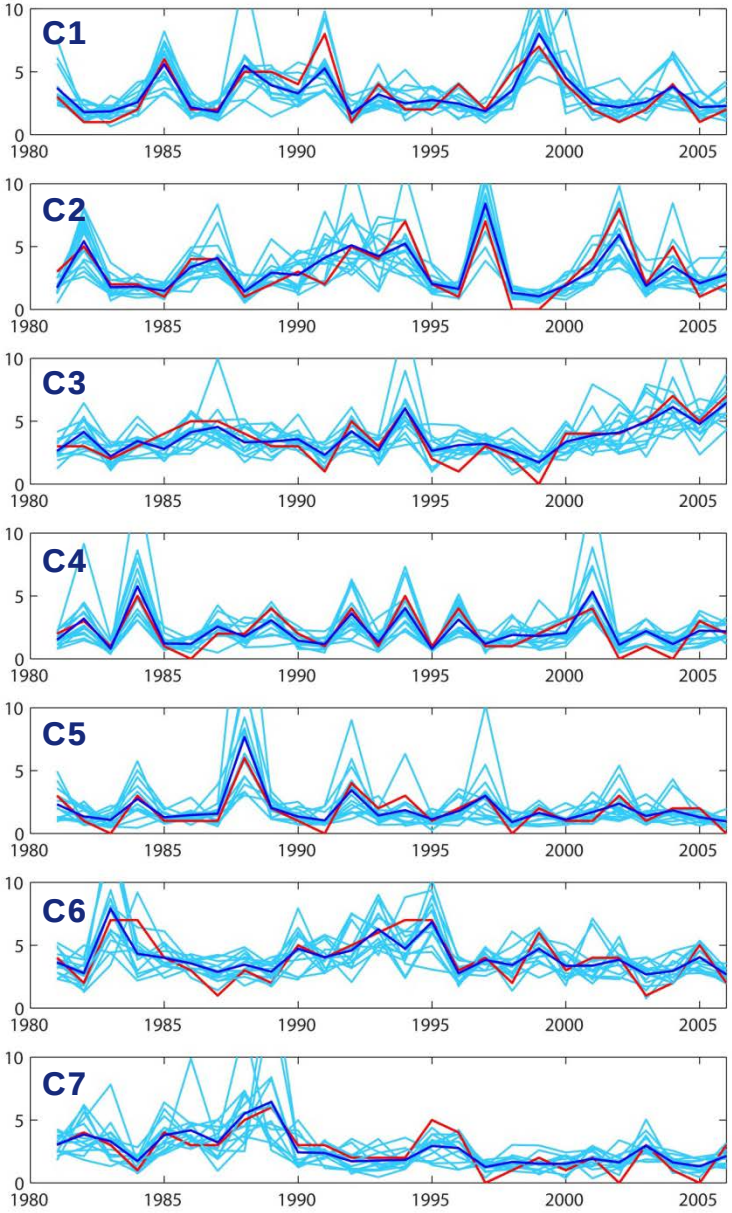

RMSE=0.94

RMSE=1.00

RMSE=0.81

RMSE=0.74

RMSE=0.76

RMSE=1.05

RMSE=0.82

- **Predictors:**
  - **SST**
  - **50-hPa zonal wind (QBO)**
  - **850-hPa relative vorticity**
  - **500-hPa geopotential height**
  - **Vertical wind shear**

Red : observation
Light blue : 15 ensemble members
Blue : ensemble mean

The each ensemble members show large error, but their ensemble mean show good correlation with the observation.

Jackknife cross-validation method:
For prediction year Y, the training period is 1981~(Y-1) and (Y+1)~2006.

Reconstruction of TC occurrence map over the WNP

Method for probability of TC (P_{fcst}) over the WNP reconstructed from the 7 clusters

For each prediction year,

$$NTC_{fcst\ total} = \sum_{i=1}^{7} NTC_{fcst}(Ci)$$

$$P_{fcst} = \sum_{i=1}^{7} P_{clim}(Ci)\frac{NTC_{fcst}(Ci)}{NTC_{fcst\ total}}$$

$P_{clim}(Ci)$= (Grided TC_{obs} occurrencs)/(# of TC_{obs} gnensis) in cluster i

$P_{clim}(C1)$ $P_{clim}(C2)$ $P_{clim}(C3)$ $P_{clim}(C4)$

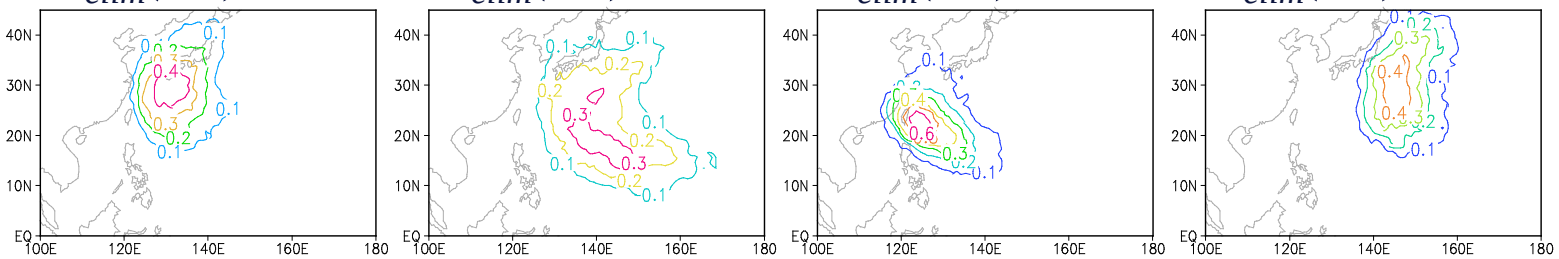

$P_{clim}(C5)$ $P_{clim}(C6)$ $P_{clim}(C7)$

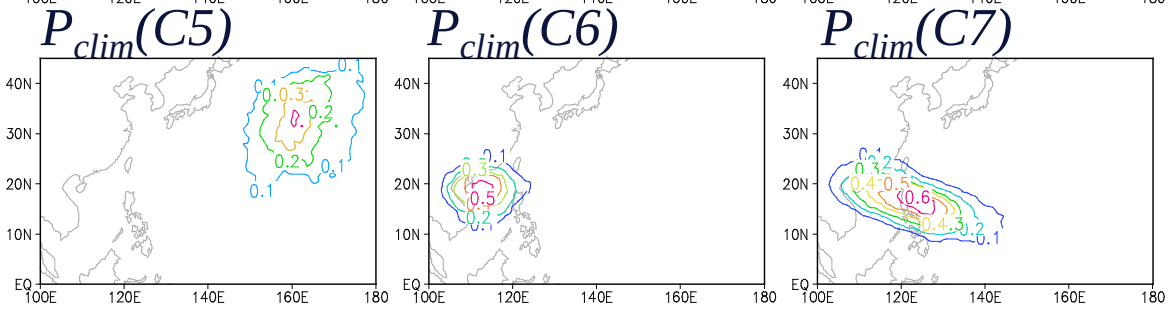

Reconstruction results (anomalous P_{fcst})

Observation | Hindcast | Observation | Hindcast

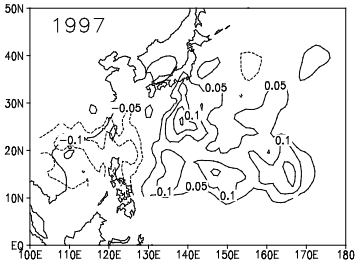

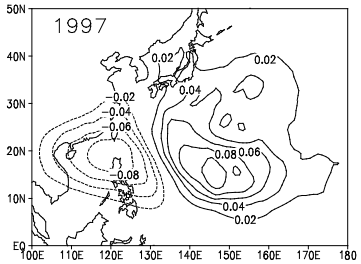

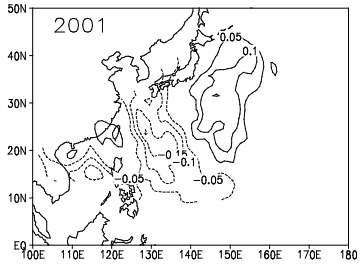

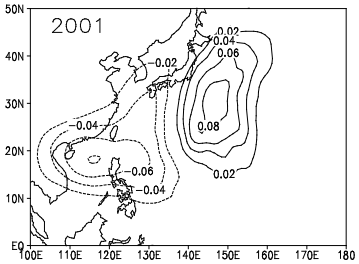

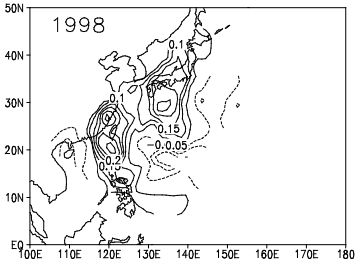

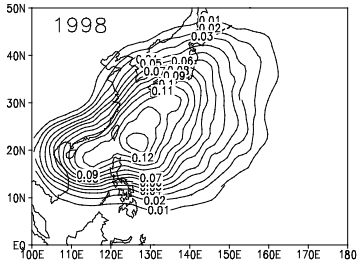

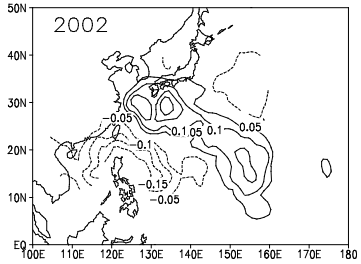

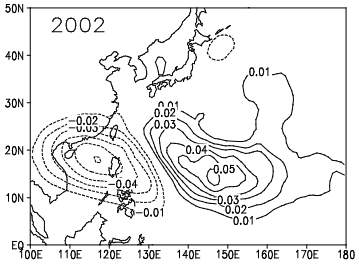

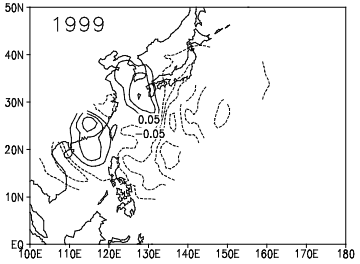

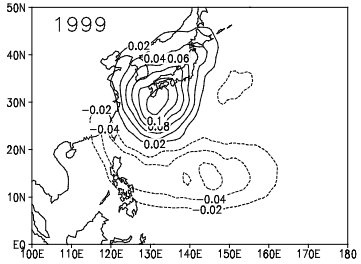

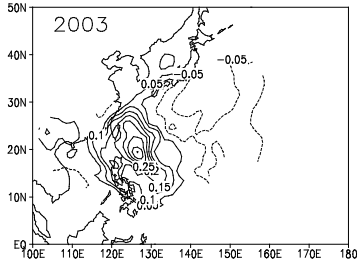

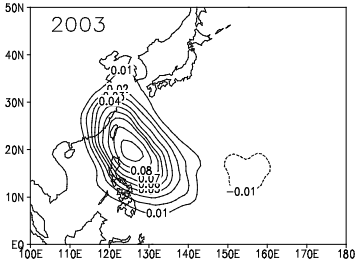

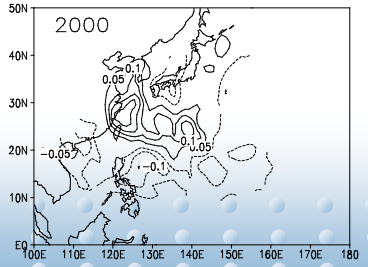

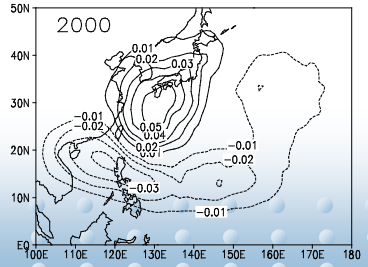

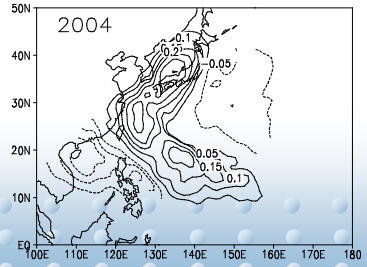

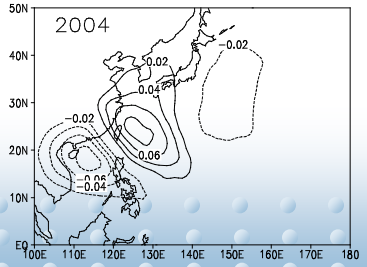

Summary

- **The summertime TC tracks over the WNP are objectively classified into 7 clusters using the fuzzy clustering method.**
- **The classified TC track patterns are well related with the large-scale circulation such as the ENSO and QBO**
- **The seasonal forecast is attempted for the TC frequency in each fuzzy cluster using the NCEP CFS forecast field.**
- **The cross validation results show the each TC track patterns can be reasonably predicted.**
- **The seasonal prediction for anomalous TC passage over the entire WNP is possible using the reconstruction method.**
- **The methodology in this study can be applied to the operational prediction task.**

Tropical Cyclone Simulation and Response to CO2 Doubling in GFDL CM2.5 High-resolution Coupled Global Climate Model

GFDL CM2.5

- Derived from CM2.1
- Fully coupled atmosphere, ocean, land and cryosphere model
- Resolution: ~50 km with 32 levels for atmosphere and ~25 km with 50 levels for ocean
- Compared to CM2.1, CM2.5 shows marked improvement in simulating ITCZ, ENSO, regional rainfall features and Indian monsoon, etc. (Delworth et al. 2012, Doi et al. 2012)

Experiments

- Control : 280 year simulation with the atmospheric composition and external forcing fixed at 1990 levels.
- CO_2 Doubling : 140 year simulation with atmospheric CO_2 increases at 1% per year until doubling after 70 year.

- We analyze 91-140 years for both experiments to focus on the approximately steady state response to CO_2 doubling .

Detection of Tropical Cyclone

- Tropical cyclone detection and tracking algorithm is adopted from Zhao et al. (2009, JC)

- Using 6 hourly fields,
  - The 850-hPa relative vorticity maxima higher than 3.5×10^{-5} s^{-1} are located within a $6° \times 6°$ latitude-longitude area.
  - The local minimum of sea level pressure, which must be within 2° of the vorticity maximum is defined as the storm center.
  - The local maximum of temperature averaged between 300 and 500 hPa (warm core center) must be within 2° of the local minima of sea level pressure and the warm core temperature must be at least 1 K warmer than the surrounding local mean.
  - The initial point of the storm trajectory must be between 40°S and 40°N and the distance between two "connected" vortex locations must be less than 400 km in 6 hours.
  - The trajectory must last at least 3 days (not necessarily consecutive) with maximum winds exceeding 17 m/s.

TC tracks (OBS vs. CM2.5)

IBTrACS (1980–2000)

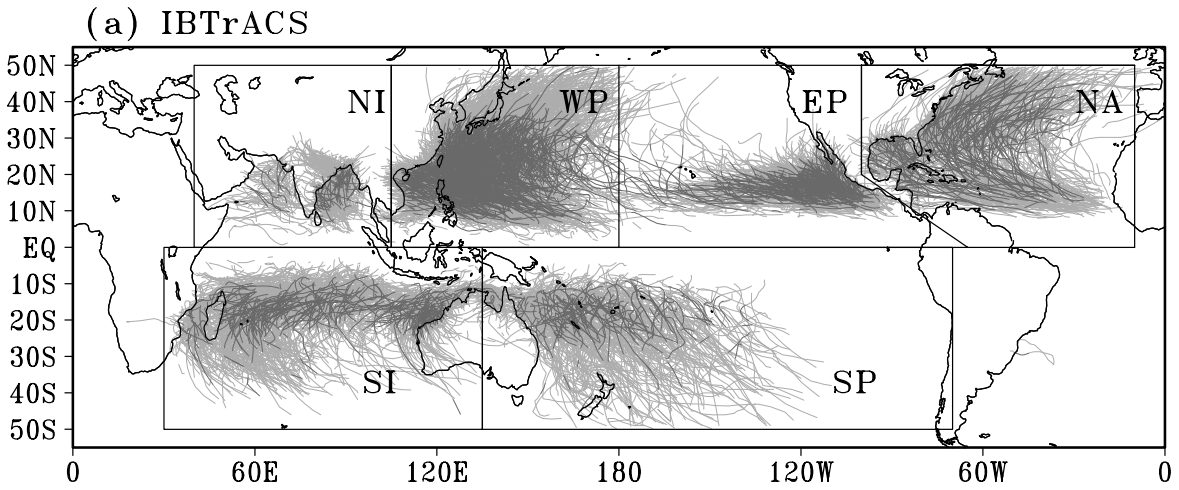

CM2.5 Control (91–110)

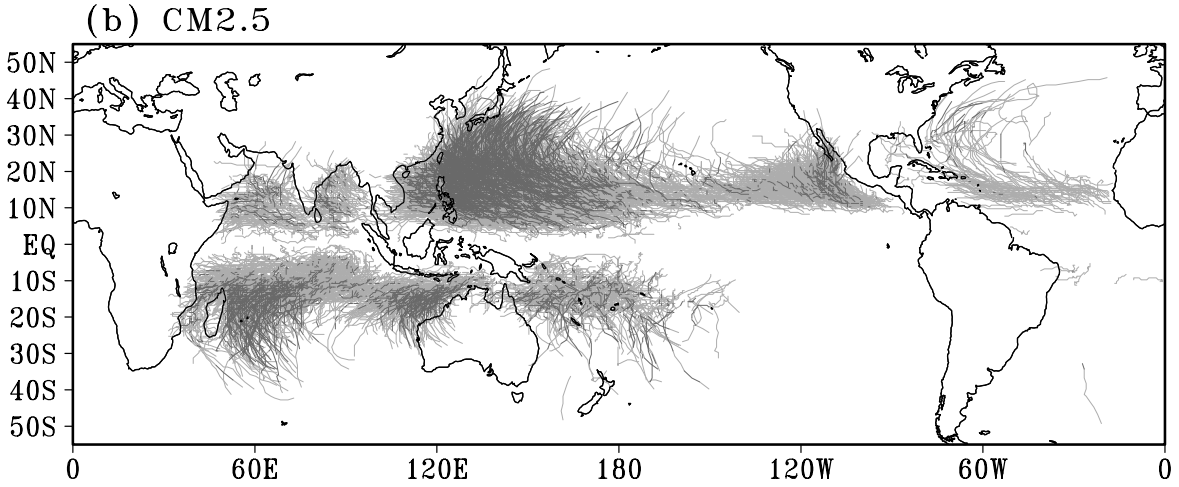

TC Climatology (OBS vs. CM2.5)

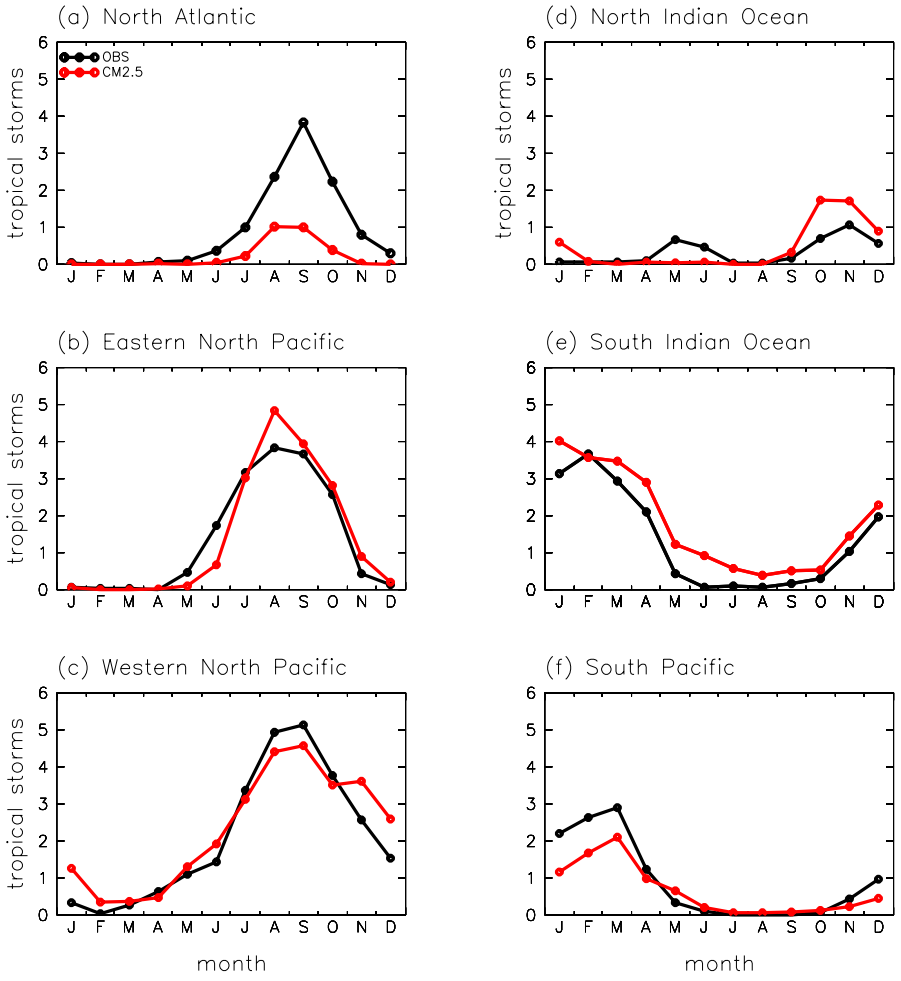

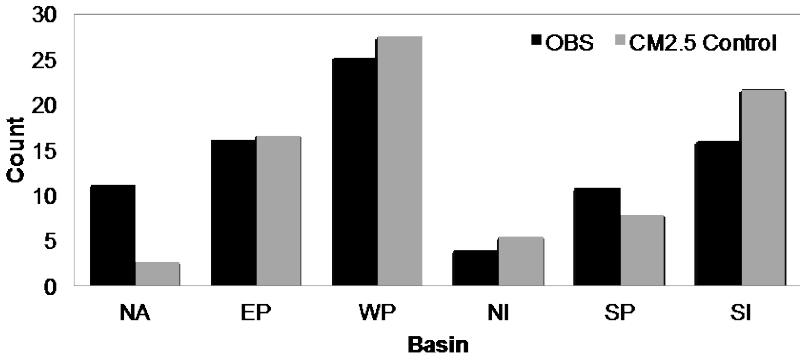

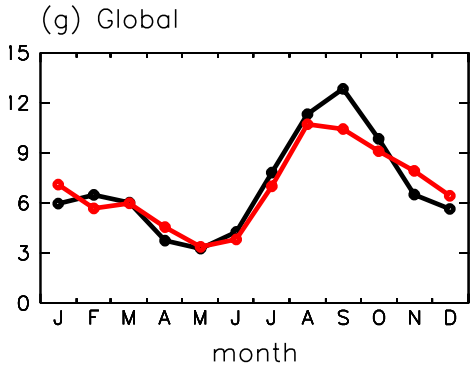

Relationship of TC Activity to ENSO

TC occurrences (5° x5°) Regressed on the NINO 3.4 Index

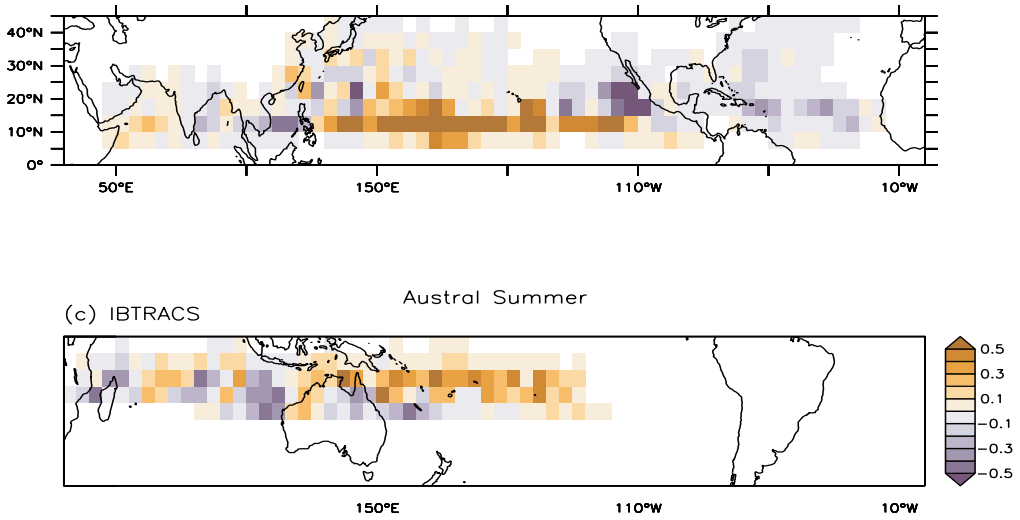

Bias in Large-scale Environments Simulated by CM2.5

CM2.5 minus OBS

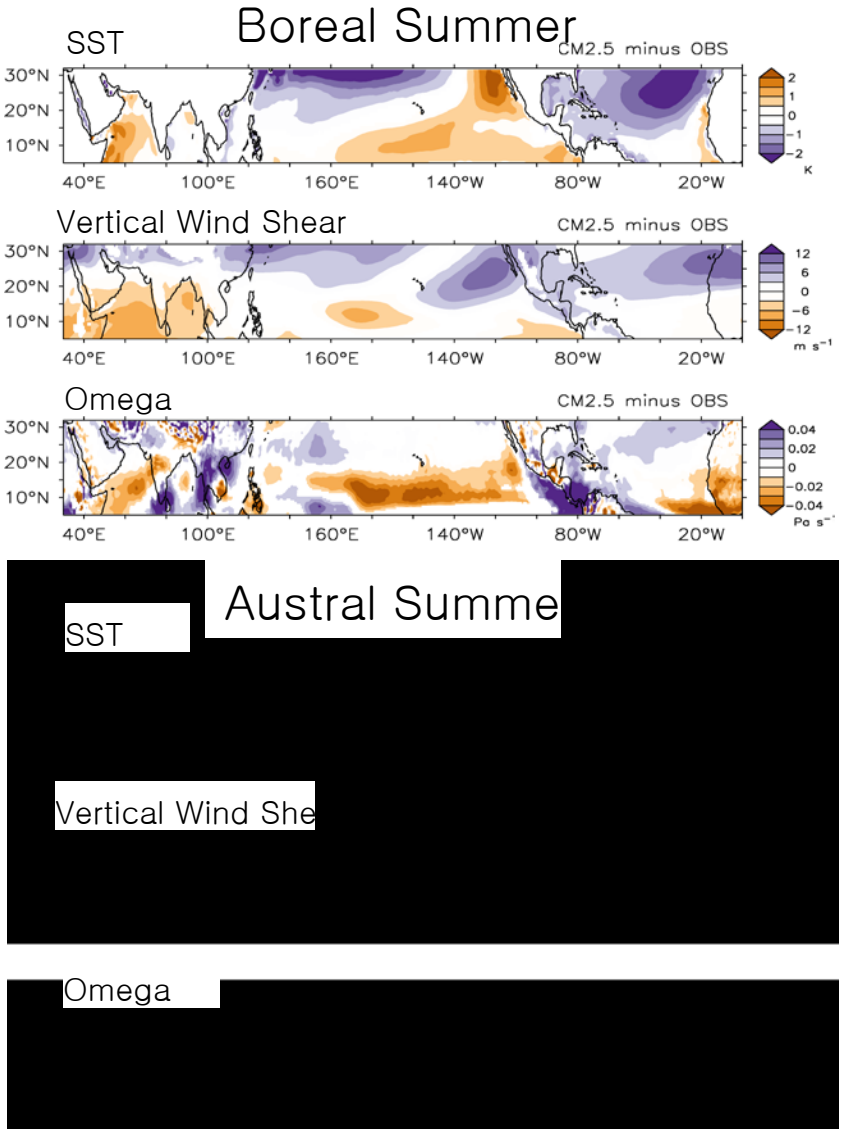

Warm color : favorable for TCs

Cold color : unfavorable for TCs

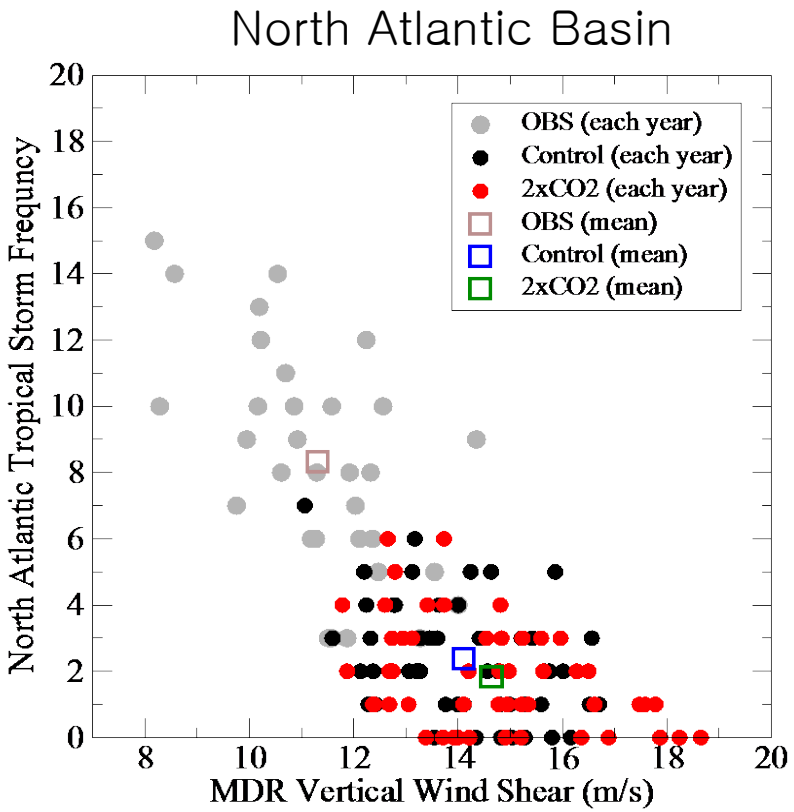

Summary (1)

- GFDL CM2.5 shows fairly realistic global TC frequency, TC seasonal cycle, and geographical distribution in the various basins.
- The model has some notable biases in regional TC activity, including simulating too few TCs in the North Atlantic basin.
- Despite these biases, the model simulates the large-scale variations of TC activity induced by El Nino/Southern Oscillation fairly realistically.
- The regional biases in TC activity are associated with simulation biases in the large-scale environments. This suggests that the simulation skill for TC activity in the model could be improved if the model biases in the environments were reduced.

Response to CO_2 doubling: TC Frequency

	> Tropical Storms (A)			> Hurricanes (B)			Ratio (B/Ax100)	
	Control (yr^{-1})	2xCO2 (yr^{-1})	Percent Change (%)	Control (yr^{-1})	2xCO2 (yr^{-1})	Percent Change (%)	Control (%)	2xCO2 (%)
Global	82.0	66.6	**-18.7**	31.6	28.7	**-9.1**	39	43
NA	2.7	1.9	**-28.4**	0.4	0.3	-11.1	13	17
EP	16.6	13.9	**-16.2**	4.0	4.5	12.1	24	32
WP	27.5	23.1	**-16.3**	13.4	12.5	-6.6	49	54
NI	5.5	4.8	-13.1	2.0	2.0	3.1	36	42
SI	21.7	16.5	**-24.0**	8.7	6.7	**-22.4**	40	41
SP	7.8	6.3	**-18.5**	3.2	2.6	-17.0	41	42

Bold : significant change at $p<0.05$

Response to CO_2 doubling: TC Maximum Wind Speed

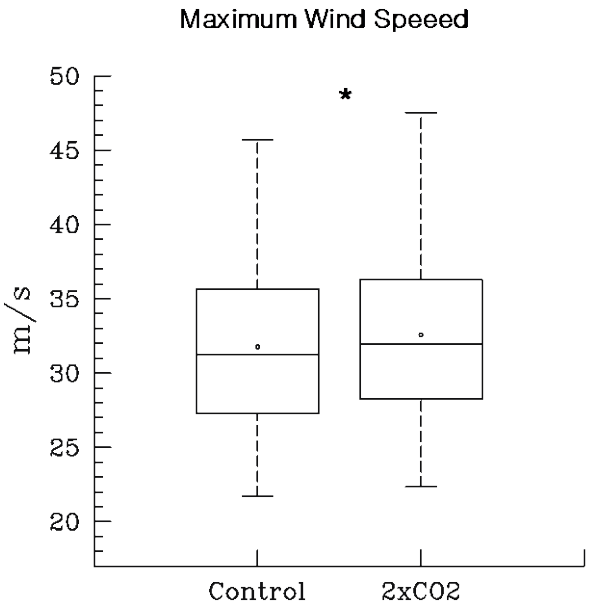

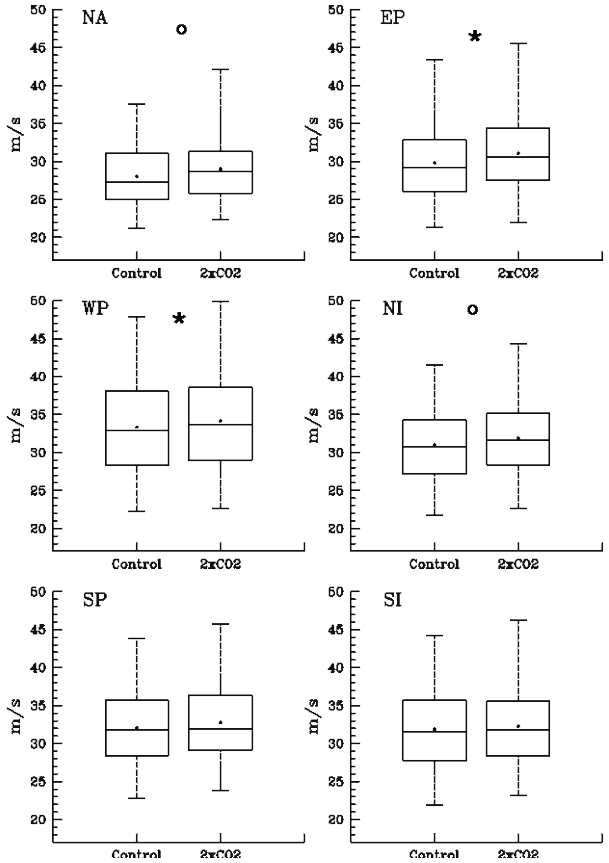

Response to CO_2 doubling: TC Activity

	Global	NA	EP	WP	NI	SP	SI
Maximum Wind Speed	* 2.7%	° 4.3%	*4.6%	*2.5%	° 3.2%	2.0%	1.5%
Lifetime	*−4.6%	−2.0%	−0.6%	*−5.8%	−3.6%	−4.4%	*−7.8%
Track Length	*−4.0%	−1.7%	0.6%	°−5.0%	−1.8%	−4.0%	*−10.5%
Translation Speed	0.6%	2.7%	0.9%	1.7%	°6.9%	−0.8%	°−3.0%
Power Dissipation Index	° 3.4%	12.7%	*12.0%	3.1%	5.0%	2.3%	−3.8%

Response to CO_2 doubling: TC Size

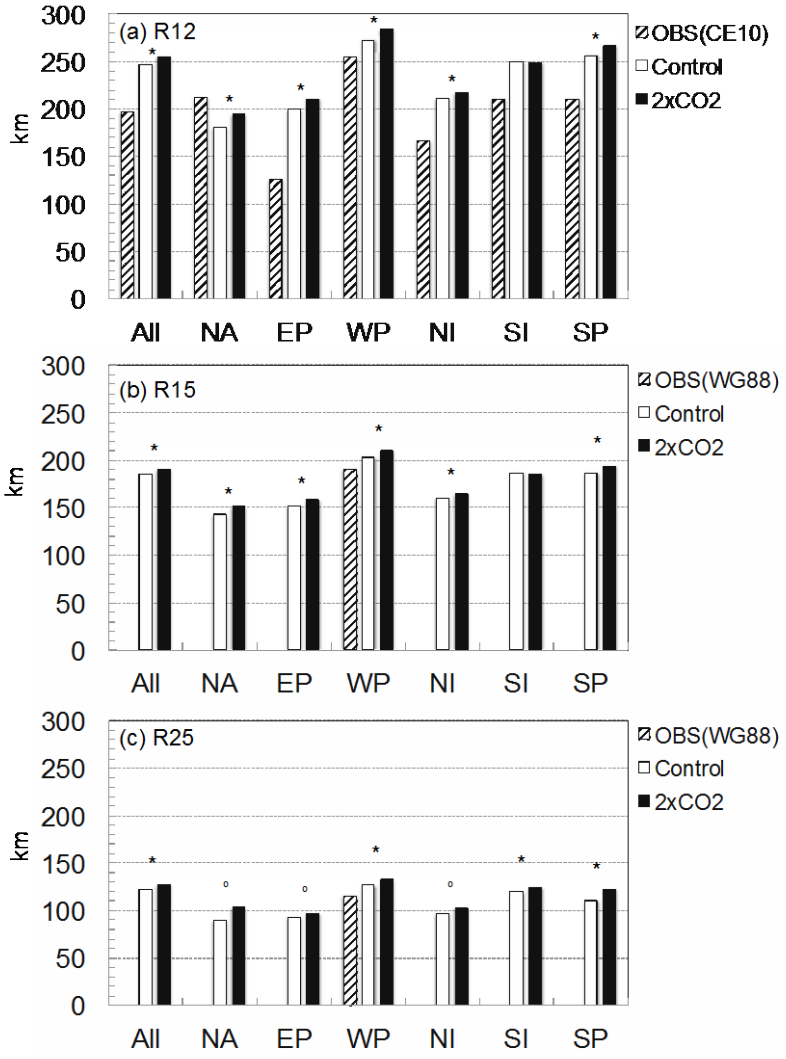

R12, R15 and R25 are the distances from the storm center at which the azimuthal-averaged (around-the-storm-averaged) tangential wind speed reaches 12, 15 and 25 m/sec, respectively.

The relative sizes of storms (differences between basins) in the control run are similar to observations (Chavas and Emanuel, 2010), except for North Atlantic.

Asterisks(*) denote a statistically significant change at the p=0.01 significance level.

Response to CO_2 doubling: TC Rainfall

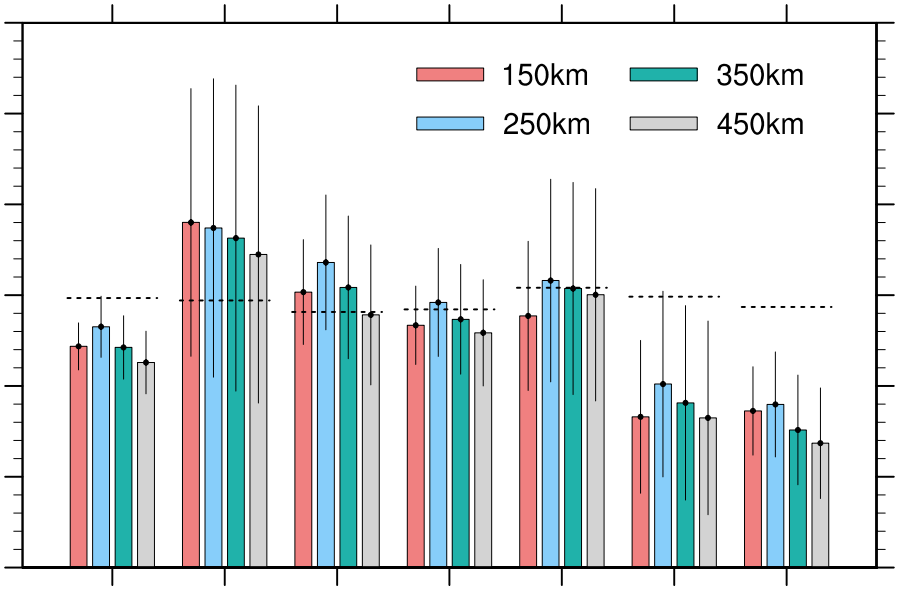

The fractional change of rainfall rate averaged within 150km, 250km, 350km and 450km of the TC center for the globe and each basin.

The dotted lines represent the approximate changes of the water holding capacity for each basin (estimated as 7% per degree C increase of basin-averaged SST).

Response to CO2 doubling: TC Regional Activity

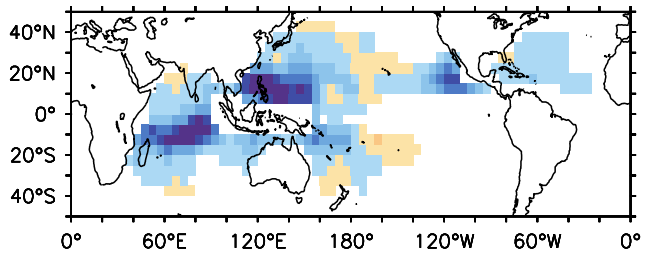

Response to CO2 doubling: Large-Scale Environments

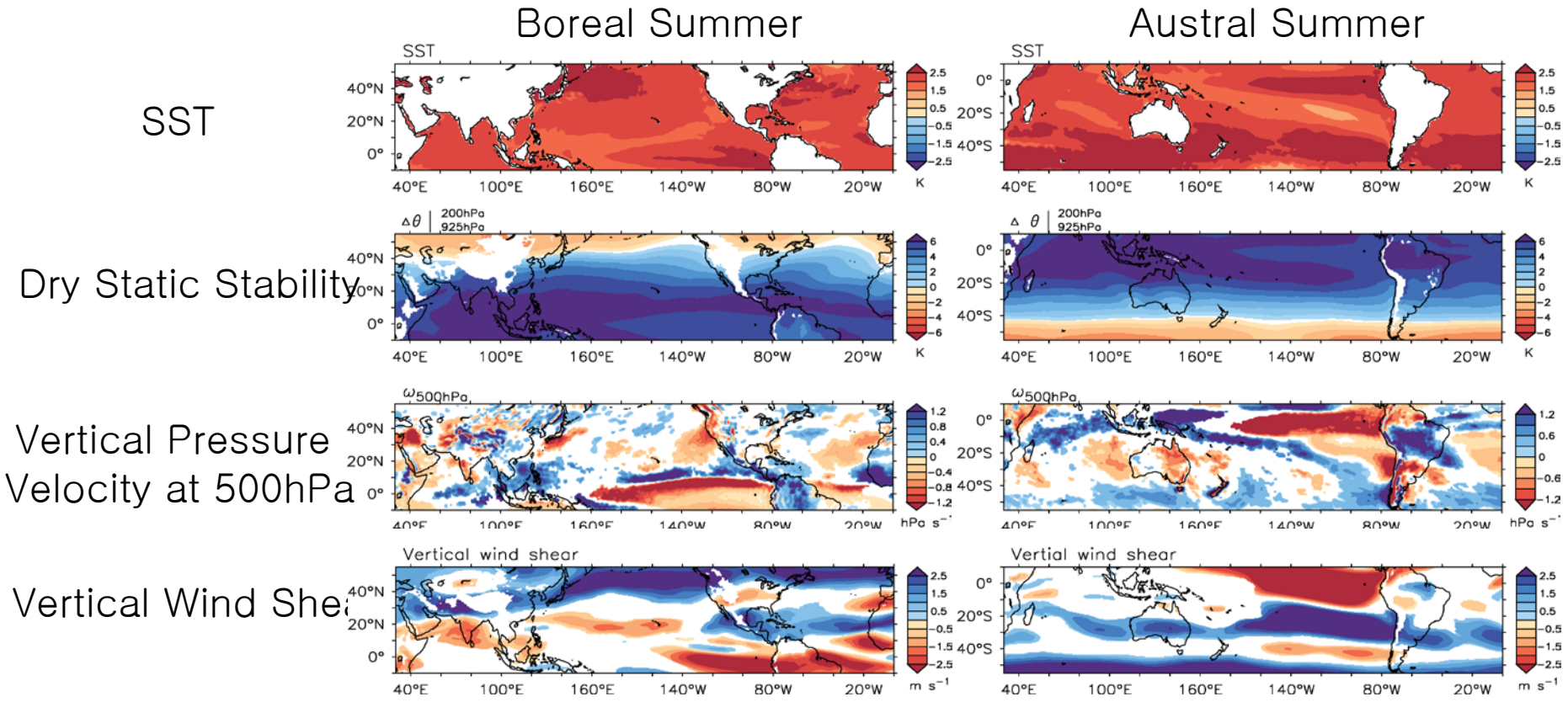

Warm color : favorable for TCs

Cold color : unfavorable for TCs

Monthly standard deviation of the interannual variation of the SST_{MDR} for the Control and the $2xCO_2$ (°C).

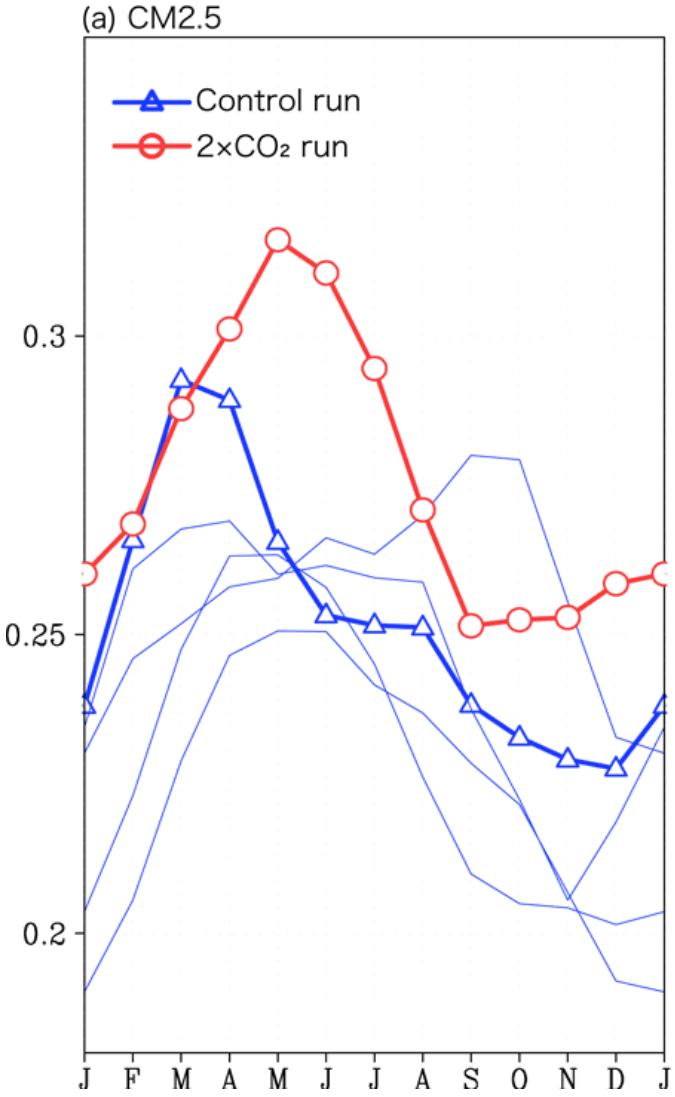

Doi et al. 2013, JC

Despite of reduction in frequency from $2xCO_2$, the warmed climate exhibits increased interannual hurricane frequency variability so that the simulated Atlantic TC activity is enhanced more during unusually warm years in the CO_2-warmed climate relative to that in unusually warm years in the control climate.

(a)	Mean TC count for all years (A)	Anomalous TC count for warm SST_{MDR} years (B)	Percentage change (B/Ax100)
Control	2.7	0.7	26.1
$2xCO_2$	1.9	1.0	50.0
2xCO2 minus Control	−0.8 (−28.3%)	0.3 (+37.1%)	

(b)	Mean PDI for all years (C)	Anomalous PDI for warm SST_{MDR} years (D)	Percentage change (D/Cx100)
Control	22.7	2.4	10.4
$2xCO_2$	20.3	9.4	46.4
2xCO2 minus Control	−2.4 (−10.7%)	7.1 (+289.1%)	

PDI unit is $10^3\ m^{-3}\ s^{-3}$

Summary (II)

- 2xCO_2 response has reduced TC frequency (-19%) increased intensity (+2.7%), shorten lifetime (-4.6%), increased size (+3%) and increased TC rainfall rates (+12%).
- The most of results are in agreement with the consensus of other climate models (Knutson et al. 2010, Nature Geoscience).
- Our analysis suggests that regional changes in several large-scale environmental factors influence the various TC characteristics at the regional scale.
- Although there is an overall reduction in frequency in the Atlantic from CO_2 doubling, the warmed climate exhibits increased interannual hurricane frequency variability so that the simulated Atlantic TC activity is enhanced more during unusually warm years in the CO_2-warmed climate relative to that in unusually warm years in the control climate.

Thank you !